Comparative field-scale assessment of the stormwater treatment effectiveness of bioswales on Maryland highways

Final Report to Chesapeake Bay Trust

Keith N. Eshleman, Ph.D.*[,1]
Briana Rice[2]
James Garlitz[2]
Trevor Frissell[3]

September 12, 2025

*Principal Investigator and corresponding author: e-mail: keshleman@umces.edu

[1]Professor, University of Maryland Center for Environmental Science, Appalachian Laboratory, 301 Braddock Road, Frostburg, MD 21532

[2]Senior Faculty Research Assistant, University of Maryland Center for Environmental Science, Appalachian Laboratory, 301 Braddock Road, Frostburg, MD 21532

[3]Faculty Research Assistant, University of Maryland Center for Environmental Science, Appalachian Laboratory, 301 Braddock Road, Frostburg, MD 21532

Executive Summary

A long-term (2017-2024) field study, supported first by Maryland Department of Transportation State Highway Administration (MDOT-SHA) and later by Chesapeake Bay Trust (CBT), addressed the management issue of the performance of bioswales in controlling stormwater runoff and stormwater pollution associated with Maryland's highway system. Bioswale performance was assessed relative to grassed swales with which the bioswales were paired at three sites across the state. Rainfall and runoff from the bioswales and grassed swales were measured from March through October at the Hagerstown site (three swales) from 2017-2018; at the Ellicott City site (three swales) from 2017-2024; and at the Lewistown site (two swales) from 2020-2024. At the three bioswales with the most extensive data, underdrainage was the dominant form of runoff, contributing 87 - 94% of total runoff over the course of the study; relative to the grassed swale controls, overland runoff from the bioswales was reduced by 87 – 96%. For all five bioswales studied, 95 – 100% of the rainfall was considered "captured and treated"—thus the technology met one of the primary stormwater management goals. We attributed the very high efficiency by which rainfall was "captured" and discharged by the bioretention cells to the extremely high measured infiltration capacity (= saturated hydraulic conductivity; 600 – 1,600 mm h^{-1}) of the engineered soil media and the associated unregulated underdrains. Unfortunately, the study produced little evidence of "extra" retention of stormwater over what the grassed swales provided. Mean storm runoff volume was significantly reduced at only one bioswale (EC-BS2) relative to the control watershed (EC-GS) which we attributed to percolation and groundwater recharge beneath the bioretention cell. At the other two bioswales with extensive data (EC-BS1 and LT-BS), either no difference in mean storm runoff volume was found or the difference could be mostly explained by differences in event rainfall. Except for EC-BS2, differences in peak runoff were also negligible or could be explained by differences in rainfall intensity between the swales—thus demonstrating little, if any, attenuation due to the presence of the bioretention cells and underscoring their hyper-efficiency at translating overland runoff into underdrainage.

Event runoff and peak runoff from the swale watersheds were shown to vary primarily as linear functions of event rainfall (or rainfall intensity) and secondarily as a function of 3-day antecedent rainfall (the latter providing a reasonable index of antecedent soil moisture). We explored the overall sensitivity of peak runoff from two of the swale watersheds to possible increases in future rainfall intensity and found nearly proportional percentage changes in runoff from a 10% increase in rainfall intensity across the entire spectrum of rainfall intensity. A scenario in which the median 3-day antecedent rainfall was increased uniformly by 10% produced negligible (< 0.2%) increases in peak runoff, however.

We found significant differences in event mean concentrations (EMCs) for 24 of the 27 constituents that were measured—including many that were our primary focus (N, P, and TSS). Analysis of event loads (computed from event runoff and EMCs of pollutants and other water quality constituents) showed fewer statistically significant differences, but some were robust and considered very important. While no differences in TSS loads were observed, mean orthophosphate-P loads were significantly lower at all three bioswales by 40 - 80%, providing strong evidence of P-chemisorption. The extremely high rates of percolation through the

biosoils promote extensive soil-water interaction that is highly conducive to chemisorption as long as the soils are not effectively P-saturated. These interactions produced very low orthophosphate-P concentrations in the underdrainage compared to overland runoff from the bioswales and from the grassed swales. Conversely, mean event NO_3-N loads from EC-BS1, EC-BS2, and LT-BS were actually higher than loads from the corresponding grassed swale controls by 190 – 790%, pointing to the bioretention cells as providing a major source of nitrate-N. The majority of the nitrate-N in the bioswale outflow was apparently generated through mineralization of soil N and subsequent nitrification within the aerobic biosoil itself. The frequent and extensive percolation of water through the biosoil provided a rapid and efficient means of extracting and transporting the accumulated nitrate-N—a mobile, negatively-charged, and highly soluble form of N—to the underdrain where it was routed directly to the downstream stormwater inlet.

Comparisons of mean event loads for two ancillary constituents (Cu, Zn) also produced significant results, with the bioswales consistently producing higher loads (typically by at least 200%) and suggesting a strong source in the bioretention cells, as well as a transport mechanism (leaching of trace metals complexed to dissolved organic matter). For quite a few of the constituents (i.e., Cl, Na, Mg, DON, SOC-P, DOC, and Cr), non-significant event load differences were consistent among all three swale pairs. In particular, the lack of differences in the Na and Cl loads provides strong evidence that the swale water balances have been accurately quantified, since Na and Cl inputs from road salting are likely very similar in magnitude and neither element has an obvious sink or additional source within the watershed.

From a stormwater management perspective, the data provided strong evidence that the specific bioswale design employed by MDOT-SHA is highly effective at reducing stormwater P pollution of streams and rivers across the state; percentage P reductions by these facilities exceeded 50% (in some cases 75%) which is consistent with proposed MEP (maximum extent practicable) goals for this type of stormwater best management practice (BMP). While the use of other materials or additives to biosoil to address specific stormwater pollutants is an area of active research and should probably be considered for future bioswale designs, maintaining the performance of the existing bioswale network should be top-of-mind. This means that the hydraulic performance of the bioswales should be maintained so that stormwater can continue to infiltrate and percolate through the bioretention cells. Fortunately, we found no evidence of significant clogging of these systems after nearly a dozen years of operation. One of the obvious downsides of the current bioswale design is their poor N retention capacity. The leaching of nitrate-N, as well as other constituents such as dissolved organic carbon and several trace metals, is clearly enhanced by the excessive drainage of the biosoil materials. The experimental data thus present a quandary in stormwater management given a possible trade-off in trying to optimize P vs. N retention by this particular BMP. The present design appears to be nearly optimally designed to address stormwater P pollution, but is ineffective at addressing nitrate-N pollution. Given that the eutrophication process in freshwater systems is often limited by P, not N, the current design is likely helping to achieve desired levels of pollution reduction necessary to restore these systems and should be credited with such. This is certainly not the case with nitrate-N stormwater pollution, however. While some modifications

of the biosoil media might be explored in this regard, we agree that using bioswale technology to address N pollution will likely require a significant redesign that allows for the presence of aboveground vegetation throughout the year and formation of a zone of transient water storage/saturation to support microbial denitrification.

Introduction

Bioretention is now a commonly used best management practice (BMP) for the treatment of stormwater in the U.S. and in many other countries around the world. Bioretention is typically incorporated into low impact development (LID) and environmental site design (ESD) practices (e.g., biofilters, rain gardens, and bioswales) as a means of enhancing infiltration of stormwater and promoting removal of pollutants within a biologically-active medium inhabited by growing vegetation and soil microorganisms (Roy et al. 2008; Liu et al. 2014). It has been suggested that bioretention can also contribute to achieving several important stormwater management objectives including: 1) protection of receiving surface waters from non-point source pollution; 2) attenuation of stormwater peaks; 3) diminishment of stormwater runoff volumes; and 4) support of the recharge/discharge behavior of groundwater that sustains stream baseflow (Davis et al. 2009). Optimal distribution of bioretention facilities and other BMPs distributed throughout a watershed can be used to address watershed management goals (Lee et al. 2012; Loperfido et al. 2014; Avellaneda et al. 2017; Fan et al. 2017; Hopkins et al. 2020).

Maryland—specifically Prince Georges County—was a pioneer in developing and promoting LID including the application of bioretention facilities to address urban development issues in the 1990s; despite this fact, urban flooding and damages resulting from such flooding continue to plague many areas of the state, in particular the Baltimore metropolitan area (Smith et al. 2013). Urban stormwater, including runoff from highways, has been identified as a major contributor to surface water pollution across a large portion of the Chesapeake Bay watershed (Chanat and Yang 2018). Urban stormwater is presently regulated by Maryland Department of the Environment (MDE) through the National Pollutant Discharge Elimination System (NPDES) Municipal Separate Storm Sewer System (MS4) discharge permitting program under the Clean Water Act. In 2015, MDE reissued a stormwater permit to Maryland Department of Transportation State Highway Administration (MDOT-SHA) covering stormwater discharges from the stormwater conveyance system owned and operated by the state. A major component of MDOT-SHA's plan under the MS4 permit has been the application of bioretention technology, either employed separately or as part of a bioretentive swale ("bioswale"), to treat runoff from the state's major highways. According to data displayed at the MDOT Bay Restoration website/on-line viewer (https://maryland.maps.arcgis.com/apps/webappviewer/index.html?id=cd43b2ce1f8c482d8ec070aac94bfd54), as of 2025, MDOT-SHA has constructed 499 new stormwater facilities across the state to help it achieve its stormwater management goals.

Experimental Design/Study Sites

We designed the present study to assess the performance of highway bioswales as an ESD approach to controlling stormwater and stormwater pollution associated with Maryland's highway system. Specifically, we were interested in evaluating the capacity of bioswales to: 1) reduce stormwater volumes; 2) attenuate stormwater peaks; and 3) reduce stormwater pollution from highway surfaces. Since many of the bioswales that MDOT-SHA has constructed

are effectively retrofits (i.e., conversions of existing grassed swales to bioswales) to meet more stringent wasteload allocations of N, P, and suspended matter than could be achieved using other practices, we designed a comparative field study to assess bioswale performance *relative to existing legacy grassed swales* (i.e., the latter were used as experimental "controls" against which bioswale performance was compared). A related, secondary objective was to determine how differences in the flowpaths of water within the bioswale (i.e., surface vs. subsurface) affected the concentrations of pollutants and other constituents measured at the swale outlet and thus contributed to (or reduced) overall stormwater pollution (again, relative to the grassed swale control).

Most field-scale studies of urban BMP effectiveness for pollution control experimentally derive average removal or retention percentages by comparing input and output loads or concentrations from particular facilities (e.g., Yu et al. 2001; Barrett 2008; Hatt et al. 2009; Stagge et al. 2012). Our study took a different approach, because stormwater pollutant inputs to highway swales are extremely difficult to measure accurately due to the diffuse nature of the temporally- and spatially-variable flowpaths (principally overland flow and direct precipitation). While it may be reasonable to assume that direct precipitation onto a particular facility is spatially-uniform, the same assumption would unlikely hold for overland flow that would expectedly vary as a function of surface imperviousness, local topography, soil properties, and other watershed features. For this reason, we opted to perform a comparative analysis of stormwater *outputs* from paired systems to address the question of whether LID/ESD practices incorporating bioretention (i.e., bioswales) provide significantly greater benefits than alternative or legacy practices (i.e., grassed swales).

The paired experimental design was replicated at three sites in two different physiographic provinces: 1) a site on U.S. Rt. 40 west of Hagerstown (HT) in the Ridge and Valley province; 2) a site on U.S. Rt. 40 west of Ellicott City (EC) in the Piedmont province; and 3) a site on U.S. Rt. 15 near Lewistown (LT) in the Piedmont province. Each site is comprised of one or two recently retrofitted bioswales and a nearby grassed swale "control" that discharge highway runoff intermittently to separate stormwater concrete box inlets (i.e., "storm drains") located within the highway medians; the HT and EC sites both included two bioswales paired with a grassed swale. The five bioswales (referred to here as "HT-BS1", "HT-BS2", "EC-BS1", "EC-BS2", and "LT-BS") were constructed in 2014 and are part of MDOT-SHA's BMP network (No. 210199, 210197, 130524, 130528, and 100464, respectively). Each bioswale is comprised of a variable length of vegetated swale in which the lower soil was effectively replaced by layers of sand and coarse aggregate drained by a 15.2 cm (6 in) dia. perforated PVC pipe functioning as a sub-drain (or underdrain); the upper soil (61 cm; 24 in) was replaced by an engineered "bioretentive" medium comprised of sand, organic matter (i.e., shredded hardwood bark mulch), and fine-grained soil particles. Gravity underdrainage required obvious modification of the existing concrete or brick box inlet at the time of bioswale construction. The three paired grassed swales (referred to as "HT-GS", "EC-GS", and "LT-GS") were constructed many decades prior to the study and are considered "legacy" or "abandoned" swales by MDOT-SHA. Since we were not able to implement a full "before-after, control-impact" (BACI) design and did not attempt to

Table 1. Physical characteristics of the eight swale watersheds included in the study[1]. See Appendix A for photos of some of the swales.

Swale watershed	SHA BMP#	Lat./long. of swale outlet	Drainage area (ha)	Impervious surface area (ha)	Imperv-iousness (%)	Bioretention area (ha)
HT-BS1	210199	39°39'11.7"N 77°45'08.6"W	0.47	0.12	25	0.009
HT-BS2	210197	39°39'11.7"N 77°45'13.9"W	0.39	0.13	33	0.009
HT-GS	210698	39°39'10.9"N 77°46'17.8"W	0.45	0.14	31	N/A
EC-BS1	130524	39°17'41.8"N 76°54'01.0"W	0.43	0.19	44	0.016
EC-BS2	130528	39°17'25.8"N 76°53'27.3"W	0.49	0.22	45	0.018
EC-GS	132881	39°16'40.9"N 76°50'26.3"W	0.45	0.27	60	N/A
LT-BS	100464	39°31'33.2"N 76°50'26.3"W	1.10[2]	0.69[2]	63	0.019
LT-GS	101537	39°31'26.6"N 77°25'12.1"W	0.58	0.14	24	N/A

[1]Physical characteristics for HT-BS1, HT-BS2, EC-BS1, EC-BS2, LT-BS, and LT-GS were taken directly from scale engineering drawings obtained from MDOT-SHA for these BMP's. Although HT-GS, EC-GS, and LT-GS swales are part of MDOT-SHA's NPDES Stormwater Management Facilities (SWMFAC) on-line database (https://data.imap.maryland.gov/datasets/d588b42cc24f4ef48235a86259da3270_0/about), no information on field characteristics is available for these swales. Therefore, we estimated these characteristics using field survey data to define the length of each swale and google maps (maps.google.com) to estimate drainage and impervious surface areas.

[2]MDOT-SHA engineering drawings showed a drainage area of 0.66 ha and an impervious area of 0.25 ha, but these values were determined to be substantially in error (see text). The drainage area shown is 67% higher to account for the underestimate. We assumed that the additional drainage area (0.44 ha) is all impervious area.

measure or model inputs, our experimental design explicitly assumes that each experimental pair of swales receives similar inputs of highway pollutants; each bioswale and control swale

was thus selected so as to minimize differences among them as much as possible (i.e., both swales are located in relatively close proximity along the same highway, have similar drainage areas, drain comparable areas of impervious surface, and have similar slopes and herbaceous vegetation; Table 1). We have subjected our data to careful scrutiny in order to test the hypothesis that the primary difference between these paired swales is the presence/absence of a bioretention area with an associated underdrain.

While we were not privy to the explicit design criteria for the bioswales at the beginning of the study (nor were we involved in design or construction), we were subsequently able to find a guidance document that provides specific design criteria for bioswales being constructed in Maryland (CSN 2011). These criteria build on technical approaches used for sizing stormwater facilities by first determining the water quality volume (WQ_V) to be "captured and treated" by a particular stormwater facility or BMP (MDE 2009). The WQ_V is defined as the storage volume needed to capture and treat 90% of the average annual rainfall (recognizing that 10% of the rainfall will not be captured and treated). Once the WQ_V is estimated, the facility can be sized accordingly. The other major design criteria refer to two different levels of P removal: 50% and 75% (the latter considered commensurate with an MEP goal). For 75% (i.e., MEP) P retention, all of the following are required: 1) filtering of at least 75% of the WQ_V; 2) a minimum swale filter bed depth of 61 cm (24 in); 3) use of a filter medium consisting of 85-88% sand, 8-12% fines, and 3-5% organic matter; 4) an effective swale slope < 2%; 5) use of a stone sump; and 6) sub-soil permeability testing to ensure minimum infiltration rate of 1.3 cm h^{-1} (0.5 in h^{-1}; with an underdrain, sub-soil testing requirement is waived) (CSN 2011). To our knowledge, no design criteria have been established for N retention by bioswales in Maryland, however.

Early on in the study it became apparent that event runoff values computed for LT-BS were much higher than at LT-GS and at the other swales; event runoff coefficients frequently exceeded unity—a physical impossibility. Among the seven swales studied, LT-BS was the only swale that showed substantial channel erosion and breaching of the four check dams that had been constructed—suggesting that discharge was much higher than expected. Event loads for many constituents, including some (e.g., Cl) that can be considered conservative tracers, were also considerably higher than at the other swales. The only logical explanation was that the watershed area for LT-BS (obtained from MDOT-SHA engineering drawings) was significantly underestimated, so we adjusted the watershed and impervious areas for LT-BS accordingly (see details in Table 1).

Methods

Field methods. Soil infiltration capacity was characterized at the sites using multiple double-ring infiltrometer measurements. For each measurement, two cylindrical steel rings (i.d. of outer buffer ring = 61.0 cm, i.d. of inner measurement ring = 30.5 cm, height of rings = 30.5 cm) were driven about halfway into the soil with the smaller ring centrally nested inside the larger one. A Mariotte bottle was constructed from a 1.2 m long section of 10.2 cm (4") dia. schedule 40 PVC pipe, cemented endcaps with two outlet tubes, and transparent plastic measurement

tube. The bottle was filled with water and suspended from a surveyor's tripod directly over the inner ring. Water was quickly ponded onto the soil surface within both rings at the same time that the outlets of the Marriotte bottle were opened, and measurements of the water level inside the bottle were taken manually at fixed time intervals (15 - 60s) from the plastic tube using a measuring tape as a reference. A cumulative infiltration capacity (mm min^{-1}) curve was plotted after correcting the Mariotte readings using the ratio of the cross-sectional areas (πr^2) of the reservoir and inner ring, and a steady-rate infiltration capacity (slope of the cumulative infiltration capacity curve, $f_i*(\infty)$ = saturated hydraulic conductivity, *K*) was computed using linear regression (omitting measurements showing clear evidence of a non-linear response due to soil capillarity upon initial wetting; Fatehnia et al. 2016). We tested for differences in mean *K* between the bioswales and control swales using t-tests (assuming unequal variances).

The bioswales and grassed swale controls were similarly instrumented to monitor stormwater and pollutant responses to rainfall events during three growing seasons (approximately March through October). Monitoring was performed over two years (2017, 2018) at HT, eight years (2017-24) at EC, and five years (2020-24) at LT. Runoff responses consisted of ***overland flow*** (discharge and pollutant concentrations) at the outlets of all eight swales and ***underdrainage*** (discharge and pollutant concentrations) at the five bioswale outlets. The grassed swales are not underdrained. Common monitoring equipment consisted of: 1) a prefabricated, fiberglass truncated Parshall flume (15.24 cm = 6.0 in throat width; maximum capacity of 0.1107 $m^3 s^{-1}$ = 1,755 gal min^{-1} at H = 45.7 cm = 1.50 ft; Tracom Fiberglass Products, Alpharetta, GA) installed at the outlet of each swale (i.e., the flume was sited directly over a stormwater inlet box to maintain critical flow conditions in the flume throat by avoiding submergence/backwater effects); 2) wingwalls ($\geq$ 30 cm high) constructed from pressure-treated timbers to channel surface runoff from the swale into the flume (flume discharge of 0.058 $m^3 s^{-1}$ at H = 30 cm); 3) an ultrasonic water level sensor and module (Teledyne ISCO No. 2110) to monitor and record water levels in the flume; 4) a portable sequential water sampler (Teledyne ISCO No. 3700) capable of collecting 24 discrete 1L stormwater samples; 5) an interface module/data logger (Teledyne ISCO No. 2105) used to store data and trigger the samplers using inputs from the water level sensors; 6) a solar panel/battery charging apparatus to maintain continuous 12V DC power to the equipment; and 7) a pre-fabricated instrument shelter housing the samplers, batteries, and interface modules.

Unfortunately, we were initially unable to obtain permission from MDOT-SHA to install this standard monitoring equipment at EC-GS due to highway safety concerns, so we were forced to gauge the overland flow at this station using a Hobo water level logger (Onset Computer Corp. No. U20L-01) and a staff gauge attached to a rebar post installed within the grass swale just upstream of the stormwater inlet. Installation was completed on May 12, 2017. Manual "wading" discharge measurements were made periodically using a Marsh-McBirney digital electromagnetic current meter attached to a top-setting wading rod to define a rating curve (i.e., log discharge vs. log[gage height – ε]; ε = offset computed by trial and error; Rantz et al. 1982). The Hobo level logger was programmed to provide continuous 5-min data. We observed a backwater effect at the EC-GS inlet during several storms due to discharge apparently exceeding the capacity of the inlet culvert; Manning's equation suggested a peak culvert

discharge of about 0.095 $m^3 s^{-1}$. This value was assigned to a few gage height measurements that exceeded a stage of 30 cm. This equipment was employed in 2017 through early 2019 when we finally obtained permission to install the standard equipment at EC-GS; installation was completed on March 29, 2019.

Additionally, the underdrain pipe outlets at the bioswales were equipped with a plastic catch basin (NDS Inc.) housing a second ultrasonic water level sensor and an inlet line leading to a second portable sequential sampler housed in the instrument shelter; each catch basin was covered with a sheet metal cover to prevent interaction of underdrain water with overland flow spilling into the inlet from the flume. Flume and underdrain water level readings were recorded at two different frequencies depending upon the level within the flume or catch basin: every four hours when the water level was less than 1.3 cm and every five minutes when the reading was greater than or equal to 1.3 cm. Flume discharge was computed using the water level data and a rating curve obtained from the flume manufacturer, while the underdrain outlets were manually calibrated using "bucket and stopwatch" discharge measurements to define an empirical rating curve comparable to the rating curve developed for EC-GS.

Tipping bucket gages (Teledyne ISCO No. 674) located at HT-BS1, EC-BS1, and EC-GS (operational 2020-21) were interfaced to the data logger and used to characterize the rainfall for each pair of swales; rainfall data were recorded at 15-min intervals. For storms at EC-GS from 2017-19, we estimated storm rainfall using NEXRAD (WSR-88D) instantaneous rainfall intensity (dual polarization) data that were downloaded and processed using NOAA's Weather and Climate Toolkit (WCT); the NEXRAD data were aggregated on a storm-by-storm basis and bias-corrected using station data from EC-BS1 (see details on methodology in Appendix B).

The sequential samplers were programmed to capture the initial flush of stormwater; the overland flow samplers were programmed to trigger sampling when the water level within a flume reached 1.3 cm. The first sample was collected immediately upon activation, with three subsequent samples collected at 5-minute intervals. Remaining samples (maximum of 20) were collected after a preset volume (3.78 – 9.46 m^3) of discharge had passed since the previous sample or until the flow declined to a rate less than 1.1×10^{-5} $m^3 s^{-1}$ as estimated by the level module. The underdrain samplers were equipped with water level actuators that activated the sampler when the water level within the catch basin was high enough to cause any discharge at the outlet. The program allowed the first sample to be collected immediately upon activation, with the next three collected at 15-min intervals; additional underdrain samples were collected at 60-, 90-, or 120-min intervals (depending on the expected duration of the storm) until underdrainage ended.

Overland flow sampling at EC-GS in 2017 and 2018 was conducted differently: in 2017, field personnel manually collected 1L "grab" samples at discrete (typically 30-min) time intervals. Beginning in spring 2018, however, we were able to deploy an automated sequential sampler that was manually activated at the time at which swale discharge was first observed; typically, the first four samples were collected at 15-min intervals and subsequent sampling at 60-min intervals.

During three major stormflow events (event #133: 4/28/23; event #144: 3/23/24; and event #148: 4/3/24) at the EC site, we conducted synoptic stormwater surveys of both bioswales and grassed swales that are located on the same section of highway (U.S. Rte. 40) as our intensively-monitored stations. The objectives were: 1) to sample a sufficient number of swales so that we could test the (null) hypothesis that the mean water quality at the bioswales is not different from the grassed swales; and 2) to test the hypothesis that the gaged watersheds are not unrepresentative of the "populations" of swale watersheds in the same area with respect to water quality responding to the same rainfall driver. We used a portable, battery-powered electric drill equipped with a peristaltic pump head and an appropriate length of pump tubing to "grab" a water sample from each swale. This required carefully lowering the tubing into the storm drain at each bioswale to sample underdrainage near the underdrain pipe; the same process was used to sample shallow overland flow at the grassed swale outlets. The pump flow rate was kept sufficiently slow to avoid entraining sediment into the sample bottle.

All samples were collected in pre-cleaned, 1L polyethylene bottles. Samples were kept on ice during transit to our laboratory in Frostburg, Maryland where they were refrigerated and later processed for chemical analysis (typically within 24-48 h of collection). No water sampling or chemical analyses were performed in 2022 due to funding constraints.

Laboratory methods. Sample analysis focused on three key water contaminants – nitrogen (N), phosphorus (P), and suspended matter—the pollutants of primary interest for downstream water quality; concentrations of a large number of secondary constituents (e.g., metals, cations, etc.) were also measured. Sub-samples for total nitrogen (TN) and total phosphorus (TP) analyses were prepared by pouring off a well-mixed portion into labeled containers. Specific conductance (SC) and pH were measured on raw water subsamples. Total suspended solids (TSS) were measured gravimetrically following filtration of a measured volume through a pre-weighed Whatman glass fiber filter (0.70 μm) under vacuum (EPA 160.2); the filtrate was aliquoted for measurement of a variety of dissolved constituents. Total N, total dissolved N (TDN), TP, and total dissolved P (TDP) were measured using a combined, two-step persulfate digestion process followed by analysis for nitrate-N and orthophosphate-P via flow injection colorimetry on a Lachat QuikChem 8000 (Valderrama 1981). Major anions were quantified using ion chromatography (Dionex DX-120; APHA 4110-2005). Cations (Na, K, Mg, Ca) were measured by flame atomic absorption spectrometry (Perkin Elmer AAnalyst 800; APHA 3111(B)–2005) from 2017-21 and by inductively coupled plasma mass spectrometry (Agilent 7900) in 2023-24. Inorganic nutrients were measured via flow injection colorimetry (Lachat QuikChem 8000): nitrate-N, nitrite-N and orthophosphate-P were measured following USEPA (1993) methods 365.2 and 365.1, respectively, and ammonium-N was quantified using the method developed by Fishman (1993). Dissolved organic N (DON) was calculated as the difference between TDN and the sum of the measured inorganic N species. Soluble organic and colloidal P (SOC-P) was computed as the difference between TDP and orthophosphate-P. Particulate-N and particulate-P were also computed by difference (i.e., TN – TDN and TP – TDP, respectively). Concentrations of a group of selected trace metals commonly associated with highway runoff (Cd, Cr, Cu, Zn, Pb) were measured in glass fiber-filtered, HNO_3-preserved aliquots by inductively coupled plasma mass spectrometry (Agilent 7900). Dissolved organic

carbon (DOC) was measured by UV-assisted persulfate digestion on a Teledyne Tekmar Fusion instrument (ASTM D4839 – 2011) and acid neutralizing capacity (ANC) was determined by automated Gran titration with standardized dilute HCl on raw water samples.

All sample analyses were completed during accepted holding times. Blanks, duplicates (~ 1 of every 10 samples), independent control samples, and spikes were used to quantify analytical error and maintain quality control. In total, we analyzed 2,763 discrete stormwater samples (11 samples from HT, 1,988 samples from EC, and 764 samples from LT) during the study; this included 63 "grab" samples analyzed as part of three synoptic stormwater surveys carried out at EC in 2023 and 2024.

Data analyses. Stormflow events, commonly 12-24 h in duration, were identified manually using the water level and rainfall records. We used a positive water level response of the underdrain in association with organized rainfall as the primary event criterion, since virtually all identified events produced this response; at the bioswales, underdrain discharge always ended last, so this component was also used to establish the event duration as well. We then identified any overland responses at the bioswale and/or at the paired grassed swale during the same time period. One result of using this identification method is that some storms produced double- or even triple-peaked hydrographs, because underdrain discharge was continuous throughout the event. For each event, we generated continuous stormflow (5-min data) hydrographs and estimates of peak instantaneous discharge for each flow component using the water level data and the appropriate rating curve. Each storm hydrograph was time-integrated and the resultant volume was normalized by drainage area to estimate a storm runoff depth (cm). Event rainfall was characterized on a depth basis, as well as by maximum *x*-h (*x* = 1, 2, 3, and 24) intensity which was translated into return periods using National Weather Service point precipitation frequency estimates for nearby stations (Bonnin et al. 2025). Three-day antecedent rainfall was computed and used as an index of antecedent soil moisture for predicting swale runoff.

A discharge-weighted event mean concentration (EMC) of each constituent was computed for each swale/event using equation (1):

$$EMC = \frac{\sum_{i=1}^{n} C_i Q_i}{\sum_{i=1}^{n} Q_i} \quad (1)$$

where C_i is the measured concentration of a particular constituent in the *i*th (*i* = 1, 2, …., *n*) sample collected during an event; Q_i is the instantaneous discharge measured at the time that the *i*th sample was collected; and *n* is the total number of samples analyzed. For EC-BS1, EC-BS2, and LT-BS (with two possible flow components: flume and underdrain), we used Eq. (1) to compute individual component EMCs for each constituent for each event for which data were available. For all storms where we had complete data for both the underdrain and flume runoff components, we computed combined EMC's by weighting the individual component EMCs by the cumulative event runoff from each component. While a few snowmelt and rain-on-snow events were characterized, they were omitted from the comparative statistical analyses. Event loads for each constituent were computed as the product of the respective runoff-weighted

EMC and the measured total event runoff and expressed in units of kg ha^{-1} (S ha^{-1} for conductivity and keq ha^{-1} for ANC). For comparisons of individual component EMC's, we tested for differences in means using a t-test (assuming unequal variances); for comparisons of "common" events, we tested for differences in mean EMC's using a paired t-test ($P \leq 0.05$). For the synoptic survey data, we used t-tests (assuming unequal variances) to compare mean sample concentrations between bioswales (underdrain samples) and grassed swales (overland runoff samples ($P \leq 0.1$).

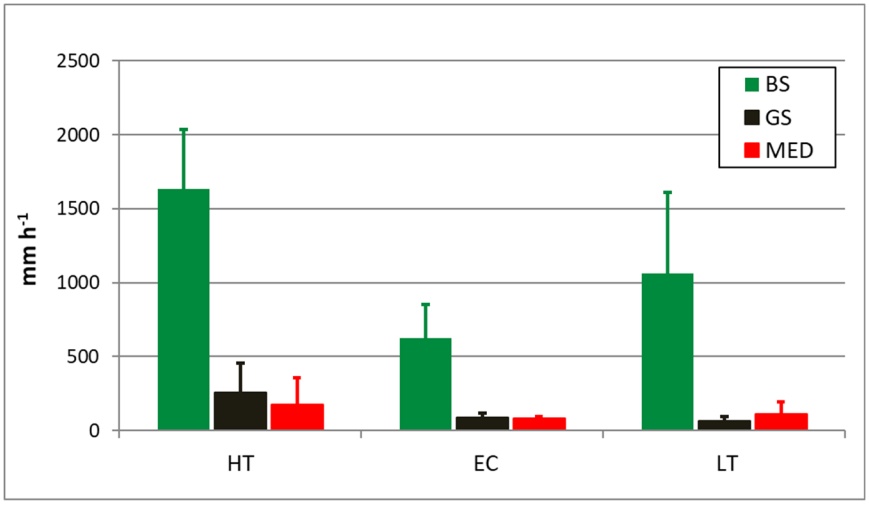

Figure 1. Mean steady-state infiltration capacity of biosoils (BS), grassed swale (GS) soils, and highway median (MED) soils measured at the three sites (HT, EC, and LT) using the double-ring infiltrometer method; error bars are 95% confidence intervals. The results are based on 22 individual measurements made at HT, 30 at EC, and 9 at LT.

Results

Soil infiltration capacity measurements. Cumulative infiltration capacity curves constructed for the bioswale soils indicated a nearly constant rate of infiltration under ponded conditions throughout the experiments. Such behavior is indicative of domination by gravity drainage through relatively coarse, highly permeable soils. In contrast, most of the curves constructed for the grass swales comprised of native soil or fills showed evidence of a sorptive phase early on in the process that is attributable to capillarity under unsaturated antecedent conditions. The cumulative infiltration capacity curves for the grassed swale soils generally became linear as the soils wetted up and capillarity declined or was eliminated, however. At all three sites, the biosoils (BS) had a higher mean *K* than soils at the paired grassed swale (GS) and of median (MED) soils surrounding the bioretention area ($P \leq 0.05$). The ratios of mean *K* in biosoils to

Table 2. Aggregated seasonal rainfall and runoff for the paired highway swale watersheds (EC-BS1/EC-GS, EC-BS2/EC-GS, and LT-BS/LT-GS) for the period 2017-2024; results include data from prior project funded by MDOT-SHA (2017-2022).

	Swale watershed					
	EC-BS1	EC-GS	EC-BS2[1]	EC-GS[1]	LT-BS[2]	LT-GS[2]
Total rainfall, m	5.55	6.15[3]	2.79	3.00	3.73	
Runoff-producing rainfall, m	3.92	4.41[3]	2.01	2.15	2.13	
Flume runoff, m	0.27	2.08	0.04	0.99	0.04	1.02
Underdrain runoff, m	1.77	0.00	0.66	0.00	1.03	0.00
Total runoff, m	2.04	2.08	0.69	0.99	1.06	1.02
Runoff coefficient, dimensionless	0.37	0.34	0.25	0.33	0.29	0.27

[1]Data from mid-August 2020 - October 2024
[2]Data from April 2019 - October 2024
[3]See text for estimation of rainfall for 2017-2019

grassed swale soils were 6, 7, and 16 at HT, EC, and LT, respectively. No differences in mean *K* were found between the BS and MED soils at any of the sites, however (Figure 1).

Hagerstown stormflow results. Only six rainfall events produced detectable storm responses at the HT site during the two-year study and all of these occurred in 2018: six responses were observed at HT-GS, while three underdrain responses were observed at HT-BS1; no responses were observed in the HT-BS1 flume or at HT-BS2, however. Each of the observed responses at HT was very fast and of short duration (i.e., a few hours), making it impossible to manually quantify underdrain flow rates and develop a rating curve. For this reason, our analysis treats these stormflow responses as binary in nature (i.e., response or no response). Qualitatively, the best single predictor of a stormflow response at these two swales was maximum 1-hr rainfall intensity. The six rainfall events that produced a response at HT-GS were ranked within the top seven in this category and only the 6th ranked maximum 1-hr rainfall intensity failed to produce a response at HT-GS; average recurrence intervals for 1-hr rainfall for these events ranged from less than one year to five years. For the HT-BS1 underdrain, maximum 1-hr rainfall intensity was also the best predictor of a response, with three of the top four rainfalls in this category producing underdrainage. Interestingly, the highest ranked maximum 1-hr intensity rainstorm that occurred on July 4, 2018 (a 5-y rainstorm) failed to produce an underdrain response. It appears that a second factor—antecedent rainfall—is also important in controlling responses of this system once a sufficient level of rainfall intensity has occurred. The 3-day antecedent rainfall on July 4, 2018 was 0.0 cm, but was 1.1 cm, 1.6 cm, and 2.0 cm for the other three events that actually produced underdrain responses at HT-BS1. It should be noted that 24-hr rainfall was a poor discriminator of stormflow responsiveness at HT-BS1 or HT-GS; none of the

events that actually produced a response at either site were in the top four in terms of 24-hr rainfall intensity (Table S1-1).

All 11 water samples collected at HT were obtained from the HT-BS1 underdrain during two separate events: 8/21/18 and 9/26/18. Obviously, the fact that no samples were collected from HT-GS for the same events makes it impossible to perform any kind of comparative water chemistry analysis for the HT swales.

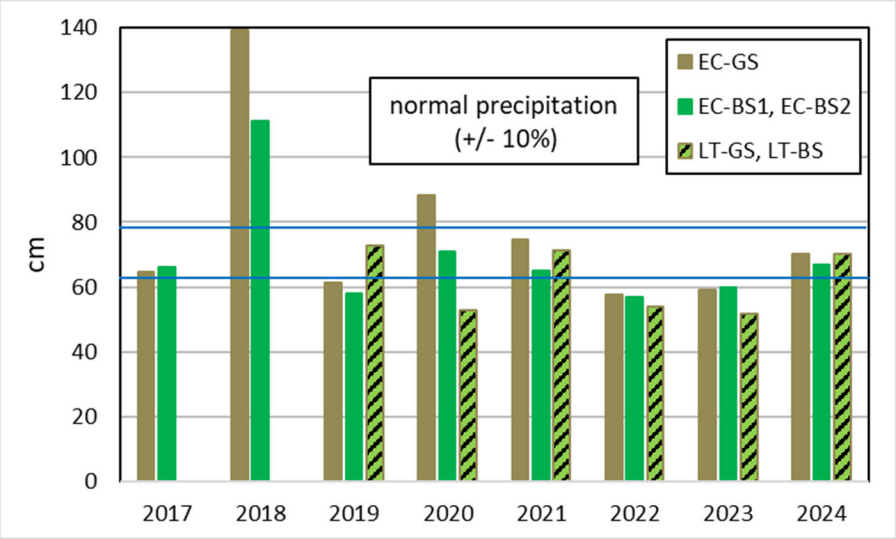

Figure 2. Seasonal (April–October) precipitation during the eight-year study at the EC and LT swales. No data for LT-GS/LT-BS in 2017 and 2018. Band of normal precipitation (blue lines, +/- 10% of the long-term mean) also shown.

Ellicott City and Lewistown stormflow results. Total precipitation (exclusively rainfall) at EC-GS and EC-BS1 during the primary monitoring period of the eight-year study was 615 cm (mean = 77 cm/monitoring season) and 555 cm (mean = 69 cm/season), respectively—reflecting an east-west gradient that has been reported by others; during the 4.3 years of monitoring at EC-BS2, seasonal rainfall was 279 cm (mean = 65 cm/season) indicating that the latter half of the eight-year study was considerably drier than the first half. At LT-GS and LT-BS, total precipitation was 373 cm (mean = 62 cm/season) during the six years of monitoring there (Table 2). Based on a comparison with long-term data from Baltimore, MD[1] and Frederick, MD[2], seasonal rainfall at the Ellicott City swale watersheds was mostly normal (i.e., within +/- 10% of the mean of 71 cm) to below normal (< 90% of the mean) during the study; the major exceptions were: 1) 2018 when seasonal rainfall was 95% and 55% greater than the long-term mean at EC-GS and EC-BS1, respectively; and 2) 2020 when seasonal rainfall at EC-GS exceeded the long-term mean value

[1] https://mesonet.agron.iastate.edu/sites/monthlysum.php?station=BWI&network=MD_ASOS
[2] https://mesonet.agron.iastate.edu/sites/monthlysum.php?network=MD_ASOS&station=FDK

by 23%. At Lewistown, seasonal rainfall was normal in 2019, 2021, and 2024, but below normal in 2020, 2022, and 2023 (Figure 2).

Seasonal runoff varied among the swale watersheds and among years—largely reflecting year-to-year variations in rainfall. Runoff was highest in 2018 at EC-GS and EC-BS1 in response to much above normal rainfall, while it was lowest in 2023 with below normal rainfall. Runoff at

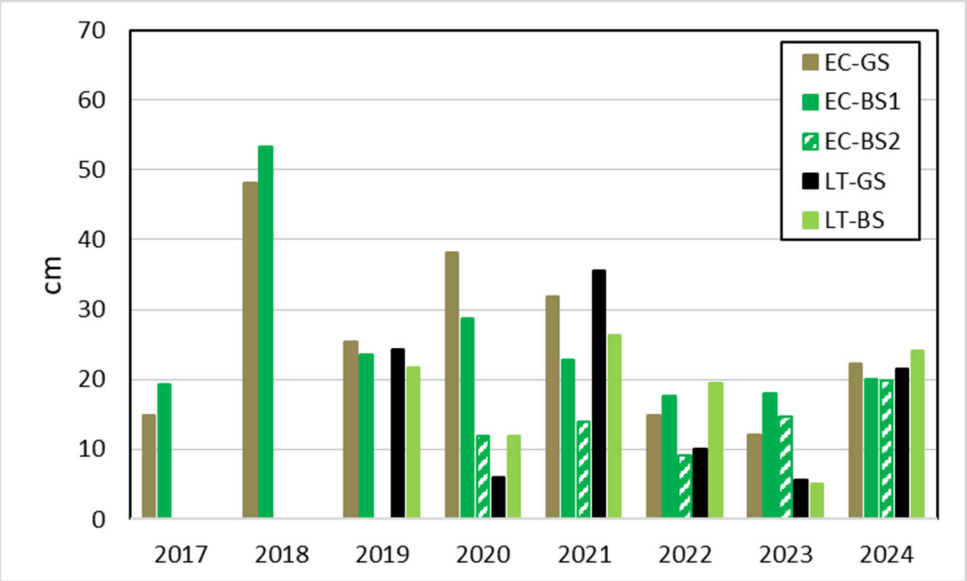

Figure 3. Seasonal (March–October) runoff from the EC and LT swales during the eight-year study. No data for EC-BS2 in 2017–2019 and partial data (August–October) in 2020; no data for LT-GS and LT-BS in 2017 or 2018.

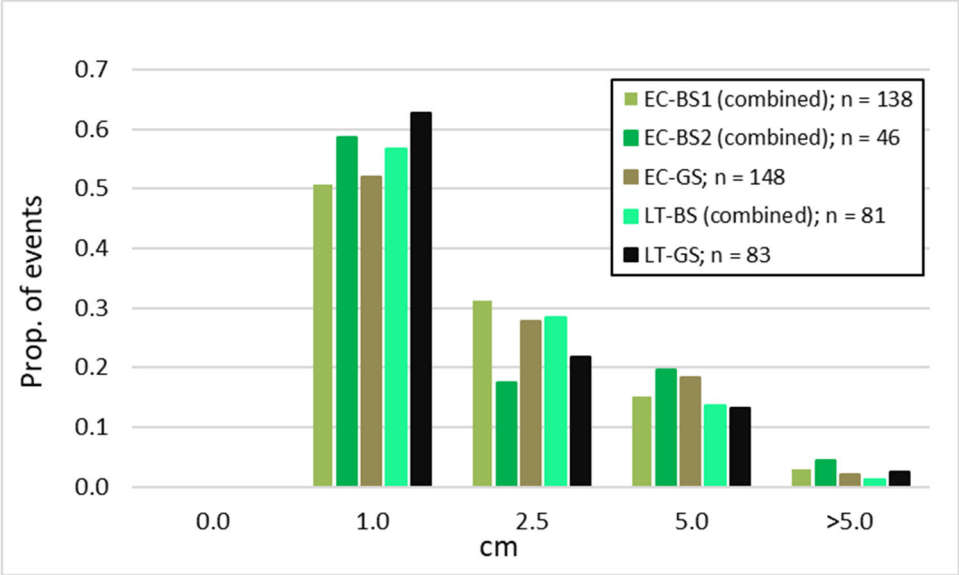

Figure 4. Proportion of runoff-producing events at each swale by event runoff depth.

EC-BS2 was highest in 2024 with above normal rainfall and lowest in 2022 with below normal rainfall. Similarly, at LT-GS and LT-BS, measured runoff was highest in the normal rainfall seasons of 2019, 2021, and 2024, and lowest during 2020, 2022, and 2023 (Figures 2, 3). Over the entire study, at least 70% of the seasonal runoff from each swale watershed could be attributed to those storm events that produced greater than 2.54 cm (1") of rainfall; the most extreme example was EC-BS2 where 93% of the runoff was due to such events (not shown).

Table 3. Statistical relationships between A) event runoff vs. event rainfall and 3-day antecedent rainfall; and B) peak runoff vs. maximum one-hour rainfall and 3-day antecedent rainfall for the five swale watersheds.

	Swales				
	EC-BS1	EC-BS2	EC-GS[1]	LT-BS	LT-GS
A) Event runoff (cm) vs. event rainfall (cm) and 3-day antecedent rainfall (cm)					
n	156	84	155	87	87
x-coef. (event rainfall)	0.74	0.71	0.53	0.72	0.84
x-coef. (3-day antecedent rainfall)	0.10	0.21	0.06	0.21	0.31
y-intercept	-0.71	-1.14	-0.26	-0.86	-1.37
Adjusted R^2	0.77	0.65	0.70	0.72	0.74
P (event rainfall)	<0.001	<0.001	<0.001	<0.001	<0.001
P (3-day rainfall)	<0.001	<0.001	<0.001	<0.001	<0.001
B) Peak (5-min) runoff (cm h^{-1}) vs. maximum 1-h rainfall (cm) and 3-day antecedent rainfall (cm)					
n	156	84	155	87	87
x-coef. (maximum 1-hr rainfall)	0.79	0.77	0.98	0.43	0.53
x-coef. (3-day antecedent rainfall)	0.06	0.08	0.04	0.04	0.07
y-intercept	-0.28	-0.35	-0.42	0.01	-0.15
Adjusted R^2	0.59	0.47	0.76	0.51	0.54
P (max. rainfall)	<0.001	<0.001	<0.001	<0.001	<0.001
P (3-day rainfall)	<0.001	0.08	0.03	0.16	0.02

[1]A small number of events at EC-GS and EC-BS lacked both on-site rainfall and NEXRAD Level III data, so we substituted data from the other paired site for these analyses

Table 4. Pair-wise comparisons of mean event runoff, event rainfall, peak runoff, and one-hour rainfall intensity for the three pairs of highway swales (EC-BS1 vs. EC-GS, EC-BS2 vs. EC- GS, LT-BS vs. LT-GS); results include data from prior project funded by MDOT-SHA (2017-2022). Paired results shown in bold italics are statistically significant (P < 0.05).

	Swale pairs					
	EC-BS1	EC-GS[1]	EC-BS2[2]	EC-GS[2]	LT-BS[3]	LT-GS[3]
A) All events						
Event runoff, cm	1.30	1.32	***0.83***	***1.18***	1.22	1.17
Event rainfall, cm	***2.50***	***2.81***	2.39	2.56	2.45	
Overland (flume) runoff, cm	***0.17***	***1.32***	***0.04***	***1.18***	***0.04***	***1.17***
Peak runoff, cm h^{-1}	***0.67***	***0.83***	***0.57***	***0.67***	0.57	0.57
Maximum one-hour rainfall intensity, cm h^{-1}	***1.09***	***1.22***	1.08	1.15	1.18	
No. of paired events	157		84		87	
B) Event subsets[4]						
Event runoff, cm	***0.47***	***0.60***	***0.10***	***0.51***	0.54	0.49
Event rainfall, cm	***1.41***	***1.52***	***1.32***	***1.47***	1.40	
Overland (flume) runoff, cm	***0.01***	***0.60***	***0.00***	***0.51***	***0.01***	***0.49***
Peak runoff, cm h^{-1}	***0.22***	***0.31***	***0.06***	***0.26***	0.41	0.36
Maximum one-hour rainfall intensity, cm h^{-1}	0.76	0.76	0.76	0.75	0.93	
No. of paired events	66		37		54	

[1]See text for estimation of rainfall for 2017-2019
[2]Data from mid-August 2020-October 2024
[3]Data from April 2019-October 2024
[4]Events with rainfall < 2.54 cm at both sites and rainfall C.V. < 0.40 (Ellicott City watersheds only)

Seasonal runoff yields showed considerable variability as well. EC-GS and EC-BS1 were the most similar in this respect, with the bioswale (EC-BS1) actually showing a slightly greater yield (0.37) than the grassed swale, EC-GS (0.34), despite receiving about 11% less runoff-producing rainfall during the study. The overall runoff yield for EC-BS2 (0.25) was appreciably lower. At Lewistown, the overall runoff yields were very similar, with LT-BS producing slightly (~5%) more runoff overall than LT-GS for the same precipitation. Aggregated runoff from all three bioswale watersheds was dominated by underdrainage. Measured underdrainage at EC-BS1, EC-BS2, and LT-BS contributed 87%, 95%, and 97% of the total runoff, respectively, demonstrating a

very high efficiency by which runoff from impervious highway surfaces was captured by the bioretention areas through the infiltration process. The slightly lower capture efficiency at EC-BS1 likely reflects at least in part the influence of above normal rainfall in 2018 when more than 1/3 of the overall flume runoff for the entire eight-year period (9.7 cm of 26.9 cm) occurred (Table 2).

Consistent with the results from HT, event rainfall and 3-day antecedent rainfall were the best predictors of event runoff ($0.65 < R^2 < 0.77$) at the five swales at EC and LT; statistically significant regression x-coefficients for the event rainfall variable varied only modestly (i.e., from 0.53 at EC-GS to 0.85 at LT-GS). Statistically significant x-coefficients for the antecedent rainfall variable ranged from 0.06 at EC-GS to 0.31 at LT-GS (Table 3). A majority of runoff-producing events at each swale produced less than 1.0 cm of runoff; depending on the swale, 17% to 31% of the events fell into the 1 cm < x $\leq$ 2.5 cm runoff range, while 13% to 20% of events produced 2.5 – 5.0 cm of runoff. Only 1 – 5% of the events exceeded 5.0 cm of runoff (Figure 4). At both EC-GS and EC-BS1, the event of record was the May 27, 2018 storm event that brought on a devastating flood in Old Ellicott City, MD. Event rainfall at EC-GS and EC-BS1 was estimated as 18.8 cm and 9.5 cm, respectively, while event runoff was measured as 8.0 cm and 7.3 cm, respectively (Table SI-2). At LT, the event of record was the September 1 – 2, 2021 event associated with the remnants of Tropical Storm Ida that delivered 12.8 cm of rainfall to LT-GS and LT-BS; event runoff was estimated as 12.8 cm and 9.4 cm, respectively (Table SI-3).

Our long-term datasets actually captured quite a few extreme events (defined here as events with 1-h rainfall exceeding the 1-yr average recurrence interval for the two sites (i.e., 2.97 cm at EC; 2.87 cm at LT; Bonnin et al. 2025). At EC-BS1, our data captured seven low-frequency events during the 8-yr project: two 2-yr storms; four 5-yr storms; and one 10-yr storm (the May 27, 2018 event). At EC-GS, the data captured eight low-frequency rainfall events: two 2-yr storms; two 5-year storms; two 10-yr storms; one 25-yr storm; and one 50-yr storm (the May 27, 2018 event). At LT, five low-frequency events occurred during the 6-year project: two 2-yr events; two 5-yr events; and one 25-yr event.

For the swale watershed pair with the longest data record (n = 157 events), there was no significant difference in mean event runoff between EC-GS (1.32 cm) and EC-BS1 (1.30 cm)—the latter based on the combination of overland and underdrain runoff; this result is somewhat misleading, however, as the mean event rainfall at EC-GS (2.81 cm) was about 12% higher than at EC-BS1 (2.50 cm). The difference in mean event runoff at EC-BS2 (0.83 cm) and EC-GS (1.18 cm) for the 2020-2024 period (n = 84 events) was statistically significant, but in this case, there was no difference in mean event rainfall (2.40 cm at EC-BS2, 2.56 cm at EC-GS) between the swale watersheds. A similar non-significant result was obtained for the LT swales with 87 characterized events (Table 4). Nineteen (12%) of the 157 events actually produced zero runoff at EC-BS1; the percentage was even higher at EC-BS2 (43%), but lower at LT-BS (8%). These "zero events" commonly occurred in mid-summer (i.e., July and August) with low antecedent rainfall amid high evapotranspirative demand.

While overland runoff was only a minor contributor to total runoff at all three bioswales (Table 2), it was often a major contributor during those events where it made a positive contribution.

For example, 46 of the 138 runoff-producing events at EC-BS1 produced measurable overland runoff (in addition to underdrainage) and, on average, 25% of the total runoff for these events was overland runoff. During one particular event (7/25/2018) that followed three events during the preceding four days, overland runoff contributed more than 85% of the total runoff; for five other events, overland runoff contributed more than 50% of the total runoff at EC-BS1. Comparable results were obtained for the other two bioswale watersheds (Tables SI-2, SI-3).

Differences in peak runoff were observed for all three pairs of swale watersheds. For the EC-BS1/EC-GS pair, we found that mean bioswale peak runoff (0.67 cm/h) was 19% lower than the corresponding grassed swale peak (0.83 cm/h); a similar result (14% difference) was observed for the other EC pair (0.57 cm h^{-1} at EC-BS2 vs. 0.67 cm/h at EC-GS). Mean peak runoff at the LT swales were identical (0.57 cm h^{-1}; Table 4). At the EC and LT swales, maximum 1-hr rainfall and 3-day antecedent rainfall were the best predictors of peak runoff ($0.47 < R^2 < 0.76$); regression x-coefficients for the 1-hr rainfall variable (all statistically significant) ranged from 0.43 at LT-BS to 0.98 at EC-GS; at several of the swale watersheds (EC-BS1, EC-GS, and LT-BS), 3-day antecedent rainfall (providing an index of antecedent soil moisture) was also a statistically significant predictor of peak runoff. At EC, the mean maximum rainfall intensity was significantly (10%) lower at EC-BS1 (1.09 cm h^{-1}) than at EC-GS (1.22 cm h^{-1}), directionally consistent with the observed difference (19%) in mean peak runoff between the swales (Table 4). The relatively higher mean peak runoff values observed at both LT swales (0.41, 0.36 cm h^{-1}) in the < 2.54 cm subset are consistent with the higher mean 1-hr rainfall at LT (0.93 cm h^{-1}) compared to EC (0.76 cm h^{-1}). The timing of event runoff is another indicator of attenuation, but the difference in the centroid of runoff for bioswale/grassed swale pairs for common events (all with low rainfall C.V.) were not significant (results not shown)

Given the goal of providing statistically valid comparisons of bioswale and grassed swale responses independent of hydro-climatological differences, paired events at EC were stratified using rainfall variation and swale design criteria; in particular, we focused solely on those events where the coefficient of variation (CV) in event rainfall was less than 0.40 and event rainfall at both paired swale watersheds (EC swales only) was less than 2.54 cm (1.0 in). For the EC-BS1/EC-GS comparison, this stratification produced a sample size of 66 events; for this subset, we observed a 21% reduction in mean event runoff at EC-BS1 (0.47 cm) compared to EC-GS (0.60 cm), despite the fact that mean event rainfall was only 7% lower (1.41 cm at EC-BS1 vs. 1.52 cm at EC-GS). For the EC-BS2 vs. EC-GS comparison, the smaller subset (n = 37 events) produced an even greater runoff reduction of 80% with a rainfall difference of 10%. Using the same approach to address peak runoff differences, we observed 29% and 78% reductions at EC-BS1 and EC-BS2, respectively, compared against EC-GS; no differences in maximum hourly rainfall intensity were observed for either comparison. At LT, a similar stratification focused on the subset of events (n = 54) with rainfall < 2.54 cm showed no differences in mean event runoff or peak runoff between the two swales (Table 4).

Among the 13 primary water quality pollutants of concern (i.e., N and P-containing contaminants and TSS), unpaired comparisons of flume and underdrain mean EMC'S computed for the three bioswales produced at least one statistically significant result for 11 of them; only NH_4-N and particulate-N EMCs showed no differences. Analyses of EMCs for five of the 13

Table 5. Flume and underdrain discharge-weighted event mean concentrations for the three bioswales in the study; numbers of runoff events characterized are shown in the column headings. Differences shown in bold are statistically significant (unpaired t-tests; $P < 0.05$).

Constituent (units*)	Swale					
	EC-BS1 Flume (n = 18)	EC-BS1 UD (n = 48)	EC-BS2 Flume (n = 8)	EC-BS2 UD (n = 21)	LT-BS Flume (n = 13)	LT-BS UD (n = 36)
Spec. cond. ($\mu S\ cm^{-1}$)	**110**	**370**	**94**	**300**	**140**	**410**
TSS	18	11	26	28	48	24
ANC ($meq\ L^{-1}$)	**0.55**	**1.9**	**0.64**	**1.4**	**0.65**	**1.8**
Chloride	**13**	**49**	**6.6**	**33**	**26**	**67**
Sulfate	**1.2**	**8.3**	**1.4**	**11**	**1.1**	**6.2**
Ortho-P	**0.27**	**0.06**	**0.53**	**0.24**	0.19	0.16
NH_4-N	0.07	0.03	0.07	0.08	0.04	0.04
NO_2-N	0.011	0.014	**0.011**	**0.018**	0.010	0.019
NO_3-N	**0.09**	**1.0**	**0.12**	**2.4**	**0.11**	**1.2**
DON	**0.72**	**1.6**	**0.66**	**1.9**	**0.50**	**1.1**
TP	**0.41**	**0.18**	**0.67**	**0.44**	0.33	0.26
TDP	**0.31**	**0.13**	**0.56**	**0.34**	0.21	0.20
SOC-P	**0.04**	**0.07**	**0.03**	**0.09**	**0.02**	**0.04**
TN	**1.36**	**3.00**	**1.33**	**4.96**	**1.10**	**2.67**
TDN	**0.89**	**2.7**	**0.85**	**4.4**	**0.65**	**2.4**
Particulate-N	0.47	0.36	0.48	0.56	0.45	0.26
Particulate-P	**0.10**	**0.05**	0.11	0.10	**0.12**	**0.07**
DOC	**11**	**24**	**9.9**	**24**	**7.3**	**16**
Na	**18**	**70**	**22**	**59**	**31**	**77**
K	**4.1**	**2.8**	7.0	5.7	1.3	1.0
Mg	**0.45**	**1.3**	**0.70**	**1.2**	**0.40**	**1.2**
Ca	**1.7**	**13**	**1.8**	**8.9**	**2.2**	**14**
Cr ($\mu g\ L^{-1}$)	**0.41**	**1.1**	1.4	1.0	1.3	0.92
Cu ($\mu g\ L^{-1}$)	**4.5**	**59**	**3.0**	**57**	**3.8**	**6.4**
Zn ($\mu g\ L^{-1}$)	**22**	**98**	**3.6**	**83**	12	20
Cd ($\mu g\ L^{-1}$)	**0.03**	**0.14**	**0.02**	**0.08**	0.06	0.05
Pb ($\mu g\ L^{-1}$)	**0.30**	**1.8**	**0.16**	**0.53**	2.3	0.52

*$mg\ L^{-1}$ unless noted otherwise

constituents (NO_3-N, DON, TN, TDN, and SOC-P) showed robust, statistically significant differences for all three swale pairs. Four other constituents (PO_4-P, TP, TDP, and particulate-P) were statistically significant at two of the three bioswale watersheds. TSS EMCs were only significantly different at EC-BS2 where the underdrainage actually had the higher concentration. For the N and P pollutants, a consistent pattern emerged in which EMCs for the

Table 6. Bioswale and grassed swale discharge-weighted event mean concentrations for the three bioswales and two paired grassed swales in the study; bioswale runoff is combined underdrain and flume. Differences shown in bold are statistically significant (paired t-tests; $P < 0.05$).

Constituent (units*)	Swale					
	EC-BS1	EC-GS	EC-BS2	EC-GS	LT-BS	LT-GS
	(n = 43[1])		(n = 20)		(n = 34)	
Spec. cond. (µS/cm)	330	300	270	220	**410**	**320**
TSS	13	11	**26**	**11**	26	27
ANC (meq L^{-1})	**1.8**	**1.4**	1.3	1.2	**1.8**	**1.0**
Chloride	41	44	28	29	68	60
Sulfate	**7.4**	**3.9**	**9.6**	**2.6**	5.9	4.8
Ortho-P	**0.07**	**0.53**	**0.24**	**0.38**	**0.16**	**0.43**
NH_4-N	**0.03**	**0.13**	0.08	0.10	0.04	0.05
NO_2-N	**0.01**	**0.02**	0.02	0.02	0.02	0.03
NO_3-N	**0.975**	**0.314**	**2.30**	**0.331**	**1.12**	**0.204**
DON	1.5	1.5	**1.6**	**1.1**	1.1	1.1
TP	**0.19**	**0.68**	0.41	0.50	**0.27**	**0.58**
TDP	**0.14**	**0.59**	0.31	0.42	**0.20**	**0.47**
SOC-P	0.07	0.06	0.07	0.05	0.04	0.04
TN	**2.9**	**2.4**	**4.5**	**2.0**	**2.5**	**1.9**
TDN	**2.6**	**2.0**	**4.0**	**1.6**	**2.3**	**1.4**
Particulate-N	0.37	0.42	0.55	0.44	**0.27**	**0.50**
Particulate-P	**0.05**	**0.09**	0.10	0.08	**0.07**	**0.11**
DOC	**23**	**18**	**21**	**13**	16	16
Na	**63**	**52**	48	36	**78**	**63**
K	**2.9**	**6.5**	5.5	5.6	**1.0**	**2.4**
Mg	1.2	1.2	1.3	1.0	1.2	1.2
Ca	**12**	**8.9**	9.3	7.2	**13**	**8.0**
Cr (µg L^{-1})	**1.1**	**0.79**	**0.86**	**0.56**	0.95	0.88
Cu (µg L^{-1})	**57**	**8.9**	**48**	**6.9**	**6.4**	**4.6**
Zn (µg L^{-1})	**91**	**17**	**83**	**7.9**	**20**	**6.8**
Cd (µg L^{-1})	**0.14**	**0.06**	**0.07**	**0.05**	**0.05**	**0.03**
Pb (µg L^{-1})	**1.7**	**0.82**	**0.45**	**0.57**	0.58	0.64

[1]n = 41 events for ANC and DOC
*mg L^{-1} unless noted otherwise

N-containing pollutants were higher in the underdrainage than in the flume discharge, while the opposite result was found for the P-containing contaminants. The only exception to this pattern was SOC-P in which higher mean concentrations were observed in the underdrainage. Computed mean EMCs for specific conductance, ANC, Cl, SO_4, Na, Mg, Ca, and Cu each produced significant differences for all three bioswales, with higher concentrations observed in

Table 7. Bioswale and grassed swale mean event loads for the three bioswales and two paired grassed swales in the study; bioswale runoff is combined underdrain and flume. Differences shown in bold are statistically significant (paired t-tests; P < 0.05).

Constituent (units*)	Swale					
	EC-BS1	EC-GS	EC-BS2	EC-GS	LT-BS[2]	LT-GS
	(n = 43[1])		(n = 20)		(n = 34)	
Spec. cond. (S ha^{-1})	56	50	39	49	**64**	**49**
TSS	2.6	2.2	4.3	2.2	4.4	4.8
ANC (keq ha^{-1})	0.31	0.26	0.23	0.27	**0.32**	**0.20**
Chloride	6.6	6.6	2.8	6.2	9.8	8.7
Sulfate	**1.2**	**0.64**	**1.3**	**0.62**	0.83	0.58
Ortho-P	**0.017**	**0.085**	**0.053**	**0.088**	**0.025**	**0.055**
NH_4-N	**0.0058**	**0.021**	**0.0093**	**0.019**	0.0055	0.0064
NO_2-N	**0.0022**	**0.0047**	0.0023	0.0039	0.0022	0.0024
NO_3-N	**0.18**	**0.062**	**0.39**	**0.076**	**0.16**	**0.018**
DON	0.25	0.26	0.26	0.25	0.17	0.16
TP	**0.038**	**0.11**	0.081	0.12	**0.042**	**0.077**
TDP	**0.028**	**0.094**	0.065	0.098	**0.031**	**0.060**
SOC-P	0.011	0.0097	0.012	0.0095	0.0064	0.0059
TN	0.49	0.43	0.75	0.45	**0.37**	**0.26**
TDN	0.44	0.35	0.65	0.36	**0.33**	**0.19**
Particulate-N	0.060	0.085	0.097	0.098	**0.041**	**0.073**
Particulate-P	**0.010**	**0.016**	0.016	0.017	**0.011**	**0.017**
DOC	3.7	3.1	3.5	3.0	2.5	2.3
Na	10	8.8	7.6	8.0	12	10
K	**0.54**	**1.2**	1.0	1.4	**0.16**	**0.32**
Mg	0.23	0.23	0.22	0.25	0.19	0.18
Ca	2.1	1.7	1.5	1.7	**2.2**	**1.2**
Cr (g ha^{-1})	0.17	0.17	0.14	0.14	0.16	0.12
Cu (g ha^{-1})	**9.3**	**1.6**	**7.5**	**1.6**	**0.98**	**0.62**
Zn (g ha^{-1})	**17**	**3.7**	**14**	**1.8**	**2.9**	**0.92**
Cd (g ha^{-1})	**0.022**	**0.014**	0.010	0.011	**0.0082**	**0.0045**
Pb (g ha^{-1})	**0.27**	**0.16**	**0.072**	**0.14**	0.097	0.093

[1]n = 41 events for ANC and DOC

[2]Computed loads adjusted using a watershed area of 1.1 ha (see text for rationale)

*kg ha^{-1} unless noted otherwise

the underdrainage—suggesting that the bioretention areas may provide sources of these constituents (Table 5).

Similar patterns emerged when comparing runoff-weighted combined (flume and underdrain) bioswale EMCs with grassed swale EMCs, albeit with fewer statistically-significant differences. For the N-containing pollutants, only three constituents (NO_3-N, TN, TDN) produced consistent differences for all the three pairs; in each case, the higher concentration was observed in the

Table 8. Results from the synoptic stormwater surveys conducted at EC in 2023/2024. Differences shown in bold italics are statistically significant (t-test; P < 0.10).

Constituent (units)	Bioswales (n = 26)	Grassed swales (n = 34)
Spec. cond. (µS)	280	230
TSS	***9.3***	***18***
ANC (meq L^{-1})	***1.4***	***1.2***
Chloride	38	32
Sulfate	**3.1**	**1.4**
Ortho-P	***0.13***	***0.18***
NH_4-N	0.027	0.031
NO_2-N	0.007	0.007
NO_3-N	***0.34***	***0.022***
DON	0.85	0.76
TP	***0.21***	***0.28***
TDP	0.17	0.20
SOC-P	0.034	0.028
TN	1.38	1.14
TDN	***1.22***	***0.82***
Particulate-N	***0.16***	***0.33***
Particulate-P	***0.040***	***0.075***
DOC	12	9.9
Na	53	44
K	***2.7***	***1.8***
Mg	***0.95***	***0.72***
Ca	***8.2***	***6.0***
Cr (µg L^{-1})	0.59	0.77
Cu (µg L^{-1})	***27***	***4.9***
Zn (µg L^{-1})	***34***	***6.6***
Cd (µg L^{-1})	***0.048***	***0.024***
Pb (µg L^{-1})	0.36	0.35

*mg L^{-1} unless noted otherwise

combined bioswale runoff. For P, only the behavior of PO_4-P was consistent across all three pairs, with significantly lower mean concentrations observed in bioswale runoff. For two of the pairs, however, mean EMCs of TP, TDP, and particulate-P were also significantly lower in bioswale runoff. No differences in mean EMCs of TSS were found. Among the group of ancillary constituents, only a few displayed consistent variations among the swales; Cu, Zn, and Pb mean EMCs were all significantly higher in combined runoff from the three bioswales—another possible indicator of source behavior. Two constituents (Cl, Mg) showed no differences among any of the pairs (Table 6).

Analysis of event loads (computed from event runoff and EMCs of pollutants and other water quality constituents) showed even fewer statistically significant differences. Mean event NO_3-N loads for EC-BS1, EC-BS2, and LT-BS were higher than loads from the corresponding grassed swale controls by 190%, 410%, and 790%, respectively. Mean PO_4-P loads were significantly lower at all three bioswales by 80%, 40%, and 55%, respectively. No TSS load differences were found. Comparisons of mean event loads for two ancillary constituents (Cu, Zn) also produced significant results for all three swale pairs, with the bioswales consistently producing the higher loads (typically by at least 200%). For quite a few of the constituents (i.e., Cl, Na, Mg, DON, SOC-P, DOC, and Cr), non-significant event load differences were consistent among all three swale pairs. In particular, the lack of differences in the Na and Cl loads provides strong evidence that the swale water balances have been accurately quantified, since Na and Cl inputs from road salting are likely very similar in magnitude and neither element has an obvious sink or additional source within the watershed (Table 7). For many of the constituents (e.g., TP, ortho-P, TN, TSS), event runoff was a strong predictor of event load for all five swale watersheds; for NO_3-N, however, event runoff was only a significant predictor of event load for the three bioswale watersheds, but not for the two grassed swales (results not shown).

Assuming equivalent inputs of Cl onto each swale watershed pair, the event load data for Cl can be used to address uncertainties in the swale water balances. For the EC-BS1/EC-GS pair with the longest record, mean event Cl loads (6.6 kg ha^{-1}) were identical, providing more support for the notion that all major Cl outflows from these watersheds have been accurately quantified (and watersheds properly delineated). A similar result was obtained for the LT swales where the mean event Cl load from LT-BS (9.8 kg ha^{-1}) was not significantly different from the mean Cl load from LT-GS (8.7 kg ha^{-1}). For the EC-BS2/EC-GS pair with a much shorter record, the difference in mean Cl loads—while not statistically significant—suggests the possibility of an additional Cl outflow from EC-BS2 (Table 7) consistent with the significant difference in mean event runoff (Table 2).

Statistically significant ($P < 0.10$) differences in mean concentrations were found for 15 of the 27 constituents measured during the synoptic water quality surveys. The mean nitrate-N concentration in runoff from the bioswale underdrains (0.34 mg L^{-1}) was higher than in overland runoff from the grassed swales, while mean PO_4-P (0.13 mg L^{-1}), particulate-P (0.04 mg L^{-1}), and TP (0.21 mg L^{-1}) concentrations were all lower—consistent with data from the paired watersheds. The mean TSS concentration in grassed swale runoff (18 mg L^{-1}) was higher than in underdrain runoff—a result that was different from the paired swale results presented earlier. ANC, sulfate, Ca, Mg, and K were all higher in underdrain runoff, while Cl concentrations were not. For the trace metals, Cu, Zn and Cd showed higher underdrain concentrations consistent with the paired swale results (Table 8).

Discussion

Results from this long-term study of the hydrologic and water quality responses of highway bioswale and grassed swale watersheds in Maryland revealed both consistent and inconsistent

differences that require further analysis before any firm conclusions regarding the relative effectiveness of these different types of green stormwater infrastructure can be drawn. A simple conceptual model of a highway bioswale watershed is a "grassed swale watershed in which a bioretention cell with the capacity of conveying water to a stormwater inlet through both overland and subsurface (i.e., underdrain) pathways" has been added. This model really isn't strictly "conceptual", however, since in many cases (i.e., along existing highways in Maryland) bioswales were actually constructed by retrofitting existing grassed swales. Since a primary goal of the bioswales is to increase infiltration in order to reduce infiltration-excess overland flow, the most important and consistent hydrologic results from the study are: 1) the significantly higher steady-state infiltration capacity of the biosoils relative to the other soils in the highway medians; and 2) the impressive reduction in overland runoff (relative to the grassed swale control) resulting from the inclusion of a sized bioretention area and underdrain in each bioswale watershed.

The measured saturated hydraulic conductivity (*K*) of the median and grassed swale soils at the three sites (Figure 1) fall into the range of either Hydrologic Soil Group A (HT: $K > 144$ mm h^{-1}) with low runoff potential or B (ES and LT: $36 < K \leq 144$ mm h^{-1}) with moderately low runoff potential (USDA 2009). All of the mean biosoil *K* values greatly exceed the 144 mm h^{-1} threshold by factors of 4.4 (EC), 7.4 (LT), and 11.3 (HT)—indicating that these soils should probably be classified as having *extremely* low runoff potential and are *excessively well-drained*. Claytor and Schueler (1996) suggested a minimum *K* value for biosoil of 12.5 mm h^{-1}; while Le Coustemer et al. (2009) reported on *K* values (mean = 95 ± 40 mm h^{-1}) from field infiltrometer measurements at 37 biofilter sites in Australia. Interestingly, *K* values for our median and grassed swale soils at EC and LT fall into this range for biofilters, while the mean biosoil *K* values at our three sites all three sites (569 – 1533 mm h^{-1}) greatly exceed this range (Figure 1). Our mean *K* value for the HT grassed swale (259 mm h^{-1}) agrees with a value recently reported for a bioswale in Norway (259 mm h^{-1}; Monrabal-Martinez et al. 2018). Le Coustumer et al. (2009) hinted at the existence of a "hydraulic sweet-spot" such that biosoils should drain quickly, but not too quickly, in order to provide sufficient time for chemical interactions to take place, thus facilitating a role in pollutant retention. While an argument can certainly be made that if the soils do not drain rapidly enough, overland runoff is produced and a considerable portion of the runoff would be effectively discharged "untreated", it is clear that MDOT-SHA bioswales provide for much more rapid drainage than what others have recommended.

The extremely high drainage efficiency of the MDOT-SHA biosoils predicted by our infiltration measurements is confirmed by the very small amounts of flume runoff (R_F) produced by the bioswales and, conversely, by the extremely high percentage reductions (87 - 96%) in overland runoff observed in the study. Moreover, assuming that R_F is the only stormwater not "captured and treated", the data presented in Table 2 can be used to directly compute the percentage of rainfall (*P*) that was "captured and treated" (PRCT) by each of the five bioswales (i.e., $PRCT = 100(P - R_F)/P$). At Hagerstown, where no flume runoff was measured (i.e., $R_F = 0$), PRCT values for HT-BS1 and HT-BS2 are both 100%. At EC-BS1, EC-BS2, and LT-BS, PRCT values are 95%, 99%, and 99%, respectively. While our "seasonal" (April – October) results are not directly applicable to an entire year, it is very likely that the specific stormwater management goal of

"capturing and treating" at least 90% of the annual rainfall is being consistently achieved by the specific bioswale design employed by MDOT-SHA. The effectiveness of the actual "treatment" is discussed later using the water quality data.

Evidence for significant reductions in runoff volume by the bioswales (relative to the paired grassed swales) was less consistent among the paired swale watersheds. Results from the EC-BS1/EC-GS pair with the longest data record (157 events over eight years) are perhaps the most straightforward to interpret in this regard, given the general similarity of the aggregated seasonal hydrologic responses and event-based runoff metrics. First of all, we found that the computed runoff yields (0.34, 0.37; Table 2) from these watersheds were not only quite similar, but they were both quite close to the long-term mean runoff yield (0.365) for the Little Patuxent River at Guilford, MD watershed gaged by USGS and computed for the same eight-month monitoring period. Second, the identical mean event Cl loads (6.6 kg/ha) computed for these watersheds provides additional evidence that the computed hydrologic fluxes are essentially correct. While modest differences in total rainfall and event rainfall were complicating factors for this particular swale pair, the reduction in overland runoff (1.808 m) at EC-BS1 relative to EC-GS was merely translated into underdrain runoff (1.766 m) of nearly the same magnitude. The result of this "translation" is that, to a first approximation, there was no significant overall reduction in runoff volume at EC-BS1; thus, mean event runoff from these watersheds were nearly identical (1.30 cm, 1.32 cm; Table 3A). This interpretation should be tempered, however, given the fact that the subset of events with lower (i.e., < 2.54 cm) rainfall and less rainfall variability showed a statistically significant (22%) runoff volume reduction in the bioswale watershed (Table 3B).

Data from the EC-BS2/EC-GS pair provide stronger evidence for substantial runoff volume reduction. In this case, not only is the decrease in seasonal overland runoff (0.96 m) greater than the increase in underdrain runoff at EC-BS2 (0.66 m; Table 2), but the event-based analysis showed a statistically-significant difference (30%) in runoff as well (Table 3A). As in the case of the EC-BS1/EC-GS pair, exclusion of events with greater rainfall (and greater rainfall variability) produced an even higher mean volume reduction (80%). Finally, while EMCs of Cl were nearly identical (28, 29 mg L^{-1}; Table 5), results from the Cl load analysis would appear to allow for an additional runoff pathway from EC-BS2 while maintaining comparable Cl total loads—assuming that the Cl concentration in this additional pathway was similar to the measured EMCs. The most logical pathway would be downward percolation of water (and Cl) below the EC-BS2 underdrain (i.e., local groundwater recharge). In fact, if the underdrain runoff from every event at EC-BS2 were increased by 50% to include this percolation pathway while maintaining the underdrainage EMC for each of the 20 events at the original value, the mean Cl load—including both pathways—would increase from 2.8 kg ha^{-1} to 4.2 kg ha^{-1} and the paired difference with EC-GS would still not be statistically significant. In other words, Cl would still be considered roughly in balance, with the additional pathway (representing recharge of about 0.66 m in 34 mo) providing a mechanistic explanation for the lower runoff yield at EC-BS2 (Table 2).

Table 9. Sensitivity of peak runoff from a bioswale watershed (EC-BS1) to possible future increases in maximum 1-hr rainfall and 3-day antecedent rainfall based on regression results presented in Table 3. Three scenarios are explored (see descriptions below).

	Average Recurrence Interval (yr)					
	1	2	5	10	25	50
A) Base case						
1) Current median 3-day rainfall (cm)	0.61	0.61	0.61	0.61	0.61	0.61
2) Current 1-hr rainfall (cm)	2.97	3.63	4.57	5.28	6.25	6.99
3) EC-BS1 peak runoff (cm h^{-1})	2.09	2.61	3.35	3.91	4.67	5.24
B) Scenario #1: Increase median 3-day rainfall by 10%						
1) Future median 3-day rainfall (cm)	0.67	0.67	0.67	0.67	0.67	0.67
2) Future 1-hr rainfall (cm)	2.97	3.63	4.57	5.28	6.25	6.99
3) Future EC-BS1 peak runoff (cm h^{-1})	2.10	2.62	3.35	3.91	4.67	5.25
4) Change from base case (%)	0.18	0.15	0.12	0.10	0.08	0.07
C) Scenario #2: Increase 1-hr rainfall by 10%						
1) Future median 3-day rainfall (cm)	0.61	0.61	0.61	0.61	0.61	0.61
2) Future 1-hr rainfall (cm)	3.27	4.00	5.03	5.81	6.87	7.68
3) Future EC-BS1 peak runoff (cm h^{-1})	2.33	2.90	3.71	4.32	5.16	5.79
4) Change from base case (%)	11.1	10.9	10.7	10.6	10.5	10.5
D) Scenario #3: Increase 1-hr rainfall and 1-hr rainfall by 10%						
1) Future median 3-day rainfall (cm)	0.67	0.67	0.67	0.67	0.67	0.67
2) Future 1-hr rainfall (cm)	3.27	4.00	5.03	5.81	6.87	7.68
3) Future EC-BS1 peak runoff (cm h^{-1})	2.33	2.90	3.71	4.33	5.16	5.80
4) Change from base case (%)	11.3	11.1	10.8	10.7	10.6	10.5

An alternative explanation for the difference in yields between the three Ellicott City swales is spatiotemporal variability in evapotranspiration (ET). While ESD practices generally promote both infiltration and ET (Li et al. 2009; Hunt et al. 2010; Jarden et al. 2016), invoking

Table 10. Sensitivity of peak runoff from a grassed swale watershed (EC-GS) to possible future increases in maximum 1-hr rainfall and 3-day antecedent rainfall based on regression results presented in Table 3. Three scenarios are explored (see descriptions below).

	Average Recurrence Interval (yr)					
	1	2	5	10	25	50
A) Base case						
1) Current median 3-day rainfall (cm)	0.61	0.61	0.61	0.61	0.61	0.61
2) Current 1-hr rainfall (cm)	2.97	3.63	4.57	5.28	6.25	6.99
3) EC-GS peak runoff (cm h^{-1})	2.51	3.16	4.08	4.77	5.72	6.44
B) Scenario #1: Increase median 3-day rainfall by 10%						
1) Future median 3-day rainfall (cm)	0.67	0.67	0.67	0.67	0.67	0.67
2) Future 1-hr rainfall (cm)	2.97	3.63	4.57	5.28	6.25	6.99
3) Future EC-GS peak runoff (cm h^{-1})	2.52	3.16	4.08	4.78	5.72	6.44
4) Change from base case (%)	0.10	0.08	0.06	0.05	0.04	0.04
C) Scenario #2: Increase 1-hr rainfall by 10%						
1) Future median 3-day rainfall (cm)	0.61	0.61	0.61	0.61	0.61	0.61
2) Future 1-hr rainfall (cm)	3.27	4.00	5.03	5.81	6.87	7.68
3) Future EC-GS peak runoff (cm h^{-1})	2.80	3.51	4.53	5.29	6.33	7.12
4) Change from base case (%)	11.6	11.2	11.0	10.8	10.7	10.6
D) Scenario #3: Increase 1-hr rainfall and 1-hr rainfall by 10%						
1) Future median 3-day rainfall (cm)	0.67	0.67	0.67	0.67	0.67	0.67
2) Future 1-hr rainfall (cm)	3.27	4.00	5.03	5.81	6.87	7.68
3) Future EC-GS peak runoff (cm h^{-1})	2.81	3.52	4.53	5.29	6.33	7.12
4) Change from base case (%)	11.7	11.3	11.0	10.9	10.7	10.6

dramatically higher ET at EC-BS2 is physically unrealistic given very similar vegetation, imperviousness, and hydroclimatological conditions at the other two EC swales (especially EC-BS1). The presence of a well-drained bioretention cell would be expected to reduce—not increase—ET, at least for the small portion of the watershed occupied by the cell (Table 1). Moreover, higher ET at EC-BS2 would necessitate a substantially higher EMC of Cl in EC-BS2

runoff than the concentration that was actually observed (28 mg L^{-1}; Table 5) in order to produce the same mean Cl load of 2.8 kg ha^{-1} (Table 6).

The groundwater recharge mechanism is also likely contributing to the observed peak runoff attenuation at EC-BS2 (relative to EC-GS) that is particularly evident in the < 2.54 cm event rainfall subset (Table 3B). Assessing this mechanism requires a more complex model that incorporates the interaction of the bioretention cell with the surrounding hydrogeological environment, however. It is worth noting that the EC-BS2 swale was constructed on highway fill materials, such that the local groundwater table is likely several meters below the level of the swales—thus providing a natural downward hydraulic gradient between transiently-saturated media surrounding the swale underdrain and the underlying (unsaturated) fill materials. Invoking a Darcian hydrogeological mechanism, the other key factor to be considered is the permeability of the underlying fill materials; all else being equal, the higher the permeability of those materials, the greater the expected overall rate (and volume) of percolation through the substrates underlying the bioswale to the water table. Since EC-BS1 was constructed to the same specifications as EC-BS2 and is also located on another section of highway fill, it is not clear why the same phenomenon does not appear to be important in that watershed as well.

It is interesting that none of the results from LT provide any support whatsoever for runoff reduction or peak runoff attenuation by the LT-BS bioswale—even when confining the analysis to the < 2.54 cm event rainfall subset (Table 3). The most obvious explanation is that unlike the EC swales where imperviousness was somewhat greater in the grassed swale watershed (EC-GS) than in the bioswales (EC-BS1, EC-BS2), the opposite is true at LT: imperviousness at LT-BS (63%) is more than a factor of two greater than at LT-GS (24%; Table 1). Based on these observations, it must be conceded that the differences in imperviousness among the individual swale watersheds may be more important hydrologically than was assumed *a priori*.

If we assume that greater imperviousness produces greater runoff volumes and higher runoff peaks in highway swale watersheds regardless of whether a bioretention is in place, then we would predict that the differences in stormflow responses between bioswale and grassed swale watersheds with the same amount of imperviousness would be somewhat smaller than the differences shown by the EC watersheds. Considering all runoff-producing events, it is therefore unlikely that mean percent runoff volume and peak runoff reduction by highway bioswales in Maryland exceeds 10% (relative to grassed swales with the same imperviousness), although the data indicate that percentages increase when only smaller storm events are considered (Table 3).

The strong predictive relationships between peak runoff and maximum rainfall intensity and antecedent rainfall for the swale watersheds provide an opportunity for exploring the sensitivity of runoff from these systems to future hydro-climatic changes (i.e., increasing rainfall/rainfall intensity). We used current point precipitation frequency estimates of 1-hr rainfall for the sites to explore three different scenarios: 1) scenario #1: 3-day antecedent rainfall is increased by 10% from the present median value; 2) scenario #2: maximum 1-hr rainfall is increased by 10%; and 3) scenario #3: both 3-day antecedent rainfall and maximum

1-hr rainfall are increased by 10%. We evaluated these scenarios using data from EC-BS1 and EC-GS (for both swales, 1-hr rainfall and 3-day antecedent rainfall were statistically significant predictors of peak runoff; Table 3). The results clearly showed that future peak runoff is nearly insensitive to a 10% increase in antecedent rainfall: at both sites, the increase in runoff was less than 0.2%. Future peak runoff is highly sensitive to increasing rainfall intensity, however, with increases ranging from 10 – 12% (depending slightly on the swale, the specific scenario, and the average recurrence interval; Tables 9, 10).

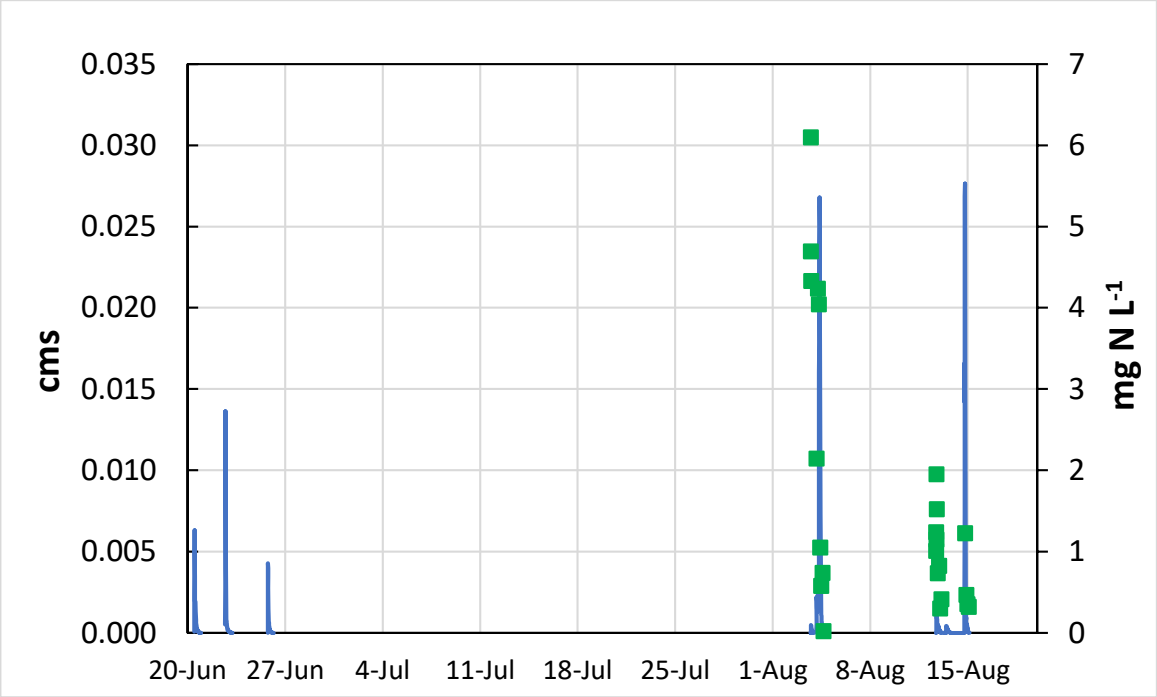

Figure 5. Measured underdrain discharge (cms = m^3 s^{-1}) and nitrate-N concentrations (mg N L^{-1}) at EC-BS1 during early summer 2020.

Results from both the intensive and synoptic water chemistry monitoring showed that highway bioswales can have significant influences on concentrations and loads of many pollutants and other water quality constituents as has been demonstrated for ESD/LID practices in general (Bäckström 2003; Bedan and Clausen 2009; Davis et al. 2009; Stagge et al. 2012; Shetty et al. 2018; Burgis et al. 2020; Smith et al. 2023). Since our bioswale results were made relative to the paired grassed swales, we attribute the differences primarily to the performance of the bioretention cells, including the underdrain systems. Many other studies have focused on the potential water quality benefits associated with bioretention systems (see interpretive summaries by Ekka et al. 2021 and Vijayaraghavan et al. 2021), including both mesocosms (Hsieh and Davis 2005; Blecken et al. 2010) and field-scale (Davis 2008; Brown and Hunt, 2011; Burgis et al. 2020) research. While experimental results have been mixed and dependent upon the design of the bioretention cells (including depth of engineered media, media properties, presence of internal water storage zone, etc.), the specific pollutant(s) being analyzed, and the time over which performance has been assessed, the emerging consensus is that bioretention

has the potential to 1) control stormwater N loads through denitrification where anaerobic conditions can be created using an internal water storage (IWS) zone; and 2) control P loads through the process of chemisorption of orthophosphate-P onto Fe- and Al-oxides present in the engineered biosoil (Ekka et al. 2021).

Our results are very consistent with the emerging consensus. In the case of N, the lack of an IWS zone in the highway bioswales appears to have greatly limited the role of denitrification in reducing nitrate-N loads from the highway bioswale watersheds. The majority of the nitrate-N in the bioswale ouflow appears to have been generated through mineralization of soil N and subsequent nitrification within the aerobic biosoil itself. The frequent percolation of water through the biosoil provided a rapid and efficient means of extracting and transporting the accumulated nitrate-N—a mobile, negatively-charged, and highly soluble form of N to the underdrain where, in the absence of an IWS, it was routed directly to the downstream stormwater inlet. The progressive flushing or leaching of accumulated nitrate-N (including atmospheric N deposited during the antecedent period) from the bioswales can be clearly observed in the underdrainage data.

As an example, data for EC-BS1 during the summer of 2020 reveals the occurrence of a long droughty period from the end of June through the beginning of August; no runoff from the bioswale watershed occurred during this period. On the afternoon of August 3rd, a 1.4 cm rainstorm produced 0.05 cm of underdrain runoff and the nitrate-N concentrations (4 – 6 mg N L^{-1}) were among the highest ever recorded at this swale due ostensibly to the flushing of accumulated nitrate-N from the biosoil. A larger rainstorm (5.5 cm) the following day produced a much larger underdrainage peak and by the end of that event, nitrate-N concentrations in underdrain runoff had declined to 0.02 mg N L^{-1} over a period of less than 24 h. Subsequent events in early- to mid-August in the same year continued to progressively flush nitrate-N from the biosoil, producing very low concentrations by the end of each event (Figure 5). Nitrate-N data from EC-BS2 for the same events (#74 - #78) show a similar pattern (Table SI-10), while data from EC-GS do not show this pattern (Table SI-8)—suggesting that 1) nitrate leaching from these highway bioswales is ubiquitous; and 2) nitrate leaching in grassed swales is either less intense or the tall fescue vegetation growing during mid-summer is more N-retentive than bioswale vegetation or both.

With respect to P, our data are strongly supportive of the P chemisorption mechanism of orthophosphate-P retention. The extremely high rates of percolation through the biosoils promotes extensive soil-water interaction that is highly conducive to chemisorption as long as the soils are not effectively P-saturated. These interactions produced very low orthophosphate-P concentrations in the underdrainage from the bioswales compared to overland (“flume”) runoff from the bioswales and from the grassed swales. The relative orthophosphate-P load reductions at the three swales ranged from 40% (EC-BS2) to 80% (EC-BS1), while the synoptic results based on three storm events at EC suggested a 30% reduction. These reductions are comparable to results that have been published from other studies based on TP input-output measurements (Hunt et al. 2006; Davis 2007; Passeport et al. 2009) and mesocosm experiments (Davis et al. 2001; Hsieh et al. 2007). Since our reductions were measured relative to the grassed swale controls, the percentage reductions would be even

higher if the grassed swales themselves provided the level of net retention of P (20 – 23%) measured by Lucke et al. (2014). At the conservative end, adding a 40% reduction on top of a 20% reduction produces a combined reduction of 52%; at the upper end, an 80% reduction on top of a 23% reduction produces a combined reduction of 85%. The higher level suggests that the MEP stormwater goal of 75% reduction can likely be achieved with the highway bioswales, while the lower level would fall short of achieving the MEP goal (CSN 2011).

The rapid percolation of water through the biosoils, resulting from the high *K* media and hyper-efficient underdrain, is consistent with the fact that we found little evidence of significant particle filtration capacity being provided by these bioretention cells. TSS EMCs and loads were either not significantly different among the swale pairs or, in the case of EC-BS2, the bioswale TSS concentration was actually higher (Table 6). The only evidence for enhanced TSS particle filtration by the bioswales was from the synoptic surveys where we found about a 50% reduction (Table 8). Other field-scale bioretention studies have shown consistently high TSS retention (Davis 2007; Hatt et al. 2009; Trowsdale and Simcock 2011), but it appears that the sand content of the biosoils used in those studies was much less than in the present work. Alternately, it is also conceivable that the grassed swale portion of the highway bioswales was highly effective in reducing TSS (Barrett et al. 1998; Yu et al. 2001; Stagge et al. 2012)—thus lowering the TSS "baseline" against which any additional retention by the bioretention cells was computed (Trowsdale and Simcock 2011). Visually, the grassed swales, as well as the grassed

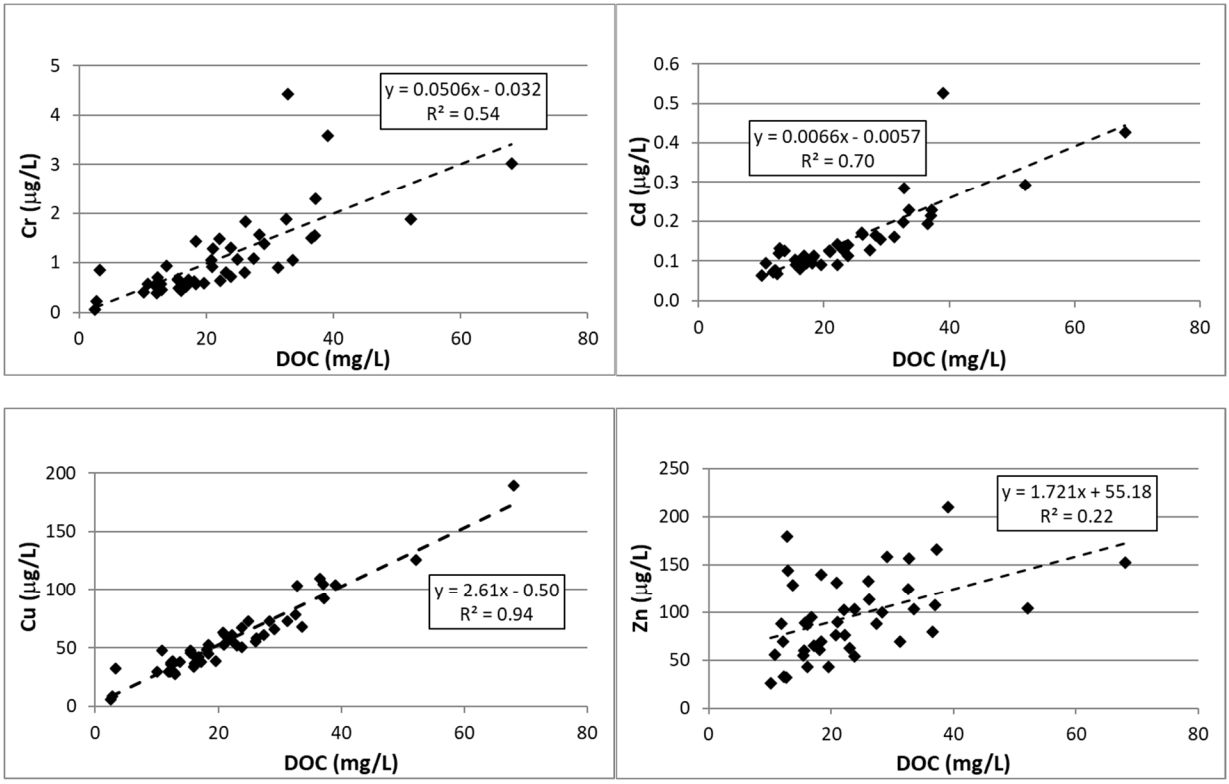

Figure 6. Relationships between trace metal and DOC EMCs in underdrain runoff from EC-BS1.

swale portion of the bioswales, studied in Maryland had vigorously growly vegetation through most of the year, while the vegetation in the bioretention cells was dormant through much of the spring and autumn sampling period.

The excessive percolation of water through the bioretention cells produced at least one other undesirable consequence: the leaching of trace metals (most notably Cu and Zn, but also Cr and Cd) into underdrain runoff at all three bioswale watersheds (Tables 6, 7, 8). While others have attributed trace metal leaching to the application of road salts in the Chesapeake Bay watershed and elsewhere (Bäckström et al. 2004; Galella et al. 2021; 2023), we found that the best predictor of trace metal concentrations in underdrainage was DOC—not Na or Cl levels. DOC concentration explained 22% (Zn) to 94% (Cu) of the total variation in dissolved trace metal concentrations in EC-BS1 underdrainage (Figure 6), suggesting a key role for the formation of organic ligand-trace metal complexes in the percolation process. The very strong statistical relationship between EMCs of trace metals and DOC in underdrain runoff is strongly suggestive of ligand-trace metal complexation (Tang et al. 2001; Craven et al. 2012). Natural dissolved organic matter is known to form stable complexes with many trace metals, particularly the humic and fulvic acid fractions of DOC; Cu^{2+} and Pb^{2+} have been shown to be strongly complexed by humic acid (Kerndorff and Schnitzer 1980) and another study showed that the solubility of Zn and Cd were enhanced by formation of complexes with DOC (Almås et al. 1999). Others have documented increased solubility and mobility of trace metals in municipal landfill (Kaschl et al. 2002) and mine tailing (Kalinowski et al. 2004) leachates that were attributed to complexation by natural dissolved organic matter. In both examples, the strong interaction of water containing natural organic ligands with unconsolidated materials laden with trace metals resulted in an observed enhancement in metal solubility. Given the physical similarity of these environments with the studied bioretention cells, our observations of trace metal mobilization were perhaps not surprising, although the conventional wisdom is that bioretention in most cases reduces trace metal loads (Davis 2007; Davis et al. 2009; Trowsdale and Simcock 2011; Hunt et al. 2012).

Conclusions and Recommendations

Our experimental data from a long-term hydrologic study of highway swales in Maryland shows that the bioswale design employed by MDOT-SHA does a reasonable job of “mimicking” the response of typical grassed swales to stormflow-producing rainstorms across the state—while offering some potential for both retention and detention of stormwater runoff from impervious highway surfaces, as well for addressing some types of stormwater pollution. Functionally, due primarily to the very high saturated hydraulic conductivity of the biosoil media (i.e., high sand content) and the inclusion of hyper-efficient underdrain systems, the bioretention cells were effective at “capturing” (i.e., infiltrating) nearly all (i.e., 95% - 100%) of the stormwater runoff generated during the study while “translating” most of the captured runoff into underdrainage. We found evidence of significant stormwater volume reduction (in excess of levels of retention by the paired grassed swale) at only one of the bioswales (EC-BS2) located along a section of highway fill, but none of the other bioswales produced the same effect. We attributed the

"extra" volume reduction at EC-BS2 to percolation of water into pervious strata below the underdrain and subsequent recharge of local groundwater. MDOT-SHA should explore whether there are ways of enhancing the passive recharge of groundwater from these stormwater management facilities, especially as part of any new highway construction, although questions about possible groundwater contamination by highway stormwater pollution through this process would undoubtedly need to be addressed (Granato et al. 1995).

Due primarily to the rapid hydrologic responses of the bioretention/underdrain systems, attenuation of peak runoff (again, in excess of levels measured at the paired grassed swales) was modest, but expectedly more significant for smaller rainstorm events (i.e., < 2.54 cm) for which these facilities were designed to address. Since most of the stormwater runoff in Maryland is apparently associated with larger, less frequent rainstorm events, the capacity of the bioswales to effectively address the stormwater goal of "detention" is clearly limited, however. The most obvious way of increasing the detention capacity of the bioswales would be to modify the design of the bioretention cells to increase their hydraulic residence time (HRT) by expanding the "footprint" (surface area) of these cells or the depth of the cells or both. Increasing the depth of the cells (i.e., by expanding the depth of aggregate material surrounding the underdrain pipe) could also allow for the provision of an internal water storage (IWS) zone advocated by others (e.g., Hunt et al. 2012) to encourage the denitrification process (see more below). Increasing the size of the bioretention cells would also be expected to reduce stormwater volumes as discussed above.

With respect to the "treatment" of stormwater pollution, our data provided strong evidence that the bioswale design employed by MDOT-SHA is very effectively reducing stormwater P pollution of streams and rivers across the state; percentage P reductions by these facilities exceeded 50% (in some cases 75%) which is consistent with proposed MEP goals for this type of stormwater BMP. The most likely explanation for the P retention is chemisorption of orthophosphate-P onto biosoil media that is not presently "P-saturated"—a process that is magnified by extensive interactions between biosoil and percolating water. This interpretation is consistent with the experimental data that showed few, if any, significant differences in concentrations and loads of other forms of P (e.g., SOC-P, particulate-P) among the different swales. While the use of other materials or additives to biosoil to address specific stormwater pollutants is an area of active research (Vijayaraghavan et al. 2021) and should probably be considered by MDOT-SHA for future bioswale designs, maintaining the performance of MDOT-SHA's existing bioswale network should be top-of-mind. From a P-sorption

Figure 7. Photo showing evidence of tampering with cap on underdrain clean-out pipe at EC-BS2.

perspective, this means that the hydraulic performance of the bioswales should be maintained so that stormwater can continue to infiltrate and percolate through the bioretention cells. Fortunately, we found no evidence of significant clogging of these systems after nearly a dozen years of operation—although we did find evidence of tampering with or inadvertent damage to the water-tight caps on some of the clean-out pipes (Figure 7) at one of the bioswales. If the caps are compromised, a portion of the stormwater could effectively bypass ("bio-pass"?) treatment by the bioretention cell under conditions of surface soil saturation.

One of the obvious downsides of the current bioswale design is their poor N retention capacity. Our data provided strong evidence that the bioretention cells are a major source of the nitrate-N that is presently discharged from the underdrains at all of the bioswales studied. One factor in regulating nitrate-N losses is the presence of vegetation that has the capacity to sequester N in plant biomass and soil organic matter. Unfortunately, the bioswale bioretention areas that we studied were devoid of aboveground vegetation through much of the year (i.e., from the first freeze in the fall through early- to mid-spring). This was not the case with the grassed swales which maintained aboveground vegetation throughout the year. A second factor is likely the productivity of aboveground vegetation and here again the grassed swales have a clear advantage (even during the middle of the growing season). Perhaps most importantly, the leaching of nitrate-N, as well as other constituents such as dissolved organic carbon and several trace metals, is clearly enhanced by the very high *K* and excessive drainage of the biosoil materials—the same soil property that is at least partially responsible for superior orthophosphate-P retention. The experimental data thus present a quandary in stormwater management given a possible trade-off in trying to optimize P vs. N retention by these BMPs. The present design appears to be nearly optimally designed to address stormwater P pollution, but is largely ineffective at addressing nitrate-N pollution. Given that the eutrophication process in freshwater systems is often limited by P, not N, the current design is likely helping to achieve desired levels of pollution reduction necessary to restore these systems and should be credited with such. This is certainly not the case with nitrate-N stormwater pollution, however. While some modifications of the biosoil media might be explored in this regard, we agree that using bioswale technology to address N pollution will likely require a significant redesign that allows for 1) the presence of aboveground vegetation throughout the year; and 2) formation of a zone of transient water storage/saturation to support microbial denitrification.

Acknowledgments

We sincerely thank both Chesapeake Bay Trust (2022-2025) and MDOT-SHA (2014-2022) for financial support of our research over multiple phases of the project. Eighty percent of MDOT-SHA project funding was provided by the Federal-Aid Highway Program (CFDA 20.205). MDOT-SHA district offices also supported the research by providing traffic control, where necessary, and supplying water for infiltration measurements. Thanks to Sam Kane for facilitating construction of guardrails at one of the swales to protect the field instrumentation and provide a safer working environment for our research team. Raymond P. Morgan II and Kathleen Kline were co-principal investigators on the initial phases of the project. Ian Smith assisted with

instrumenting several of the swale watersheds and trouble-shooting the hydrologic instrumentation. Pavithra S. Pitumpe Arachchige, Stephanie Siemek, Joseph Acord, Jessica Shipley, and Ev DeMott assisted with many of the laboratory analyses.

References

Almås, S, BR Sing, and B Salbu. 1999. Mobility of cadmium-109 and zinc-65 in soil influenced by equilibration time, temperature, and organic matter. *J. Environ. Qual*. 28**:**1742.

Avellaneda, PM, AJ Jefferson, JM Grieser, and SA Bush. 2017. Simulation of the cumulative hydrological response to green infrastructure. *Water Resour. Res.* 53:3087-3101.

Bäckström, M. 2003. Grassed swales for stormwater pollution control during rain and snowmelt. *Water Sci. and Technol.* 48:123-134.

Bäckström, M., S. Karlsson, L. Bäckman, L. Folkeson, and B. Lind. 2004. Mobilisation of heavy metals by deicing salts in a roadside environment. *Water Res.* 38:720732.

Barrett, ME. 2008. Comparison of BMP Performance Using the International BMP Database. *J. Irrig. Drain. Eng.* 134:556-561.

Barrett, ME, PM Walsh, JF Malina Jr., and RJ Charbeneau. 1998. Performance of vegetative controls for treating highway runoff. *J. Environ. Eng.* 124:1121-1128.

Bedan, ES, and JC Clausen. 2009. Stormwater runoff quality and quantity from traditional and low impact development watersheds. *J. Amer. Water Resour. Res.* 45:998-1008.

Blecken, G-T, Y Zinger, A Deletic, TD Fletcher, A Hedström, and M Viklander. 2010. Laboratory study on stormwater biofiltration: nutrient and sediment removal in cold temperatures. *J. Hydrol.* 394:507-514.

Bonnin, GM, D Martin, B Lin, T Parzybok, M Yekta, and D Riley. 2025. Point precipitation frequency estimates for Ellicott City, Maryland, USA. NOAA Atlas 14, Vol. 2, Version 3; https://hdsc.nws.noaa.gov/hdsc/pfds/pfds_map_cont.html.

Brown, RA, and WF Hunt. 2011. Underdrain configuration to enhance bioretention exfiltration to reduce pollutant loads. *J. Environ. Eng.* 137:1082-1091.

Burgis, CR, GM Hayes, W Zhang, DA Henderson, SA Macko, and JA Smith. 2020. Tracking denitrification in green stormwater infrastructure with dual nitrate stable isotopes. *Sci. Tot. Environ.* 747:141281.

Chanat, JG, and G Yang. 2018. Exploring drivers of regional water-quality change using differential spatially referenced regression—a pilot study in the Chesapeake Bay watershed. *Water Resour. Res.* 54:8120-8145.

Claytor, R, and T Schueler. 1996. Design of Stormwater Filtering Systems. Center for Watershed Protection, Ellicott City, MD; 220 pp. https://owl.cwp.org/mdocs-posts/design-of-sw-filtering-systems/

CSN. 2011. Environmental site design criteria in the Maryland critical area. Chesapeake Stormwater Network; May 24, 2011 draft.

Craven, AM., GR Aiken, and JN Ryan. 2012. Copper(II) binding by dissolved organic matter: Importance of the copper-to-dissolved organic matter ratio and implications for the biotic ligand model. *Environ. Sci. Technol.* 46:9948–9955.

Davis, AP. 2007. Field performance of bioretention: water quality. *Environ. Eng. Sci.* 24:1048-1063.

Davis, AP. 2008. Field performance of bioretention: hydrology impacts. *J. Hydrol. Eng.* 13:90-95.

Davis, AP, M Shokouhian, H Sharma, an C Minami. 2001. Laboratory study of biological retention for urban stormwater management. *Water Environ. Res.* 73:5-14.

Davis, AP, WF Hunt, RG Traver, and M Clar. 2009. Bioretention technology: Overview of current practice and future needs. *J. Environ. Eng.* 135:109-117.

Ekka, SA, H Rujner, G Leonhardt, G-T Blecken, M Viklander, and WF Hunt. 2021. Next generation swale design for stormwater runoff treatment: a comprehensive approach. *J. Environ. Manage.* 279:111756.

Fan, R, STY Tong, and JG Lee. 2017. Determining the optimal BMP arrangement under current and future climate regimes: case study. *J. Water Resour. Plan. Manag.* 143.

Fatehnia, M, K Tawfiq, and M Ye. 2016. Estimation of saturated hydraulic conductivity from double-ring infiltrometer measurements. *Eur. J. Soil Sci.* 67:135-147.

Fishman, MJ. 1993. Methods of analysis by the U.S. Geological Survey National Water Quality Laboratory—determination of inorganic and organic constituents in water and fluvial sediments. *U.S. Geological Survey Open-File Report 93-125.*

Galella, JG, SS Kaushal, KL Wood, JE Reimer, and PM Mayer. 2021. Sensors track mobilization of "chemical cocktails" in streams impacted by road salts in the Chesapeake Bay watershed. *Environ. Res. Let.* 16; 10.1088/1748-9326/abe48f.

Galella, JG, SS Kaushal, PM Mayer, CM Maas, RR Shatkay, and RA Stutzke. 2022. Stormwater best management practices: experimental evaluation of chemical cocktails mobilized by freshwater salinization syndrome. *Front. Environ. Sci.* 11; 10.3389/fenvs.2023.1020914.

Granato, GE, PE Church, and VJ Stone. 1995. Mobilization of major and trace constituents of highway runoff in groundwater potentially caused by deicing chemical migration. *Transportation Research Record* 1483:92-104.

Hatt, BE, TD Fletcher, and A Deletic. 2009. Hydrologic and pollutant removal performance of stormwater biofiltration systems at the field scale. *J. Hydrol.* 365:310-321.

Hopkins, KG, AS Bhaskar, SA Woznicki, and RM Fanelli. 2020. Changes in event-based streamflow magnitude and timing after suburban development with infiltration-based stormwater management. *Hydrol. Process.* 34:387-403.

Hsieh, C-H, and AP Davis. 2005. Evaluation and optimization of bioretention media for treatment of urban storm water runoff. *J. Environ. Eng.* 131:1521-1531.

Hsieh, C-H, AP Davis, and B Needelman. 2007. Nitrogen removal from urban stormwater runoff through layered bioretention columns. *Water Environ. Res.* 79:177-184.

Hunt, WF, AR Jarrett, JT Smith, and LJ Sharkey. 2006. Evaluating bioretention hydrology and nutrient removal at three field sites in North Carolina. *J. Irrigat. Drain. Eng.* 132:600-608.

Hunt, WF, JM Hathaway, RJ Winston, and SJ Jadlocki. 2010. Runoff volume reduction of a level spreader-vegetated filter strip system in suburban Charlotte, N.C. *J. Hydrol. Eng.* 15:499-503.

Hunt, WF, AP Davis, and RG Traver. 2012. Meeting hydrologic and water quality goals through targeted bioretention design. *J. Environ. Eng.* 138(6):698-707.

Jarden, KM, AJ Jefferson, and JM Grieser. 2016. Assessing the effects of catchment-scale urban green infrastructure retrofits on hydrograph characteristics. *Hydrol. Process.* 30:1536-1550.

Kalinowski, BE, A Oskarsson, Y Albinsson, J Arlinger, A Ödegaard-Jensen, T Andlid, and K Pedersen. 2004. Microbial leaching of uranium and other trace elements from shale mine tailings at Ranstad. *Geoderma* 122: 10.1016/j.geoderma.2004.01.007.

Kaschl, A, V Römheld, and YN Chen. 2002. Trace metal distribution in soluble organic matter from municipal solid waste compost determined by size-exclusion chromatography. *Environ. Toxicol. Chem.* 21:1775-1782; 10.1002/etc.5620210903.

Kerndorff, H, and M Schnitzer. 1980. Sorption of metals on humic acids. *Geochim. Cosmochim. Acta*. 44:1701.

Le Coustemer, S, TD Fletcher, A Deletic, S Barraud, and JF Lewis. 2009. Hydraulic performance of biofilter systems for stormwater management: influences of design and operation. *J. Hydrol.* 376:16-23.

Lee, JG, A Selvakumar, K Alvi, J Riverson, JX Zhen, L Shoemaker, and F Lai. 2012. A watershed-scale design optimization model for stormwater best management practices. *Environ. Model. Software* 37:6-18.

Li, H, LJ Sharkey, WF Hunt, and AP Davis. 2009. Mitigation of impervious surface hydrology using bioretention in North Carolina and Maryland. *J. Hydrol. Eng.* 14:407-415.

Liu, J, DJ Sample, C Bell, and Y Guan. 2014. Review and research needs of bioretention used for treatment of urban stormwater. *Water* 6:1069-1099.

Loperfido, JV, GB Noe, ST Jarnagin, and DM Hogan. 2014. Effects of distributed and centralized stormwater best management practices and land cover on urban stream hydrology at the catchment scale. *J. Hydrol.* 519:2584-2595.

Lucke, T, MAK Mohamed, and N. Tindale. 2014. Pollutant removal and hydraulic reduction performance of field grassed swales during runoff simulation experiments. *Water* 6:1887-1904; doi:10.3390/w6071887.

MDE. 2009. Maryland Stormwater Design Manual, Chap. 5 Environmental Site Design. Maryland Department of the Environment, Baltimore, MD. https://mde.maryland.gov/programs/water/StormwaterManagementProgram/Pages/stormwater_design.aspx.

Monrabal-Martinez, C, J Aberle, TM Muthanna, and M Orts-Zamorano. 2018. Hydrological benefits of filtering swales for metal removal. *Water Res.* 145:509-517.

Passeport, E, WF Hunt, DE Line, RA Smith, and RA Brown. 2009. Field study of the ability of two grassed bioretention cells to reduce storm-water runoff pollution. *J. Irrigat. Drain. Eng. 135*:505-510.

Rantz et al. 1982. Measurement and computation of streamflow: Volume 1. Measurement of stage and discharge. *Geological Survey Water-Supply Paper 2175*, Washington DC.

Roy, AH, SJ Wenger, TD Fletcher, CJ Walsh, AR Ladson, WD Shuster, HW Thurston, and RR Brown. 2008. Impediments and solutions to sustainable, watershed-scale urban stormwater management: lessons from Australia and the United States. *Environ. Manag.* 42:344-359.

Shetty, N, R Hu, J Hoch, B Mailloux, M Palmer, DN Menge, K McGuire, W McGillis, and P Culligan. 2018. Quantifying urban bioswale nitrogen cycling in the soil, gas, and plant phases. *Water* 10(11):1627.

Smith, BK, JA Smith, ML Baeck, G Villarini, and DB Wright. 2013. Spectrum of storm event hydrologic response in urban watersheds. *Water Resour. Res.* 49:2649-2663.

Smith, JS, RJ Winston, DM Wituszynski, RA Tirpak, KM Boening-Ulman, and JF Martin. 2023. Effects of watershed-scale green infrastructure retrofits on urban stormwater quality: a paired watershed study to quantify nutrient and sediment removal. *Ecol. Eng.* 186:106835; doi:10.1016/j.ecoleng.2022.106835.

Stagge, JH, AP Davis, E Jamil, and H Kim. 2012. Performance of grass swales for improving water quality from highway runoff. *Water Res.* 46:6731-6742.; doi:10.1016/j.watres.2012.02.037.

Tang, D., K.W. Warnken, and P.H. Santschi. 2001. Organic complexation of copper in surface waters of Galveston Bay. *Limnol. Oceanogr.* 46(2):321–330.

Trowsdale, SA, and R Simcock. 2011. Urban stormwater treatment using bioretention. *J. Hydrol.* 397:167-142; doi:10.1016/j.hydrol.2010.11.023.

USDA. 2009. National Engineering Handbook. Part 630 Hydrology. Chapter 7 Hydrologic Soil Groups. US Department of Agriculture, Washington, DC.

USEPA. 1993. Methods for the Determination of Inorganic Substances in Environmental Samples. *EPA/600/R-93/100*, U.S.EPA National Exposure Research Laboratory (NERL) Microbiological and Chemical Exposure Assessment Research Division (MCEARD), Cincinnati, OH.

Valderrama, JC. 1981. The simultaneous analysis of total nitrogen and phosphorus in natural waters. *Mar. Chem.* 10: 109-122.

Vijayaraghavan, K, BK Biswal, MG Adam, SH Soh, DK Tsen-Tieng, AP Davis, SH Chew, PY Tan, V Babovic, and R Balasubramanian. 2021. Bioretention systems for stormwater management: recent advances and future prospects. *J. Environ. Manag.* 292:112766; doi:10.1016/j.jenvman.2021.112766.

Yu, LS, J-R Kuo, AE Fassman, and H Pan. 2001. Field test of grassed-swale performance in removing runoff pollution*. J. Water Resour. Manag.* 127:168-171.

Yu, J, H Yu, and L Xu. 2013. Performance evaluation of various stormwater best management practices. *Environ. Res. Pollut. Res.* 20:6160-6171.

Appendix A. Photos of some of the swales monitored as part of the project.

Figure A-1. Photo of EC-BS1 swale watershed on US Rte. 40 in Ellicott City, MD with above-ground instrumentation.

Figure A-2. Photo of EC-GS swale watershed on US Rte. 40 in Ellicott City, MD (instrumentation not shown).

Figure A-3. Photo of LT-BS swale watershed on US Rte. 15 near Lewistown, MD prior to installation of monitoring equipment.

Figure A-4. Photo of LT-GS swale watershed on US Rte. 15 near Lewistown, MD with instrumentation shown.

Appendix B. Use of NEXRAD Level III Rainfall Data

Introduction

As a hydrologic variable, precipitation is notoriously variable both in space and in time. The layperson regularly confronts the problem of spatial variability in his/her daily life: most of us have experienced the situation where it poured down raining on one end of the street, while the other end stayed completed dry. With respect to the current project, we were unable to monitor rainfall at one of our swales (ET-GS) in Ellicott City, Maryland from 2017-19 due to highway safety issues that precluded us from installing a gage on this section of U.S. Rte. 40. In an earlier iteration of our paired hydrologic analysis, we attempted to use on-site, tipping bucket rainfall data from the other swale (EC-BS1) located about 5.5 km to the west as the precipitation input for both sites, but this turned out to be unsatisfactory due to the high spatial variability of rainfall between the two swales. This was perhaps best illustrated for the May 28, 2018 runoff event that devastated Old Ellicott City (see Figure A-1 reproduced from NWS imagery); while the EC-BS1 swale is located in the dark blue-shaded area indicated 3 – 4 in (7.6 – 10.2 cm) of rainfall, the EC-GS swale is located in the orange-shaded area indicating between 6 in (15.2 cm) and 8 in (20.3 cm) of total rainfall (Figure A-1). Moreover, Smith et al. (2012) used data from the Hydro-NEXRAD system to document a steep decline in the occurrence of moderate to high-intensity rainfall events west of the city of Baltimore—including the area of Howard County in which the swales are located—for the ten-year period from 2000-2009. Urbanization and/or the presence of mountainous terrain west of the city could be reasonable climatological explanations for these observations. Regardless, in order to properly characterize the hydrologic responsiveness of EC-GS, we needed an alternate method.

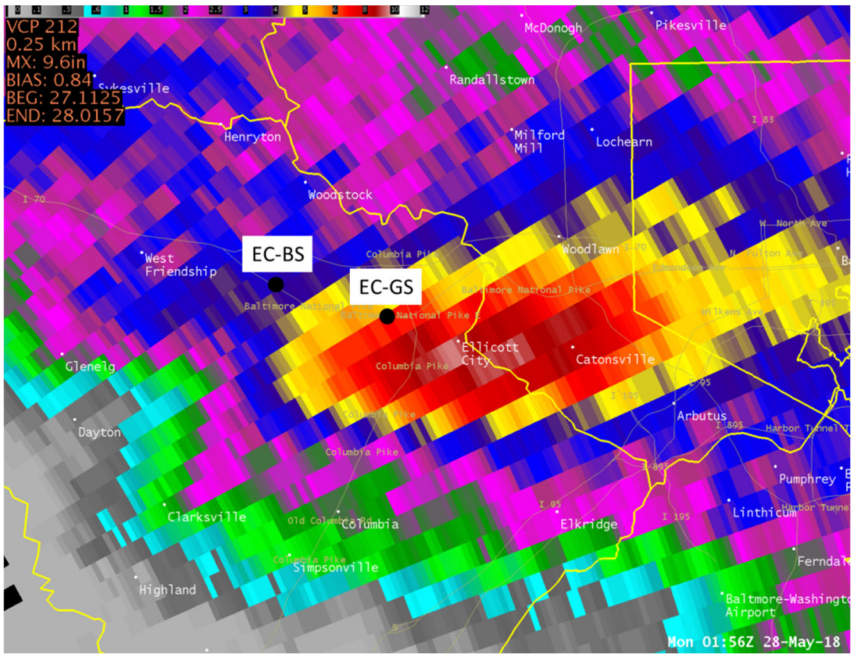

Figure B-1. Radar-rainfall map generated by National Weather Service for May 28, 2018 for suburban Baltimore, Maryland area (downloaded from https://www.weather.gov/lwx/EllicottCityFlood2018); locations of EC study swales also shown. Data reported in inches.

The most obvious solution to this problem was to utilize high resolution rainfall data based on Weather Surveillance Radar Doppler (WSR-88D) radar reflectivity fields that can be obtained from archived records by the National Weather Service. Several other recently-published studies conducted in the Baltimore-Washington metropolitan area have used these datasets based on radar reflectivity reported by the Sterling, Virginia radar (Smith et al., 2012; Smith et al., 2013). The standard method is to "correct" the rainfall data on a daily (or storm-by-storm) basis to account for any bias in the radar-based estimation scheme (Wright et al., 2014):

$$B_i = \frac{\sum_{S_i} G_{ij}}{\sum_{S_i} R_{ij}} \quad \text{[A-1]}$$

where B_i is the bias factor for event i, G_{ij} is the rainfall accumulation for rain gage j for event i, and R_{ij} is the radar rainfall accumulation for the location of rain gage j for event i.

Methods

We downloaded NEXRAD Level III 5-min rainfall a) intensity (dual polarization) and b) one-hour accumulation (dual polarization[3]) data for the Sterling, Virginia radar for each day for each storm event from the NOAA NCEI website (https://www.ncdc.noaa.gov/nexradinv/) and processed the requisite binary data files using NOAA's Weather and Climate Toolkit (WCT). We note here that radar data for some dates were missing from the NEXRAD Level III permanent archive, but interestingly when data were missing for the Sterling radar, data from the other closest radars were missing as well—suggesting a data archiving issue rather than a radar failure per se. The primary WCT processing tool was the "point subset tool" which allowed us to select intensity and one-hour accumulation values for only the specific points of interest to us (i.e., geographic coordinates of the EC and LT swales). For each day of data processed, the point subset tool produced a .csv file which was easily imported into Excel and used to compute a value of R_{ij} by numerical integration of rainfall intensity for the storm duration that could be paired with G_{ij} from our small gage network; in some cases, our "event" data files required us to merge data from multiple daily files. Similarly, we imported each one-hourly accumulation file into Excel and calculated the maximum one-hour accumulation for each storm event as well. Note that for Lewistown (2019-21) and for Ellicott City prior to 2020 when a rain gage at EC-GS was operational, we operated only one gage at each location (i.e., j = 1); therefore, computation of B_i in Eq. [A-1] did not actually involve summation (rather $B_i = R_i/G_i$). We statistically analyzed the relationships between R_i and G_i for each gage and provided several goodness-of-fit indices with which to summarize the results: 1) root mean square error (RMSE) of the accumulated event rainfall; 2) Nash-Sutcliffe efficiency (NSE) of the overall statistical relationship between R_i and G_i; 3) cumulative bias factor (given by integrating B_i over all i events); and 4) the overall percentage of events for which R_i is within +/- a factor of two of G_i. We used the first three of these metrics for comparing the maximum one-hour rainfall data as well.

[3] Dual polarization radars are thought to improve rainfall estimation because they can distinguish between different hydrometeor types (e.g., hail vs. rain). See Cunha et al. (2013) for more details.

Results and Discussion

Relationships between R_i and G_i for the three swale stations are shown in Figures A-2 (EC-BS1), A-3 (EC-GS), and A-4 (LT-BS). The statistical results show reasonable agreement between R_i and G_i, with RMSE's in the range of 1.0 to 1.2 cm, NSE's in the range of 0.56 to 0.67, and cumulative bias factors ranging from 1.10 to 1.36 (Table A-1). Early efforts from the 1990's to try to quantify the errors in estimating accumulated rainfall using NEXRAD concluded that without bias-correction, NEXRAD radar rainfall was usually within +/- a factor of two of gage rainfall about 75% of the time. Our results suggest that we can now do a little better than that, at least for runoff-producing events, with 80 – 88% of the events falling within the factor of two criterion (Table A-1, Figures A2 – A4). This analysis did not consider the significant number of events for which we were unable to find radar rainfall data in the NOAA archive, however (including those events would have lowered these percentages considerably). This missing data problem is perhaps the biggest issue in making use of NEXRAD radar rainfall data, but we do not have enough experience to be able to say whether this is a recent archiving problem or one that has plagued the system from the onset.

When we used gage data from EC-BS1 and NEXRAD data to estimate bias-corrected rainfall for EC-GS, we found that the errors were reduced even further; the RMSE (0.57 cm) was only half as large, the NSE was 0.90, and the cumulative bias factor (1.02) dropped nearly to one (Table A-1). Finally, a comparison of radar vs. gage one-hour maximum rainfall values seemed even more promising; we found that the RMSE's were about 50% as large as for the accumulated rainfall RMSE's and that cumulative bias for this measure (0.94 to 1.10) was even lower than for accumulated rainfall and appears to be about zero based on a mean for the three stations (Table A-2).

Overall, these results (and those of others) support the use of bias-corrected NEXRAD Level III data for estimating event rainfall for EC-GS for storms for which gage data are unavailable. As noted, this was the case for the period from 2017-19 when we could not operate an on-site gage at EC-GS due to safety concerns. However, we have also learned that operating rain gage networks is not infallible, so the technique that we used here can also be extended to situations where a particular gage is inoperable due to mechanical difficulties or where data are lost due to programming or data failures, etc. Aside from the errors associated with the methodology, the main limitation seems to be related to the NEXRAD archiving schemes that are all too often unreliable. Among the 111 runoff-producing events storm events that we monitored at EC-GS, there were 16 for which NEXRAD Level III data were unavailable at the NOAA NCEI server. Fortunately, by the end of the project, we learned that NEXRAD data for the *most recent* 30-day period are also archived by Unidata on the THREDDS data server at UCAR and can be downloaded and processed using the WCT using the same procedure. Oddly, we even found several occurrences where recent data were available from UCAR that could not be obtained from NOAA NCEI. The availability of historical NEXRAD Level III data, in combination with the apparent need to bias-correct the data on an event-by-event basis, hampers widespread adoption and application in hydrology (and presumably other fields as well). The development of HydroNEXRAD (e.g., Wright et al., 2014) was obviously motivated by a desire to overcome

these issues and provide a reliable rainfall product to practitioners that does not require the rather laborious steps that were needed for this project.

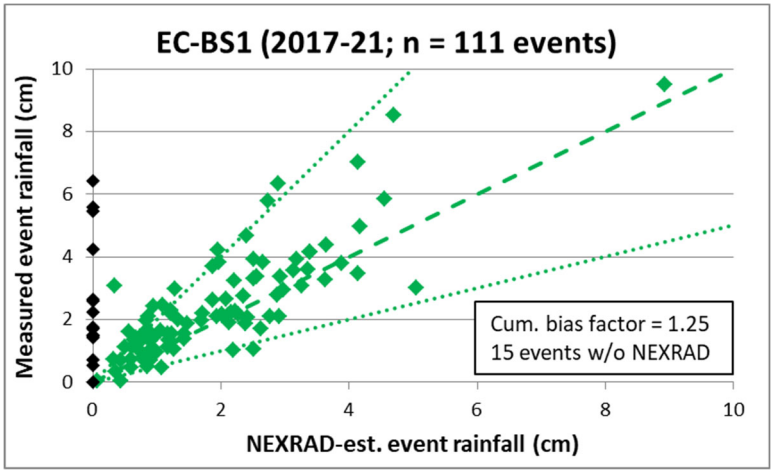

Figure B-2. Measured event rainfall vs. NEXRAD-estimated event rainfall for the EC-BS1 swale (2017-21). Points represented by black diamonds (n = 15) were missing NEXRAD Level III data.

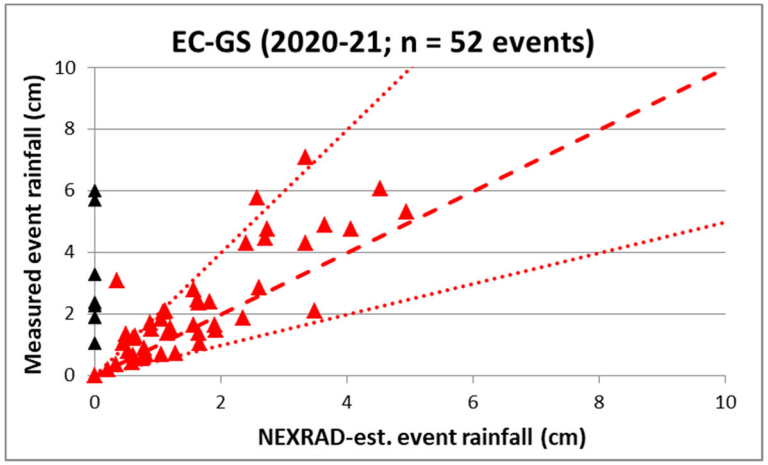

Figure B-3. Measured event rainfall vs. NEXRAD-estimated event rainfall for the EC-GS swale (2020-21). Points represented by black triangles (n = 7) were missing NEXRAD Level III data.

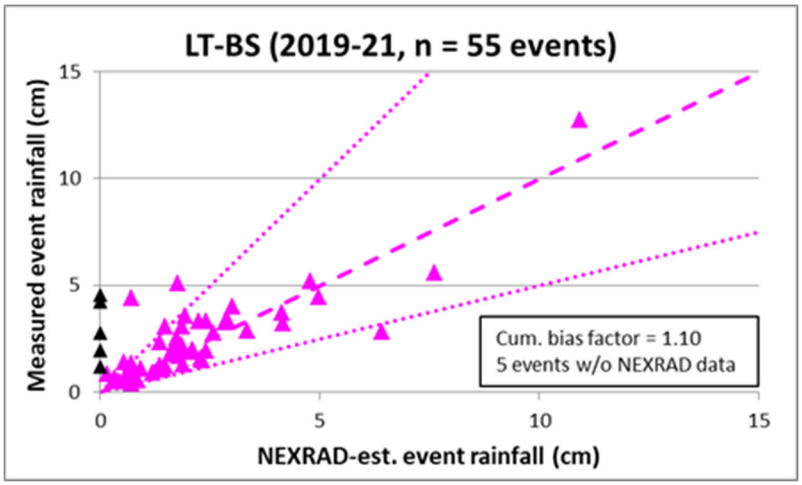

Figure B-4. Measured event rainfall vs. NEXRAD-estimated event rainfall for the LT-BS and LT-GS swales (2019-21). Points represented by black triangles (n = 5) were missing NEXRAD Level III data.

Table B-1. Statistical comparison of event rainfall results (gage vs. NEXRAD Level III) for runoff-producing events at the three swale sites with rainfall gages: LT (Lewistown) and EC (Ellicott City).

Site	No of Events[1]		Event rainfall (cm): gage/NEXRAD						RMSE (cm)	NSE	Cum. Bias Factor	Events within +/-a factor of two of observed rainfall (%)
	Total	Analyzed	Minimum		Mean		Maximum					
LT-BS	55	50	0.38	0.16	2.44	2.22	12.75	10.93	1.14	0.67	1.10	88
EC-BS1	111	91	0.03	0.06	2.46	1.97	9.50	8.93	1.06	0.62	1.25	80
EC-GS	52	45	0.00	0.00	2.27	1.67	7.09	4.94	1.16	0.56	1.36	86
EC-GS[2]	52	41	0.00	0.00	2.27	2.21	7.09	7.05	0.57	0.90	1.02	90

[1]The difference between total events and events analyzed is due to the fact that there were some events for which either (or both) gage data or NEXRAD Level III data were unavailable.

[2]EC-GS event rainfall was predicted from NEXRAD Level III data that was bias-corrected using the observed EC-BS1 rainfall; the number of events analyzed is smaller due to four events for which EC-BS1 observed rainfall was unavailable.

Table B-2. Statistical comparison of maximum one-hour rainfall results (gage vs. NEXRAD Level III) for runoff-producing events at the three swale sites with rainfall gages: LT (Lewistown) and EC (Ellicott City).

Site	No of Events[1]		Event rainfall (cm): gage/NEXRAD						RMSE (cm)	NSE	Cum. Bias Factor
	Total	Analyzed	Minimum		Mean		Maximum				
LT-BS	55	50	0.28	0.07	1.21	1.29	3.45	4.87	0.56	0.41	0.94
EC-GS	52	47	0.00	0.01	1.10	1.00	5.77	4.86	0.52	0.78	1.10
EC-BS1	111	93	0.00	0.04	1.06	1.06	4.39	3.92	0.43	0.72	1.00

[1]The difference between total events and events analyzed is due to the fact that there were some events for which either (or both) gage data or NEXRAD Level III data were unavailable.

References

Cunha, L.K., J.A. Smith, M.L. Baeck, and W.F. Krajewski. 2014. An early performance evaluation of the NEXRAD dual-polarization radar rainfall estimates for urban flood applications. *Weather and Forecasting* 28:1478-1497.

Smith, J.A., M.L. Baeck, G. Villarini, C. Welty, A.J. Miller, and W.F. Krajewski. 2012. Analyses of a long-term high-resolution radar rainfall data set for the Baltimore metropolitan region. *Water Resources Research* 48:W04504.

Smith, B.K., J.A. Smith, M.L. Baeck, G. Villarini, and D.B. Wright. 2013. Spectrum of storm event hydrologic response in urban watersheds. *Water Resources Research* 49:2649-2663.

Wright, D.B., J.A. Smith, G. Villarini, and M.L. Baeck. 2014. Long-term high-resolution radar rainfall fields for urban hydrology. *Journal of the American Water Resources Association* 50(3):713-734.

Table SI-1. Rainfall and runoff events at Hagerstown (2017-2018)

Dates[1]	1-hr Rainfall			24-hr Rainfall			3-day antecedent rainfall (cm)	Runoff Response (Y or N)	
	Depth (cm)	Average recurrence interval (y)[2]	Rank	Depth (cm)	Average recurrence interval (y)[2]	Rank		HT-BS1 underdrain	HT-GS flume
5/4-5/2017	0.76	<1		5.92	1	4	0.13	N	N
10/29-30/2017	0.25	<1		5.03	<1	6	0.13	N	N
10/8-9/2017	0.81	<1		3.35	<1	9	0.25	N	N
4/15-16/2018	1.37	<1	6	5.99	1	3	0.00	N	N
7/4/2018	4.14	5	1	4.50	<1	7	0.00	N	Y
7/17/2018	0.89	<1	9	1.91	<1		0.00	N	N
7/21/2018	0.91	<1	8	6.40	1	2	0.00	N	N
7/25/2018	0.84	<1		1.68	<1		3.15	N	N
8/1/2018	2.44	1	3	5.05	<1	5	1.63	Y	Y
8/3/2018	1.60	<1	5	2.34	<1		7.32	N	Y
8/8/2018	1.35	<1	7	2.29	<1		0.13	N	Y
8/21/2018	3.73	5	2	4.50	<1	7	1.07	Y	Y
9/9/2018	0.71	<1		7.85	2	1	1.52	N	N
9/26/2018	2.11	<1	4	2.13	<1		1.96	Y	Y

[1]Event dates were determined using hourly rainfall data to maximize 24-hour rainfall depth; 3-day antecedent rainfall was determined accordingly.

[2]Based on NOAA Atlas 14 Point Precipitation Frequency Estimates (Bonnin et al. 2025): https://hdsc.nws.noaa.gov/pfds/pfds_map_cont.html?bkmrk=md

Table SI-2. Rainfall and runoff data for 158 runoff-producing events monitored at three Ellicott City (EC) swales during the project (2017-2024). Events with data shown in bold were common events used for water quality comparisons. Data shaded in yellow were collected as part of the CBT-funded project (2022-2025).

Event No.	Dates	EC-GS		EC-BS1				EC-BS2			
		Rainfall (cm)	Runoff (cm)	Rainfall (cm)	Under-drain runoff (cm)	Flume runoff (cm)	Total runoff (cm)	Rainfall (cm)	Under-drain runoff (cm)	Flume runoff (cm)	Total runoff (cm)
1	**5/12/2017**	1.85	1.30	1.60	1.02	0.00	1.02				
2	5/19/2017	2.02	1.04	1.88	1.52	0.00	1.52				
3	5/25/2017	1.95	0.71	3.07	1.60 [e]	0.08	1.68 [e]				
4	7/6/2017	4.33	0.36	4.67	1.68	0.00	1.68				
5	**7/28/2017**	5.36	3.40	5.84	2.46 [e]	0.00	2.46 [e]				
6	8/15/2017	3.90	1.73	4.14	1.78 [e]	0.64	2.41 [e]				
7	8/18/2017	4.66	2.95	3.94	0.99 [e]	1.24	2.24 [e]				
8	9/2/2017	1.24	0.10	1.52	0.48	0.00	0.48				
9	9/5/2017	2.01	2.84	3.28	1.40 [e]	0.36	1.75 [e]				
10	10/11/2017	2.14	0.15	1.96	1.27	0.00	1.27				
11	11/4/2017	1.75	0.13	1.24	0.61	0.00	0.61				
12	11/7/2017	2.65	0.23	2.29	2.11	0.00	2.11				
13	**4/16/2018**	4.48	1.70	3.81	3.56 [e]	0.00	3.56 [e]				
14	**4/27/2018**	1.09	0.13	0.94	0.46	0.00	0.46				
15	5/14/2018	1.36	1.57	1.37	0.74	0.00	0.74				
16	**5/15/2018**	2.83	2.24	3.00	2.26	0.36	2.62				
17	5/17/2018	2.58	0.46	1.96	1.75	0.03	1.78				
18	5/28/2018	18.80	7.98	9.50	4.78	2.51	7.29				
19	5/31/2018		1.65	2.24	1.14	0.25	1.40				
20	**6/2/2018**	0.76	0.41	1.40	0.71	0.03	0.74				
21	6/3/2018		4.65	6.43	2.31	1.52	3.84				
22	**6/10/2018**	5.95	6.10	4.95	1.78	1.68	3.45				

23	**7/21/2018**	12.81	5.23	8.53	6.17	0.71	6.88				
24	**7/22/2018**	4.56	3.10	2.95	1.93	0.43	2.36				
25	7/23/2018	2.76	0.81	1.09	0.61	0.00	0.61				
26	7/24/2018	5.38	1.09	2.64	1.85	0.33	2.18				
27	7/25/2018	3.61	2.34	2.62	1.85	0.64	2.49				
28	7/31/2018	3.09	0.89	2.74	1.80	0.66	2.46				
29	8/1/2018	1.92	1.68	1.52	0.74	0.13	0.86				
30	8/21/2018	4.21	1.52	3.58	0.99	0.00	0.99				
31	8/31/2018	2.63	0.51	1.52	0.10	0.00	0.10				
32	9/7/2018		0.20	3.07							
33	9/8/2018		0.03	1.47	0.94	0.03	0.97				
34	9/9/2018		0.69	4.24	2.95	0.00	2.95				
35	9/17/2018	2.44	0.38	1.35	0.00	0.00	0.00				
36	9/23/2018	2.38	0.03	1.98	0.81	0.00	0.81				
37	9/27/2018	5.27	1.35	3.68	2.57	0.43	3.00				
38	10/4/2018	1.60	1.37	2.16	0.00	0.00	0.00				
39	**10/26/2018**	3.33	0.20	2.46	0.84	0.00	0.84				
40	3/21-22/19	6.22	3.02	6.32	2.26	1.27	3.53				
41	**5/5/2019**	2.21	0.28	1.63	0.18	0.00	0.18				
42	5/10/2019	2.39	1.69	2.79	0.89	0.81	1.70				
43	5/11-12/19	2.77	2.22	2.97	1.52	0.61	2.13				
44	5/13/2019		1.55	1.50	1.04	0.20	1.24				
45	5/30/2019	2.27	0.32	1.91	0.15	0.00	0.15				
46	6/13/2019	0.75	0.23	0.33	0.00	0.00	0.00				
47	7/4/2019	2.48	0.51	1.02	0.00	0.00	0.00				
48	7/6/2019	0.83	0.90	1.04	0.00	0.00	0.00				
49	**7/8/2019**	3.13	3.39	3.45	1.52	0.00	1.52				
50	7/11/2019	1.03	0.32	2.26	0.64	0.00	0.64				
51	**7/17/2019**	0.97	0.18	1.70	0.18	0.00	0.18				
52	8/22/2019		0.46	2.64	0.00	0.00	0.00				
53	8/23/2019		0.23	0.71	0.00	0.00	0.00				

54	10/16/2019	3.58	0.25	3.56	0.81	0.00	0.81				
55	**10/20/2019**	3.19	1.71	2.18	0.99	0.00	0.99				
56	10/22/2019		0.67	1.70	0.71	0.00	0.71				
57	**10/27/2019**	3.25	2.66	3.30	3.07	0.00	3.07				
58	**10/30/2019**	1.45	0.97	1.32	1.14	0.00	1.14				
59	**10/31/2019**	6.09	3.81	3.35	4.42	1.19	5.61				
60	3/18-19/2020	1.70	0.95	1.45	0.99	0.00	0.99				
61	3/28/2020	1.83	1.34	1.68	0.99	0.00	0.99				
62	4/12-13/2020	4.47	3.65	7.01	3.02	1.57	4.60				
63	4/24/2020	2.08	0.97	2.11	0.79	0.00	0.79				
64	4/26/2020	1.30	1.18	1.35	0.74	0.00	0.74				
65	4/30/2020	3.30	2.52	2.59	1.63	0.00	1.63				
66	5/3-4/2020	0.89	0.32	0.71	0.13	0.00	0.13				
67	5/6-7/2020	1.07	0.62	1.12	0.36	0.00	0.36				
68	5/8-9/2020	0.79	0.39	0.69	0.18	0.00	0.18				
69	6/5/2020	2.87	0.35	2.11	0.08	0.00	0.08				
70	6/11/2020	1.65	0.25	2.16	0.38	0.00	0.38				
71	6/20/2020	4.90	3.02	2.06	0.71	0.00	0.71				
72	6/22/2020	6.07	3.99	2.21	1.50	0.15	1.65				
73	6/25/2020	0.20	0.00	1.12	0.36	0.00	0.36				
74	**8/3/2020**	1.91	0.58	1.42	0.05	0.00	0.05				
75	**8/4/2020**	6.02	4.92	5.46	5.99	0.05	6.05	5.46	4.95	0.03	4.98
76	**8/12/2020**	2.29	0.81	1.75	0.28	0.00	0.28	1.75	0.03	0.00	0.03
77	8/13/2020	0.56	0.32	0.46	0.13	0.00	0.13	0.46	0.00	0.00	0.00
78	**8/14-15/2020**	2.79	1.96	4.37	2.51	1.27	3.78	4.37	3.02	1.22	4.24
79	8/15-16/2020	2.11	1.75	2.41	0.94	0.00	0.94	2.41	0.84	0.00	0.84
80	8/17/2020	0.69	0.30	0.71	0.23	0.00	0.23	0.71	0.00	0.00	0.00
81	8/24/2020	1.07	0.23	0.00	0.00	0.00	0.00	0.00	0.00	0.00	0.00
82	8/29/2020	0.71	0.44	0.76	0.20	0.00	0.20	0.76	0.00	0.00	0.00
83	9/3/2020	1.35	0.92	1.04	0.41	0.00	0.41	1.04	0.18	0.00	0.18
84	9/29-30/2020	2.39	0.92	0.53	0.00	0.00	0.00	0.53	0.00	0.00	0.00

85	10/11-13/2020	3.07	1.45	3.02	0.71	0.00	0.71	3.02	0.00	0.00	0.00
86	**10/29-30/2020**	5.77	4.02	4.22	2.41	0.00	2.44	4.22	1.57	0.00	1.57
87	3/18-19/2021	1.50	0.72	1.40	0.28	0.00	0.28	1.40	0.00	0.00	0.00
88	3/24/2021	4.78	3.19	3.94	1.70	0.41	2.13	3.94	1.27	0.00	1.27
89	3/28-29/2021	1.65	1.32	1.02	0.33	0.00	0.33	1.02	0.00	0.00	0.00
90	3/31-4/1/2021	2.39	2.31	2.18	1.35	0.00	1.35	2.18	0.56	0.00	0.56
91	4/11/2021	1.22	0.51	1.12	0.43	0.00	0.43	1.12	0.05	0.00	0.05
92	4/11-12/2021	0.36	0.28	0.03	0.00	0.00	0.00	0.03	0.00	0.00	0.00
93	5/8/2021	0.66	0.00	0.51	0.08	0.00	0.08	0.51	0.00	0.00	0.00
94	**5/28-29/2021**	4.29	2.75	3.81	1.30	0.00	1.30	3.81	0.20	0.00	0.20
95	6/14-15/2021	2.11	1.32	1.67	1.02	0.00	1.02	1.67	0.00	0.00	0.00
96	6/21/2021	1.88	0.28	1.17	0.00	0.00	0.00	1.17	0.00	0.00	0.00
97	6/22/2021	0.69	0.35	0.58	0.08	0.00	0.08	0.58	0.00	0.00	0.00
98	**7/01-02/2021**	2.36	0.28	3.25	0.53	0.00	0.53	3.25	0.00	0.00	0.00
99	7/17-18/2021	1.07	0.00	2.11	0.03	0.00	0.03	2.11	0.00	0.00	0.00
100	7/29/2021	2.46	0.30	1.57	0.00	0.00	0.00	1.57	0.00	0.00	0.00
101	8/1/2021	1.55	0.37	0.46	0.00	0.00	0.00	0.46	0.00	0.00	0.00
102	8/10/2021	1.47	0.09	1.02	0.00	0.00	0.00	1.02	0.00	0.00	0.00
103	**8/17-19/2021**	5.31	3.21	3.38	1.17	0.00	1.17	3.38	0.00	0.00	0.00
104	8/20/2021	1.40	0.76	0.97	0.00	0.00	0.00	0.97	0.00	0.00	0.00
105	**9/1-2/2021**	4.75	2.61	4.14	2.03	0.00	2.03	4.14	0.36	0.00	0.36
106	9/9/2021	1.37	0.07	1.32	0.05	0.00	0.05	1.32	0.00	0.00	0.00
107	9/16-17/2021	0.43	0.00	2.13	0.56	0.00	0.56	2.13	0.00	0.00	0.00
108	9/17/2021	0.00	0.00	0.05	0.00	0.00	0.00	0.05	0.00	0.00	0.00
109	9/22-23/2021	4.29	2.10	3.78	1.96	0.00	1.96	3.78	2.59	0.00	2.59
110	10/25-26/2021	5.72	3.23	5.59	3.10	0.05	3.15	5.59	3.96	0.00	3.96
111	**10/29/2021**	7.09	5.89	5.77	5.77	0.64	6.40	5.77	4.80	0.10	4.90
112	4/05-07/2022	3.15	3.15	2.82	1.40	0.00	1.40	2.82	0.76	0.00	0.76
113	4/07-08/2022	1.63	1.63	1.52	1.07	0.00	1.07	1.52	0.60	0.00	0.60
114	4/18-19/2022	2.67	2.67	2.16	0.76	0.00	0.76	2.16	0.19	0.00	0.19
115	5/03-04/2022	1.35	1.35	1.45	0.25	0.00	0.25	1.45	0.00	0.00	0.00

116	5/06-08/2022	6.50	6.50	2.74	3.33	0.10	3.43	2.74	1.57	0.08	1.65
117	5/16/2022	0.79	0.79	0.53	0.18	0.00	0.18	0.53	0.00	0.00	0.00
118	5/22-23/2022	1.65	1.65	1.96	0.48	0.00	0.48	1.96	0.00	0.00	0.00
119	5/27-28/2022	2.41	2.41	3.30	0.86	1.02	1.88	3.30	1.47	0.64	2.10
120	6/8/2022	2.82	2.82	2.87	0.71	0.00	0.71	2.87	0.64	0.01	0.65
121	6/9/2022	0.66	0.66	0.81	0.43	0.04	0.47	0.81	0.19	0.00	0.19
122	7/1/2022	1.72		2.29	0.14	0.00	0.14	2.29	0.00	0.00	0.00
123	7/02-03/2022	0.80		0.36	0.00	0.00	0.00	0.36	0.00	0.00	0.00
124	7/9/2022	1.37	1.37	1.27	0.38	0.00	0.38	1.27	0.00	0.00	0.00
125	8/5/2022	0.74	0.74	1.50	0.23	0.00	0.23	1.50	0.00	0.00	0.00
126	9/05-06/2022	6.27	6.27	5.77	2.96	0.05	3.00	5.77	2.00	0.00	2.00
127	9/11/2022	2.36	2.36	1.96	0.58	0.00	0.58	1.96	0.17	0.00	0.17
128	10/01-03/2022	2.06	2.06	1.80	0.61	0.00	0.61	1.80	0.00	0.00	0.00
129	10/03-05/2022	2.59	2.59	2.84	1.68	0.00	1.68	2.84	0.79	0.00	0.79
130	10/13-14/2022	1.70	1.70	1.68	0.35	0.00	0.35	1.68	0.01	0.00	0.01
131	3/03-04/2023	1.65	1.65	2.08	0.16	0.21	0.37	2.08	0.67	0.00	0.67
132	3/24-26/2023	1.47	1.47	1.42	0.27	0.00	0.27	1.42	0.02	0.00	0.02
133	**4/28-29-2023**	4.78	4.78	4.39	1.61	0.00	1.61	4.39	0.16	0.00	0.16
134	**4/30-5/1/2023**	1.88	1.88	2.03	1.12	0.00	1.12	2.03	0.35	0.00	0.35
135	7/1/2023	1.68	1.68	0.66	0.00	0.00	0.00	0.66	0.00	0.00	0.00
136	7/21/2023	2.26	2.26	1.63	0.00	0.00	0.00	1.63	0.00	0.00	0.00
137	7/28/2023	1.75	1.75	2.67	0.10	0.00	0.10	2.67	0.00	0.00	0.00
138	**8/6/2023**	2.64	2.64	2.77	1.80	0.00	1.80	2.77	0.15	0.00	0.15
139	**9/10-11/2023**	2.31	2.31	7.16	3.72	0.56	4.27	7.16	3.68	0.00	3.68
140	9/12-13/2023	3.20	3.20	3.25	2.22	0.45	2.67	3.25	5.63	0.32	5.95
141	**9/23-25/2023**	5.64	5.64	5.28	2.75	0.00	2.75	5.28	1.18	0.00	1.18
142	**10/14-15/2023**	1.50	1.50	1.42	0.13	0.00	0.13	1.42	0.00	0.00	0.00
143	11/21-22/2023	5.99	5.99	5.46	2.90	0.04	2.94	5.46	2.45	0.00	2.45
144	**3/23/2024**	3.73	3.73	3.07	1.04	0.00	1.04	3.07	0.44	0.00	0.44
145	3/27/2024	1.57	1.57	1.12	0.28	0.00	0.28	1.12	0.00	0.01	0.01
146	**4/1/2024**	2.90	2.90	2.62	1.17	0.15	1.32	2.62	0.86	0.00	0.86

147	**4/2/2024**	4.88	4.88	4.19	1.24	1.50	2.74	4.19	2.71	0.46	3.17
148	**4/3/2024**	3.68	3.68	2.36	0.94	0.48	1.42	2.36	0.86	0.12	0.98
149	4/4/2024	0.46	0.46	0.36	0.03	0.00	0.03	0.36	0.01	0.00	0.01
150	4/12/2024	0.28	0.28	0.69	0.10	0.00	0.10	0.69	0.00	0.00	0.00
151	5/11-12/2024	1.30	1.30	1.22	0.33	0.00	0.33	1.22	0.00	0.00	0.00
152	5/27/2024	5.00	5.00	3.91	1.45	0.89	2.34	3.91	2.62	0.34	2.96
153	**6/5/2024**	4.24	4.24	3.96	1.55	0.20	1.75	3.96	1.13	0.00	1.13
154	**8/7-8/2024**	2.51	2.51	3.48	0.33	0.00	0.33	3.48	0.00	0.00	0.00
155	**8/8-9/2024**	4.65	4.65	8.19	4.39	0.76	5.16	8.19	7.17	0.17	7.34
156	**8/18/2024**	6.58	6.58	2.82	0.15	0.00	0.15	2.82	0.04	0.00	0.04
157	**9/26/2024**	3.23	3.23	4.78	2.69	0.15	2.84	4.78	2.90	0.00	2.90
158	9/27-28/2024	0.46	0.46	0.51	0.13	0.00	0.13	0.51	0.00	0.00	0.00

[e]error due to ultrasonic sensor problem in underdrain (see text for explanation)

Table SI-3. Rainfall and runoff data for 88 runoff-producing events monitored at two Lewistown (LT) swales during the project (2019-2024). Events with data shown in bold were common events used for water quality comparisons. Data shaded in yellow were collected as part of the CBT-funded project (2022-2025).

Event No.	Dates	LT-GS		LT-BS			
		Rainfall (cm)	Runoff (cm)	Rainfall (cm)	Under-drain runoff (cm)	Flume runoff (cm)	Total runoff (cm)
1	4/12-13/19	3.30	1.83	3.30	2.51	0.03	2.54
2	**4/14/2019**	1.68	1.65	1.68	1.73	0.18	1.91
3	4/15/2019	1.78	1.45	1.78	0.79	0.33	1.12
4	4/19-20/19	3.30	3.05	3.30	1.96	0.56	2.51
5	**5/3/2019**	1.93	0.94	1.93	0.71	0.05	0.76
6	5/4/2019	0.38	0.15	0.38	0.00	0.00	0.00
7	**5/5/2019**	5.11	4.52	5.11	4.90	0.30	5.21
8	5/12/2019	3.07	2.18	3.07	2.57	0.10	2.67
9	5/13/2019	1.19	0.97	1.19	1.07	0.03	1.09
10	5/25/2019	1.09	0.18	1.09	0.13	0.00	0.13
11	5/26/2019	1.47	0.76	1.47	0.89	0.00	0.89
12	5/28/2019	0.48	0.05	0.48	0.00	0.00	0.00
13	6/12/2019	1.91	0.05	1.91	0.08	0.00	0.08
14	**6/13/2019**	1.85	1.14	1.85	2.36	0.15	2.51
15	**6/17/2019**	0.99	0.08	0.99	0.71	0.00	0.71
16	**7/8/2019**	5.59	1.50	5.59	3.81	0.05	3.86
17	**7/22-23/19**	4.45	0.69	4.45	2.46	0.00	2.46
18	**10/27/2019**	4.01	1.42	4.01	3.56	0.00	3.56
19	**10/30/2019**	2.31	0.28	2.31	1.70	0.00	1.70
20	**10/31/2019**	3.28	1.45	3.28	2.18	0.36	2.54
21	4/30/2020	4.24	0.33	4.24	5.61	0.05	5.66
22	5/8/2020	1.04	0.00	1.04	0.33	0.00	0.33

23	6/22/2020	2.77	0.25	2.77	0.81	0.00	0.81
24	6/23/2020	1.02	0.18	1.02	0.51	0.00	0.51
25	8/4/2020	2.77	0.00	2.77	0.25	0.00	0.25
26	8/6/2020	1.09	0.08	1.09	0.13	0.00	0.13
27	**8/12/2020**	1.96	0.56	1.96	0.48	0.00	0.48
28	9/2/2020a	0.86	0.10	0.86	0.00	0.00	0.00
29	9/2/2020b	1.32	0.76	1.32	1.04	0.00	1.04
30	9/3/2020	0.64	0.25	0.64	0.33	0.00	0.33
31	10/11-12/2020	4.42	0.25	4.42	0.38	0.00	0.38
32	**10/29/2020**	3.05	0.46	3.05	1.52	0.00	1.52
33	**11/11/2020**	2.13	0.56	2.13	1.47	0.00	1.47
34	11/12/2020	0.53	0.03	0.53	0.30	0.00	0.30
35	11/30/2020	3.33	0.79	3.33	4.11	0.00	4.11
36	**5/3/2021**	5.18	3.53	5.18	2.69	0.66	3.35
37	5/5/2021	0.69	0.20	0.69	0.00	0.00	0.00
38	**5/28-29/2021**	2.54	0.28	2.54	0.51	0.00	0.51
39	**7/1/2021**	1.88	0.36	1.88	0.36	0.00	0.36
40	7/12/2021	1.60	0.05	1.60	0.03	0.00	0.03
41	**7/17/2021**	2.18	0.38	2.18	0.46	0.00	0.46
42	**8/16/2021**	2.82	0.41	2.82	0.76	0.00	0.76
43	**8/18/2021a**	1.98	1.55	1.98	1.55	0.03	1.57
44	**8/18/2021b**	0.58	0.71	0.58	0.41	0.00	0.41
45	8/20/2021	2.84	2.21	2.84	3.00	0.00	3.00
46	**8/25/2021**	4.55	1.83	4.55	1.45	0.38	1.83
47	8/27/2021	1.24	1.07	1.24	0.66	0.00	0.66
48	8/30/2021	1.27	0.48	1.27	0.41	0.00	0.41
49	**9/1-2/2021**	12.75	12.80	12.75	13.06	2.62	15.67
50	9/8-9/2021	3.71	2.51	3.71	3.91	0.03	3.94
51	9/15/2021	1.40	0.05	1.40	0.23	0.00	0.23
52	9/16/2021	1.22	0.48	1.22	0.94	0.00	0.94
53	9/17/2021	0.89	0.33	0.89	0.86	0.00	0.86

54	9/23/2021	3.23	3.40	3.23	4.95	0.00	4.95
55	**10/29-30/2021**	3.58	2.97	3.58	4.01	0.00	4.01
56	4/05-06/2022	1.45	0.30	1.45	0.73	0.00	0.73
57	4/7/2022	2.16	0.89	2.16	2.39	0.00	2.39
58	4/18/2022	2.11	0.15	2.11	0.43	0.00	0.43
59	5/03-04/2022	1.47	0.28	1.47	0.66	0.00	0.66
60	5/6/2022	5.03	2.79	5.03	5.00	0.00	5.00
61	5/06-07/2022	2.06	0.64	2.06	2.93	0.00	2.93
62	5/27/2022	2.03	N/D	2.03	0.67	0.00	0.67
63	7/9/2022	0.30	0.18	0.30	0.00	0.00	0.00
64	9/06-07/2022	5.74	3.76	5.74	2.74	0.09	2.83
65	9/11/2022	1.09	0.18	1.09	0.99	0.00	0.99
66	9/12/2022	1.68	0.79	1.68	0.98	0.00	0.98
67	9/30-10/1/2022	1.91	0.00	1.91	0.30	0.00	0.30
68	10/2/2022	1.30	0.03	1.30	1.08	0.00	1.08
69	10/4/2022	0.58	0.05	0.58	0.43	0.00	0.43
70	3/24/2023	0.81	0.18	0.81	0.00	0.00	0.00
71	3/25/2023	0.53	0.43	0.53	0.34	0.00	0.34
72	**4/28/2023**	3.96	2.36	3.96	2.91	0.00	2.91
73	**4/30/2023**	2.49	2.64	2.49	1.69	0.00	1.69
74	7/3/2023	1.35	0.08	1.35	0.17	0.00	0.17
75	9/12/2023	2.24	0.00	2.24	0.00	0.00	0.00
76	**3/22-23/2024**	3.18	1.42	3.18	1.14	0.00	1.14
77	**4/1/2024**	2.08	1.24	2.08	1.48	0.00	1.48
78	**4/2/2024**	2.69	2.62	2.69	2.39	0.00	2.39
79	**4/03-04/2024**	2.90	3.56	2.90	3.32	0.00	3.32
80	5/11-12/2024	1.02	0.46	1.02	0.23	0.00	0.23
81	**5/25/2024**	3.58	1.27	3.58	1.11	0.00	1.11
82	**5/26-27/2024**	1.47	0.89	1.47	0.62	0.00	0.62
83	5/27-28/2024	0.76	0.36	0.76	0.26	0.00	0.26

84	**6/5/2024**	2.11	0.15	2.11	0.08	0.00	0.08
85	**6/29-30/2024**	4.52	0.43	4.52	0.70	0.00	0.70
86	**8/07-08/24**	5.18	2.08	5.18	4.48	0.00	4.48
87	**8/08-09/24**	5.89	5.05	5.89	4.18	0.01	4.19
88	9/26/2024	2.69	1.93	2.69	4.10	0.01	4.11
N/A	5/19/2022	N/D	N/D	N/D	N/D	N/D	N/D
N/A	9/23-24/2023	N/D	N/D	N/D	N/D	N/D	N/D

Table SI-4. Maximum rainfall and peak runoff data for 158 runoff-producing events monitored at three Ellicott City (EC) swales during the project (2017-2024). Events with data shown in bold were common events used for water quality comparisons. Data shaded in yellow were collected as part of the CBT-funded project (2022-2025).

Event No.	Dates	EC-GS		EC-BS1				EC-BS2			
		Max hourly rainfall (cm)	Peak runoff (cm hr^{-1})	Max hourly rainfall (cm)	Peak under-drain runoff (cm hr^{-1})	Peak flume runoff (cm hr^{-1})	Peak total runoff (cm hr^{-1})	Max hourly rainfall (cm)	Peak under-drain runoff (cm hr^{-1})	Peak flume runoff (cm hr^{-1})	Peak total runoff (cm hr^{-1})
1	**5/12/2017**	0.16	0.356	0.36	0.203	0.000	0.203				
2	5/19/2017	1.44	0.864	1.68	1.499	0.000	1.499				
3	5/25/2017	1.12	0.381	1.55	0.940	0.203	0.991				
4	7/6/2017	0.39	0.178	1.02	0.838	0.000	0.838				
5	**7/28/2017**	1.07	1.143	1.70	0.940	0.000	0.940				
6	8/15/2017	1.76	2.235	2.59	1.194	1.143	2.108				
7	8/18/2017	3.05	5.105	2.24	0.711	2.235	2.235				
8	9/2/2017	0.37	0.102	0.56	0.102	0.000	0.102				
9	9/5/2017	1.74	0.838	2.29	0.889	0.737	0.889				
10	10/11/2017	0.72	0.203	1.24	0.660	0.000	0.660				
11	11/4/2017	0.44	0.051	0.33	0.127	0.000	0.127				
12	11/7/2017	0.34	0.051	0.38	0.381	0.000	0.381				
13	**4/16/2018**	1.14	0.813	1.52	2.134	0.000	2.134				
14	**4/27/2018**	0.64	0.102	0.33	0.127	0.000	0.127				
15	5/14/2018	1.55	1.194	0.97	0.762	0.000	0.762				
16	**5/15/2018**	3.78	2.540	1.73	1.422	0.711	1.905				
17	5/17/2018	0.42	0.203	0.51	0.254	0.076	0.330				
18	5/28/2018	6.49	7.645	4.39	2.057	3.048	4.851				
19	5/31/2018	1.91	1.143	1.91	1.219	0.584	1.626				
20	**6/2/2018**	0.42	0.178	0.64	0.330	0.076	0.381				
21	6/3/2018	1.91	2.819	1.91	0.813	2.108	2.819				

22	**6/10/2018**	2.00	2.591	1.93	1.219	2.540	3.556				
23	**7/21/2018**	1.39	1.092	1.35	1.626	0.737	1.626				
24	**7/22/2018**	2.10	2.235	1.14	0.787	0.381	1.194				
25	7/23/2018	1.77	0.737	0.53	0.305	0.000	0.305				
26	7/24/2018	0.93	0.635	1.12	0.965	0.381	1.346				
27	7/25/2018	2.00	1.753	0.97	1.295	1.245	2.362				
28	7/31/2018	2.32	0.914	2.13	1.753	1.397	1.753				
29	8/1/2018	1.00	0.660	0.61	0.330	0.178	0.381				
30	8/21/2018	0.72	0.813	1.27	0.635	0.000	0.635				
31	8/31/2018	1.47	0.559	1.37	0.076	0.000	0.076				
33	9/7/2018	0.51	0.025	0.51	0.406	0.076	0.483				
34	9/8/2018	0.46	0.127	0.46	0.229	0.000	0.229				
35	9/9/2018	1.79	0.483	0.36	0.000	0.000	0.000				
36	9/17/2018	0.30	0.025	0.46	0.178	0.000	0.178				
37	9/23/2018	1.08	0.406	1.22	0.584	0.432	0.737				
38	9/27/2018	1.78	1.270	2.06	0.000	0.000	0.000				
39	10/4/2018	0.36	0.076	0.30	0.152	0.000	0.152				
40	**10/26/2018**	0.80	0.432	1.02	0.254	0.991	1.194				
41	3/21-22/19	0.41	0.185	0.25	0.127	0.000	0.127				
42	**5/5/2019**	2.46	2.771	2.46	0.711	1.600	2.261				
43	5/10/2019	0.51	0.739	0.76	0.178	0.762	0.965				
44	5/11-12/19	0.33	0.531	0.33	0.152	0.254	0.406				
45	5/13/2019	1.72	0.693	1.60	0.178	0.000	0.178				
46	5/30/2019	0.51	0.231	0.30	0.000	0.000	0.000				
47	6/13/2019	1.29	0.877	0.46	0.000	0.000	0.000				
48	7/4/2019	1.27	0.716	0.84	0.000	0.000	0.000				
49	7/6/2019	1.33	3.117	1.45	1.168	0.000	1.168				
50	**7/8/2019**	0.74	0.254	1.07	0.254	0.000	0.254				
51	7/11/2019	1.69	0.208	1.45	0.076	0.000	0.076				
52	**7/17/2019**	2.06	0.660	2.06	0.000	0.000	0.000				
53	8/22/2019	0.43	0.076	0.43	0.000	0.000	0.000				

54	8/23/2019	1.63	0.185	1.04	0.203	0.000	0.203				
55	10/16/2019	0.43	0.457	0.36	0.152	0.000	0.152				
56	**10/20/2019**	0.69	0.323	0.69	0.203	0.000	0.203				
57	10/22/2019	1.04	1.473	0.89	1.219	0.000	1.219				
58	**10/27/2019**	0.30	0.178	0.28	0.102	0.000	0.102				
59	**10/30/2019**	3.83	4.595	2.51	1.626	1.956	2.946				
60	**10/31/2019**	0.23	0.254	0.36	0.432	0.000	0.432				
61	3/18-19/2020	0.74	0.508	0.64	0.432	0.000	0.432				
62	3/28/2020	1.14	0.739	1.19	0.787	0.864	1.067				
63	4/12-13/2020	0.36	0.203	0.48	0.203	0.000	0.203				
64	4/24/2020	0.41	0.185	0.36	0.152	0.000	0.152				
65	4/26/2020	0.74	0.406	0.56	0.000	0.000	0.229				
66	4/30/2020	0.48	0.092	0.38	0.051	0.000	0.051				
67	5/3-4/2020	0.36	0.152	0.41	0.127	0.000	0.127				
68	5/6-7/2020	0.38	0.092	0.38	0.051	0.000	0.051				
69	5/8-9/2020	0.43	0.178	0.36	0.051	0.000	0.051				
70	6/5/2020	0.46	0.185	0.74	0.229	0.000	0.229				
71	6/11/2020	4.65	4.775	1.83	0.000	0.000	0.559				
72	6/20/2020	5.77	5.182	2.16	1.219	0.406	1.600				
73	6/22/2020	0.20	0.000	1.09	0.381	0.000	0.381				
74	6/25/2020	1.68	0.531	1.22	0.051	0.000	0.051				
75	**8/3/2020**	1.55	1.422	1.73	2.388	0.152	2.388	1.73	2.438	0.102	2.543
76	**8/4/2020**	0.69	0.577	1.35	0.178	0.000	0.178	1.35	0.008	0.000	0.008
77	**8/12/2020**	0.38	0.115	0.23	0.051	0.000	0.051	0.23	0.000	0.000	0.000
78	8/13/2020	2.36	1.778	4.09	2.464	2.540	4.013	4.09	2.565	2.413	4.780
79	**8/14-15/2020**	0.66	0.508	0.71	0.203	0.000	0.203	0.71	0.277	0.000	0.277
80	8/15-16/2020	0.66	0.254	0.71	0.152	0.000	0.152	0.71	0.000	0.000	0.000
81	8/17/2020	1.07	0.323	0.00	0.000	0.000	0.000	0.00	0.000	0.000	0.000
82	8/24/2020	0.41	0.208	0.51	0.152	0.000	0.152	0.51	0.000	0.000	0.000
83	8/29/2020	1.24	0.808	0.97	0.254	0.000	0.254	0.97	0.259	0.000	0.259
84	9/3/2020	1.65	0.693	0.20	0.000	0.000	0.000	0.20	0.000	0.000	0.000

85	9/29-30/2020	0.61	0.277	0.25	0.203	0.000	0.203	0.25	0.000	0.000	0.000
86	10/11-13/2020	1.19	1.092	0.76	0.711	0.000	0.711	0.76	0.935	0.000	0.935
87	**10/29-30/2020**	0.25	0.076	0.25	0.051	0.000	0.051	0.25	0.000	0.000	0.000
88	3/18-19/2021	1.63	1.224	1.70	0.508	0.584	1.001	1.70	0.785	0.000	0.785
89	3/24/2021	0.41	0.203	0.28	0.102	0.000	0.102	0.28	0.003	0.000	0.003
90	3/28-29/2021	0.66	0.208	0.58	0.127	0.000	0.127	0.58	0.086	0.000	0.086
91	3/31-4/1/2021	0.43	0.152	0.36	0.152	0.000	0.152	0.36	0.043	0.000	0.043
92	4/11/2021	0.33	0.051	0.03	0.000	0.000	0.000	0.03	0.000	0.000	0.000
93	4/11-12/2021	0.25	0.000	0.25	0.025	0.000	0.025	0.25	0.000	0.000	0.000
94	5/8/2021	2.26	0.716	2.13	0.406	0.000	0.406	2.13	0.124	0.000	0.124
95	**5/28-29/2021**	1.80	1.062	3.44	1.041	0.000	1.041	3.44	0.008	0.000	0.008
96	6/14-15/2021	1.35	0.231	2.10	0.000	0.000	0.000	2.10	0.000	0.000	0.000
97	6/21/2021	0.30	0.152	0.46	0.025	0.000	0.025	0.46	0.000	0.000	0.000
98	6/22/2021	0.84	0.178	1.19	0.229	0.000	0.229	1.19	0.000	0.000	0.000
99	**7/01-02/2021**	0.64	0.000	1.50	0.010	0.000	0.010	1.50	0.000	0.000	0.000
100	7/17-18/2021	2.46	0.577	1.57	0.005	0.000	0.005	1.57	0.000	0.000	0.000
101	7/29/2021	1.30	0.577	0.15	0.000	0.000	0.000	0.15	0.000	0.000	0.000
102	8/1/2021	1.42	0.139	0.99	0.000	0.000	0.000	0.99	0.000	0.000	0.000
103	8/10/2021	1.68	1.247	0.48	0.218	0.000	0.218	0.48	0.000	0.000	0.000
104	**8/17-19/2021**	0.46	0.300	0.41	0.000	0.000	0.000	0.41	0.000	0.000	0.000
105	8/20/2021	2.49	2.032	2.31	1.542	0.000	1.542	2.31	0.516	0.000	0.516
106	**9/1-2/2021**	0.99	0.046	1.12	0.018	0.000	0.018	1.12	0.000	0.000	0.000
107	9/9/2021	0.20	0.000	1.83	0.498	0.000	0.498	1.83	0.000	0.000	0.000
108	9/16-17/2021	0.00	0.000	0.15	0.003	0.000	0.003	0.15	0.000	0.000	0.000
109	9/17/2021	1.80	1.501	0.89	0.607	0.000	0.607	0.89	1.623	0.000	1.623
110	9/22-23/2021	1.85	0.854	1.45	0.940	0.102	0.955	1.45	2.057	0.000	2.057
111	10/25-26/2021	1.83	1.778	1.07	1.981	0.457	2.423	1.07	1.643	0.208	1.831
112	**10/29/2021**	2.06	0.432	0.53	0.254	0.000	0.254	0.53	0.312	0.000	0.312
113	4/05-07/2022	0.64	0.254	0.08	0.137	0.000	0.137	0.08	0.071	0.000	0.071
114	4/07-08/2022	0.41	0.279	0.71	0.226	0.000	0.226	0.71	0.091	0.000	0.091
115	4/18-19/2022	0.81	0.025	0.48	0.086	0.000	0.086	0.48	0.000	0.000	0.000

116	5/03-04/2022	0.71	0.635	0.23	0.279	0.203	0.445	0.23	0.401	0.216	0.427
117	5/06-08/2022	0.94	0.356	0.53	0.119	0.000	0.119	0.53	0.000	0.000	0.000
118	5/16/2022	0.74	0.279	0.94	0.236	0.000	0.236	0.94	0.000	0.000	0.000
119	5/22-23/2022	0.69	1.676	2.54	0.660	1.905	2.487	2.54	1.753	2.040	3.345
120	5/27-28/2022	1.88	1.219	1.85	0.686	0.000	0.686	1.85	0.884	0.089	0.973
121	6/8/2022	2.13	0.203	0.76	0.203	0.124	0.203	0.76	0.076	0.000	0.076
122	6/9/2022	0.58	0.000	1.50	0.147	0.000	0.305	1.50	0.000	0.000	0.000
123	7/1/2022	1.26	0.584	0.28	0.000	0.000	0.000	0.28	0.000	0.000	0.000
124	7/02-03/2022	2.38	0.076	0.28	0.089	0.000	0.089	0.28	0.003	0.000	0.003
125	7/9/2022	0.23	0.000	1.45	0.191	0.000	0.191	1.45	0.000	0.000	0.000
126	8/5/2022	0.61	1.270	2.16	2.093	0.140	2.131	2.16	1.750	0.000	1.750
127	9/05-06/2022	2.24	0.279	0.91	0.135	0.000	0.135	0.91	0.056	0.000	0.056
128	9/11/2022	0.97	0.094	0.25	0.061	0.000	0.061	0.25	0.000	0.000	0.000
129	10/01-03/2022	0.25	0.483	0.61	0.417	0.000	0.417	0.61	0.378	0.000	0.378
130	10/03-05/2022	0.66	0.076	0.33	0.066	0.000	0.066	0.33	0.015	0.000	0.015
131	10/13-14/2022	0.51	0.327	0.89	0.210	0.427	0.637	0.89	0.712	0.012	0.712
132	3/03-04/2023	0.48	0.121	0.46	0.116	0.000	0.116	0.46	0.005	0.000	0.005
133	3/24-26/2023	0.46	0.298	0.58	0.191	0.000	0.191	0.58	0.048	0.000	0.048
134	**4/28-29-2023**	0.56	0.603	1.12	0.448	0.000	0.448	1.12	0.456	0.000	0.456
135	**4/30-5/1/2023**	1.07	0.093	0.48	0.000	0.000	0.000	0.48	0.000	0.000	0.000
136	7/1/2023	1.60	0.512	1.40	0.000	0.000	0.000	1.40	0.000	0.000	0.000
137	7/21/2023	1.93	0.477	2.01	0.115	0.000	0.115	2.01	0.000	0.000	0.000
138	7/28/2023	1.73	1.866	1.24	1.811	0.000	1.811	1.24	0.191	0.000	0.191
139	**8/6/2023**	0.74	0.000	3.99	1.738	0.975	2.549	3.99	2.046	0.000	2.046
140	**9/10-11/2023**	1.19	2.174	2.03	1.187	0.594	1.665	2.03	3.500	0.617	3.830
141	9/12-13/2023	2.11	0.578	0.84	0.682	0.000	0.682	0.84	0.768	0.000	0.768
142	**9/23-25/2023**	1.07	0.106	0.56	0.035	0.000	0.035	0.56	0.000	0.000	0.000
143	**10/14-15/2023**	0.53	1.081	1.14	0.945	0.141	1.086	1.14	1.516	0.000	1.516
144	11/21-22/2023	0.97	0.419	0.58	0.229	0.000	0.229	0.58	0.196	0.000	0.196
145	**3/23/2024**	0.69	0.168	0.38	0.102	0.000	0.102	0.38	0.003	0.000	0.003
146	3/27/2024	0.46	0.991	1.09	0.432	0.381	0.813	1.09	0.968	0.000	0.968

147	**4/1/2024**	1.35	1.753	2.01	0.203	1.321	1.321	2.01	1.676	0.572	2.164
148	**4/2/2024**	2.13	1.245	0.79	0.152	0.381	0.533	0.79	0.422	0.163	0.584
149	**4/3/2024**	1.52	0.076	0.20	0.010	0.000	0.010	0.20	0.003	0.000	0.003
150	4/4/2024	0.25	0.000	0.38	0.051	0.000	0.051	0.38	0.000	0.000	0.000
151	4/12/2024	0.20	0.305	0.79	0.203	0.000	0.203	0.79	0.000	0.000	0.000
152	5/11-12/2024	0.91	4.775	3.71	1.194	1.676	2.642	3.71	3.312	1.034	3.823
153	5/27/2024	4.72	1.499	3.00	0.940	0.483	1.397	3.00	1.240	0.000	1.240
154	**6/5/2024**	3.02	0.178	0.46	0.152	0.000	0.152	0.46	0.000	0.000	0.000
155	**8/7-8/2024**	0.58	2.261	3.72	1.753	0.914	2.642	3.72	2.863	0.607	3.216
156	**8/8-9/2024**	2.72	3.023	1.12	0.076	0.000	0.076	1.12	0.051	0.000	0.051
157	**8/18/2024**	2.67	1.372	1.45	1.854	0.356	2.162	1.45	2.868	0.003	2.868
158	**9/26/2024**	1.85	0.065	0.05	0.102	0.000	0.102	0.05	0.000	0.000	0.000

Table SI-5. Maximum rainfall and peak runoff data for 88 runoff-producing events monitored at two Lewistown (LT) swales during the project (2019-2024). Events with data shown in bold were common events used for water quality comparisons. Data shaded in yellow were collected as part of the CBT-funded project (2022-2025).

Event No.	Dates	LT-GS		LT-BS	
		Max hourly rainfall (cm)	Peak runoff (cm/hr)	Max hourly rainfall (cm)	Peak runoff (cm/hr)
1	4/12-13/19	1.17	0.762	1.17	1.52
2	**4/14/2019**	1.57	1.524	1.57	1.14
3	4/15/2019	1.17	1.168	1.17	0.67
4	4/19-20/19	1.70	1.245	1.70	1.51
5	**5/3/2019**	1.88	1.549	1.88	0.46
6	5/4/2019	0.38	0.203	0.38	0.00
7	**5/5/2019**	0.84	1.092	0.84	3.12
8	5/12/2019	0.71	0.838	0.71	1.60
9	5/13/2019	0.38	0.406	0.38	0.66
10	5/25/2019	0.97	0.178	0.97	0.08
11	5/26/2019	1.27	0.813	1.27	0.53
12	5/28/2019	0.48	0.051	0.48	0.00
13	6/12/2019	0.51	0.076	0.51	0.05
14	**6/13/2019**	1.80	1.524	1.80	1.51
15	**6/17/2019**	0.76	0.102	0.76	0.43
16	**7/8/2019**	1.78	1.422	1.78	2.32
17	**7/22-23/19**	1.93	0.686	1.93	1.48
18	**10/27/2019**	1.52	0.660	1.52	2.13
19	**10/30/2019**	0.46	0.152	0.46	1.02
20	**10/31/2019**	2.44	1.727	2.44	1.52
21	4/30/2020	1.04	0.381	1.04	3.40
22	5/8/2020	0.64	0.025	0.64	0.20
23	6/22/2020	2.39	0.559	2.39	0.49
24	6/23/2020	0.91	0.229	0.91	0.30

25	8/4/2020	0.56	0.000	0.56	0.15
26	8/6/2020	1.02	0.076	1.02	0.08
27	**8/12/2020**	1.85	0.356	1.85	0.29
28	9/2/2020a	0.28	0.051	0.28	0.00
29	9/2/2020b	1.32	0.559	1.32	0.62
30	9/3/2020	0.64	0.229	0.64	0.20
31	10/11-12/2020	0.48	0.102	0.48	0.23
32	**10/29/2020**	0.53	0.127	0.53	0.91
33	**11/11/2020**	0.53	0.406	0.53	0.88
34	11/12/2020	0.36	0.051	0.36	0.18
35	11/30/2020	0.79	0.279	0.79	2.47
36	**5/3/2021**	3.45	2.362	3.45	2.01
37	5/5/2021	0.36	0.076	0.36	0.00
38	**5/28-29/2021**	0.41	0.152	0.41	0.30
39	**7/1/2021**	1.07	0.330	1.07	0.21
40	7/12/2021	1.60	0.051	1.60	0.02
41	**7/17/2021**	1.98	0.381	1.98	0.27
42	**8/16/2021**	2.11	0.381	2.11	0.46
43	**8/18/2021a**	1.96	1.041	1.96	0.94
44	**8/18/2021b**	0.53	0.432	0.53	0.24
45	8/20/2021	1.45	0.737	1.45	1.80
46	**8/25/2021**	4.52	1.880	4.52	1.10
47	8/27/2021	1.24	0.762	1.24	0.40
48	8/30/2021	0.81	0.279	0.81	0.24
49	**9/1-2/2021**	3.00	2.413	3.00	9.40
50	9/8-9/2021	2.39	0.914	2.39	2.36
51	9/15/2021	1.19	0.051	1.19	0.14
52	9/16/2021	0.81	0.254	0.81	0.56
53	9/17/2021	0.84	0.152	0.84	0.52
54	9/23/2021	1.24	0.864	1.24	2.97
55	**10/29-30/2021**	0.97	0.813	0.97	2.41

56	4/05-06/2022	0.46	0.229	0.46	0.73
57	4/7/2022	0.66	0.508	0.66	2.39
58	4/18/2022	0.41	0.152	0.41	0.43
59	5/03-04/2022	0.58	0.305	0.58	0.66
60	5/6/2022	0.81	0.660	0.81	5.00
61	5/06-07/2022	0.41	0.229	0.41	2.93
62	5/27/2022	1.98	0.000	1.98	0.67
63	7/9/2022	0.18	0.152	0.18	0.00
64	9/06-07/2022	2.84	1.803	2.84	2.83
65	9/11/2022	0.46	0.076	0.46	0.99
66	9/12/2022	1.60	0.610	1.60	0.98
67	9/30-10/1/2022	0.66	0.000	0.66	0.30
68	10/2/2022	0.36	0.025	0.36	1.08
69	10/4/2022	0.41	0.051	0.41	0.43
70	3/24/2023	0.25	0.076	0.25	0.00
71	3/25/2023	0.51	0.229	0.51	0.34
72	**4/28/2023**	0.74	0.660	0.74	2.91
73	**4/30/2023**	0.99	0.991	0.99	1.69
74	7/3/2023	1.27	0.152	1.27	0.17
75	9/12/2023	2.16	0.000	2.16	0.00
76	**3/22-23/2024**	0.43	0.406	0.43	1.14
77	**4/1/2024**	0.71	0.381	0.71	1.48
78	**4/2/2024**	0.84	0.940	0.84	2.39
79	**4/03-04/2024**	0.89	1.194	0.89	3.32
80	5/11-12/2024	0.58	0.305	0.58	0.23
81	**5/25/2024**	3.28	1.956	3.28	1.11
82	**5/26-27/2024**	1.42	0.660	1.42	0.62
83	5/27-28/2024	0.74	0.152	0.74	0.26
84	**6/5/2024**	1.63	0.051	1.63	0.08
85	**6/29-30/2024**	2.41	0.330	2.41	0.70
86	**8/07-08/24**	1.98	0.483	1.98	4.48

87	**8/08-09/24**	1.45	0.965	1.45	4.19
88	9/26/2024	1.50	1.067	1.50	4.11
N/A	5/19/2022	N/D	N/D	N/D	N/D
N/A	9/23-24/2023	N/D	N/D	N/D	N/D

Table SI-6(A). Flume event mean concentrations (EMCs) for all events characterized at EC-BS1 (2017-24). Note that blue-shaded winter events were not included in statistical analyses. Data shaded in yellow were collected as part of the CBT-funded project (2022-2025).

Event No.	Dates	Spec. Cond. (µS/cm)	TSS (mg/L)	ANC (µeq/L)	Chloride (mg/L)	Sulfate (mg/L)	Ortho-P (mg/L)	Ammonia-N (mg/L)	Nitrite-N (mg/L)	Nitrate-N + Nitrite-N (mg/L)	Nitrate-N (mg/L)	DON (mg/L, calc.)
1	5/12/2017	68.98	8.10		5.74	0.72	0.19	0.05	0.01	0.04	0.03	0.67
16	5/15/2018	144.32	9.48	526.15	23.58	2.10	0.12	0.05	0.01	0.14	0.13	0.98
18	5/28/2018	106.16	10.56	271.17	23.79	0.83	0.31	0.02	0.00	0.01	0.00	0.39
19	5/31/2018	113.18	16.90	381.47	19.09	1.54	0.28	0.60	0.02	0.03	0.01	1.22
22	6/10/2018	110.29	6.52	500.82	15.66	1.12	0.18	0.05	0.01	0.14	0.13	0.78
23	7/21/2018	74.63	1.98	583.76	4.45	0.49	0.10	0.01	0.00	0.01	0.00	0.31
59	10/31/2019	73.87	6.73	568.85	5.79	1.14	0.34	0.03	0.01	0.06	0.05	0.71
75	8/4/2020	87.61	6.81	753.79	2.99	0.88	0.42	0.05	0.01	0.05	0.04	0.52
78	8/14/2020	45.97	5.13	317.17	2.45	0.87	0.22	0.09	0.01	0.22	0.21	0.76
N/A	12/24/2020	750.16	46.51	502.93	205.45	1.80	0.11	0.05	0.01	0.11	0.10	0.34
88	3/24/2021	733.07	35.90	694.21	205.56	2.90	0.35	0.30	0.01	0.55	0.54	1.11
111	10/29/2021	129.70	9.50	735.18	8.67	1.59	0.51	0.01	0.01	0.05	0.04	0.58
139	9/10/2023	61.43	2.20	391.51	4.28	1.47	0.31	0.01	0.01	0.11	0.10	0.64
140	9/12/2023	74.73	6.94	533.73	4.40	1.39	0.25	0.02	0.01	0.07	0.07	0.90
146	4/1/2024	243.63	47.95	738.65	48.47	1.76	0.16	0.07	0.01	0.23	0.21	0.78
147	4/2/2024	127.46	128.18	723.40	19.46	0.76	0.12	0.04	0.01	0.10	0.09	0.34
152	5/27/2024	129.15	19.22	377.81	21.35	1.33	0.48	0.08	0.02	0.20	0.18	1.02
153	6/5/2024	125.10	14.51	440.77	18.52	1.37	0.46	0.07	0.02	0.24	0.22	1.23
155	8/8/2024	116.54	6.39	891.98	6.77	1.23	0.22	0.01	0.00	0.01	0.01	0.66
157	9/26/2024	73.71	7.31	554.09	3.32	0.97	0.20	0.02	0.01	0.03	0.02	0.53

Table SI-6(B). Flume event mean concentrations (EMCs) for all events characterized at EC-BS1 (2017-24). Note that blue-shaded winter events were not included in statistical analyses. Data shaded in yellow were collected as part of the CBT-funded project (2022-2025).

Event No.	Dates	Total P (mg/L)	Total Dissolved P (mg/L)	DOP (mg/L, calculated)	Total Nitrogen (mg/L)	Total Dissolved N (mg/L)	Particulate N (mg/L, calculated)	Particulate P (mg/L, calculated)	DOC (mg/L)
1	5/5/2017	0.29	0.22	0.02	1.17	0.77	0.40	0.08	
16	5/15/2018	0.24	0.15	0.03	1.76	1.17	0.59	0.09	18.89
18	5/28/2018	0.48	0.37	0.06	0.96	0.42	0.54	0.11	8.32
19	5/31/2018	0.51	0.36	0.09	2.77	1.85	0.92	0.15	14.45
22	6/10/2018	0.31	0.21	0.03	1.53	0.98	0.55	0.10	12.07
23	7/21/2018	0.15	0.13	0.02	0.47	0.33	0.13	0.02	5.64
59	10/31/2019	0.44	0.37	0.03	1.19	0.81	0.38	0.07	10.67
75	8/4/2020	0.47	0.43	0.01	0.82	0.61	0.21	0.04	8.43
78	8/14/2020	0.37	0.33	0.11	1.32	1.07	0.25	0.04	9.90
N/A	12/24/2020	0.19	0.12	0.01	0.88	0.50	0.38	0.07	3.92
88	3/24/2021	0.50	0.39	0.04	2.53	1.96	0.57	0.11	10.36
111	10/29/2021	0.62	0.54	0.03	1.09	0.64	0.45	0.09	7.47
139	9/10/2023	0.37	0.33	0.02	1.01	0.76	0.25	0.04	10.17
140	9/12/2023	0.34	0.28	0.03	1.34	0.99	0.35	0.06	15.39
146	4/1/2024	0.34	0.18	0.03	1.55	1.07	0.48	0.16	10.11
147	4/2/2024	0.43	0.14	0.02	1.18	0.47	0.71	0.29	5.78
152	5/27/2024	0.68	0.52	0.04	2.15	1.30	0.85	0.16	13.69
153	6/5/2024	0.67	0.50	0.04	2.39	1.55	0.84	0.16	16.23
155	8/8/2024	0.30	0.25	0.02	0.99	0.68	0.31	0.06	9.77
157	9/26/2024	0.28	0.22	0.02	0.85	0.57	0.28	0.06	6.60

Table SI-6(C). Flume event mean concentrations (EMCs) for all events characterized at EC-BS1 (2017-24). Note that blue-shaded winter events were not included in statistical analyses. Data shaded in yellow were collected as part of the CBT-funded project (2022-2025).

Event No.	Dates	Cr (µg/L)	Cu (µg/L)	Zn (µg/L)	Cd (µg/L)	Pb (µg/L)	Na (mg/L)	K (mg/L)	Mg (mg/L)	Ca (mg/L)
1	5/5/2017	0.99	6.62	48.25	0.03	0.43	12.70	3.82	0.22	0.83
16	5/15/2018	0.63	14.17	66.62	0.06	0.51	27.92	1.98	0.27	1.54
18	5/28/2018	0.32	2.61	54.03	0.03	0.22	9.78	5.99	0.20	0.81
19	5/31/2018	0.43	3.92	73.89	0.05	0.44	11.22	6.73	0.47	1.84
22	6/10/2018	0.30	2.96	58.68	0.03	0.35	17.69	5.02	0.37	2.24
23	7/21/2018	0.25	2.65	16.11	0.02	0.36	15.27	1.12	0.28	1.17
59	10/31/2019	0.67	4.18	14.25	0.03	0.69	16.43	3.18	0.56	1.38
75	8/4/2020	0.29	4.29	7.91	0.02	0.19	11.81	4.68	0.83	2.19
78	8/14/2020	0.24	3.05	3.88	0.03	0.31	6.35	3.58	0.47	1.47
N/A	12/24/2020	0.18	2.31	10.71	0.03	0.11	113.15	5.00	3.29	24.43
88	3/24/2021	0.74	8.18	7.40	0.04	0.37	143.59	5.38	0.79	7.10
111	10/29/2021	0.40	3.56	5.51	0.04	0.28	24.95	4.76	0.45	1.38
139	9/10/2023	0.41	3.81	5.90	0.02	0.15	9.05	4.20	0.55	1.40
140	9/12/2023	0.29	4.41	5.72	0.02	0.22	12.35	3.05	0.73	2.38
146	4/1/2024	0.32	4.56	5.00	0.03	0.26	48.29	0.94	0.44	3.26
147	4/2/2024	0.17	2.10	1.11	0.04	0.12	27.22	0.85	0.30	1.91
152	5/27/2024	0.28	4.26	5.35	0.02	0.15	18.13	11.80	0.36	1.39
153	6/5/2024	0.69	7.08	6.28	0.03	0.23	20.05	6.31	0.38	1.50
155	8/8/2024	0.22	3.25	4.48	0.03	0.23	20.84	3.42	0.66	2.16
157	9/26/2024	0.54	3.89	4.90	0.04	0.22	12.45	2.95	0.52	1.78

Table SI-7(A). Underdrain event mean concentrations (EMCs) for all events characterized at EC-BS1 (2017-24). Note that blue-shaded winter events were not included in statistical analyses. Data shaded in yellow were collected as part of the CBT-funded project (2022-2025).

Event No.	Dates	Spec. Cond. (µS/cm)	TSS (mg/L)	ANC (µeq/L)	Chloride (mg/L)	Sulfate (mg/L)	Ortho-P (mg/L)	Ammonia-N (mg/L)	Nitrite-N (mg/L)	Nitrate-N + Nitrite-N (mg/L)	Nitrate-N (mg/L)	DON (mg/L, calc.)
N/A	4/6/2017	695.27	15.31	N/D	133.60	7.31	0.07	0.06	0.01	0.86	0.85	1.42
N/A	4/25/2017	541.67	14.75	N/D	81.55	10.57	0.06	0.04	0.02	0.43	0.41	1.95
N/A	5/5/2017	260.94	13.66	N/D	27.25	5.15	0.12	0.07	0.01	0.31	0.30	1.46
1	5/12/2017	357.50	8.20	N/D	33.00	4.19	0.06	0.03	0.01	0.11	0.09	1.63
5	7/28/2017	288.84	11.38	N/D	23.71	10.41	0.16	0.02	0.01	0.50	0.49	1.45
N/A	2/10/2018	1357.47	8.03	1038.00	353.38	7.15	0.12	0.16	0.01	1.72	1.71	0.55
13	4/16/2018	1127.14	6.33	1048.52	272.68	4.89	0.03	0.06	0.00	0.58	0.58	0.85
14	4/27/2018	790.91	8.90	2406.69	148.87	4.55	0.06	0.03	0.01	0.28	0.27	1.45
16	5/15/2018	388.42	19.15	2420.16	56.43	3.59	0.07	0.03	0.02	0.34	0.32	1.63
20	6/2/2018	445.72	6.16	2888.16	51.95	3.45	0.05	0.02	0.01	0.87	0.86	1.68
22	6/10/2018	355.44	8.26	2677.31	22.44	5.41	0.05	0.03	0.01	2.38	2.37	0.82
23	7/21/2018	166.64	11.66	1191.55	11.53	3.83	0.04	0.02	0.01	0.24	0.23	0.89
24	7/22/2018	197.63	16.53	1674.07	9.78	2.92	0.04	0.02	0.01	0.13	0.12	0.97
39	10/26/2018	245.11	3.15	1709.46	14.03	9.90	0.03	0.01	0.00	1.60	1.60	0.86
N/A	4/15/2019	1119.88	5.79	N/D	239.29	11.63	0.04	0.04	0.02	0.98	0.97	1.80
41	5/5/2019	937.61	6.75	2998.98	198.95	12.77	0.04	0.04	0.02	0.76	0.74	2.24
49	7/8/2019	304.54	26.97	2044.50	25.48	12.40	0.07	0.03	0.02	0.56	0.54	2.19
51	7/17/2019	497.11	23.13	3738.02	39.18	16.36	0.06	0.14	0.03	2.12	2.10	2.12
54	10/16/2019	370.52	8.10	1061.31	61.81	32.61	0.14	0.03	0.02	2.41	2.40	1.72
55	10/20/2019	417.30	5.28	1687.27	68.14	16.25	0.06	0.03	0.02	1.29	1.28	2.10
57	10/27/2019	284.69	9.25	1919.79	23.59	12.91	0.09	0.04	0.02	1.32	1.30	1.66

58	10/30/2019	285.64	6.14	2118.61	22.49	6.40	0.07	0.03	0.01	0.59	0.58	1.84
59	10/31/2019	241.26	10.92	2052.63	11.54	6.07	0.08	0.02	0.01	0.92	0.90	1.29
74	8/3/2020	338.63	14.82	1669.80	25.63	26.00	0.05	0.05	0.01	5.05	5.04	1.82
75	8/4/2020	199.19	10.47	1351.49	10.45	8.48	0.06	0.02	0.01	2.97	2.97	0.96
76	8/12/2020	250.27	9.38	2088.73	8.86	9.31	0.03	0.04	0.01	1.35	1.35	2.12
78	8/14/2020	155.29	5.45	1451.56	2.94	2.98	0.03	0.03	0.01	1.19	1.19	1.11
86	10/29/2020	221.57	6.99	1314.78	16.03	11.41	0.03	0.03	0.01	2.00	1.99	1.28
N/A	11/11/2020	212.72	5.68	1428.79	14.25	7.73	0.02	0.01	0.01	1.45	1.44	1.02
N/A	12/24/2020	1486.85	1.00	618.84	433.43	3.42	0.01	0.01	0.00	0.42	0.42	0.25
N/A	2/15/2021	5007.61	2.72	740.78	1843.36	11.82	0.01	0.13	0.01	1.46	1.45	0.29
N/A	3/18/2021	3376.83	3.21	1350.34	960.81	12.21	0.02	0.05	0.01	2.99	2.98	1.09
88	3/24/2021	1853.31	7.13	1434.14	502.27	8.21	0.03	0.02	0.01	2.46	2.45	0.99
90	3/31/2021	1312.21	3.92	2622.07	334.40	6.26	0.04	0.03	0.01	0.76	0.74	1.91
94	5/28/2021	634.71	19.65	1921.77	129.39	10.74	0.05	0.04	0.03	0.72	0.70	1.95
98	7/1/2021	468.98	33.96	3095.60	49.25	7.64	0.08	0.09	0.06	0.66	0.60	4.69
103	8/17/2021	537.69	15.22	3150.88	69.10	9.89	0.08	0.08	0.04	0.67	0.63	3.75
105	9/1/2021	369.17	36.51	2273.78	37.28	12.61	0.08	0.04	0.03	1.43	1.40	2.97
111	10/29/2021	131.84	11.85	1299.49	14.23	2.84	0.09	0.02	0.01	0.33	0.32	0.91
133	4/28/2023	163.91	9.58	1350.89	5.14	3.45	0.08	0.02	0.01	0.56	0.55	1.19
134	4/30/2023	169.77	12.01	1524.07	2.71	1.95	0.06	0.02	0.01	0.42	0.41	1.26
138	8/6/2023	220.07	11.51	1395.63	9.44	15.31	0.08	0.03	0.01	2.15	2.13	1.47
139	9/10/2023	144.23	14.74	953.11	7.24	7.91	0.09	0.02	0.01	0.69	0.68	1.25
141	9/23/2023	179.37	4.34	1473.95	7.41	4.60	0.05	0.02	0.01	0.16	0.16	1.14
142	10/14/2023	245.66	6.72	1667.51	16.37	9.81	0.04	0.03	0.01	0.50	0.49	1.61
144	3/23/2024	545.57	4.35	1292.97	121.12	3.36	0.05	0.02	0.01	0.40	0.39	0.89

146	4/1/2024	417.46	8.76	1962.83	65.07	3.32	0.06	0.02	0.01	0.44	0.43	1.01
147	4/2/2024	293.71	7.23	1530.29	41.67	1.44	0.06	0.02	0.01	0.09	0.09	0.78
148	4/3/2024	277.18	3.92	1594.27	34.70	1.14	0.06	0.01	0.01	0.05	0.05	0.61
153	6/5/2024	273.43	16.66	1848.83	19.50	4.55	0.08	0.04	0.01	1.49	1.48	1.66
154	8/7/2024	307.28	3.43	2070.84	24.44	6.38	0.06	0.03	0.01	0.67	0.66	2.10
155	8/8/2024	237.83	5.40	1738.23	13.95	4.67	0.08	0.02	0.01	1.19	1.18	1.31
156	8/18/2024	311.64	8.48	2376.89	10.82	8.15	0.06	0.03	0.01	2.98	2.97	1.75
157	9/26/2024	164.51	14.82	1101.77	7.62	6.96	0.07	0.03	0.01	0.61	0.60	1.27

Table SI-7(B). Underdrain event mean concentrations (EMCs) for all events characterized at EC-BS1 (2017-24). Note that blue-shaded winter events were not included in statistical analyses. Data shaded in yellow were collected as part of the CBT-funded project (2022-2025).

Event No.	Dates	Total P (mg/L)	Total Dissolved P (mg/L)	DOP (mg/L, calculated)	Total Nitrogen (mg/L)	Total Dissolved N (mg/L)	Particulate N (mg/L, calculated)	Particulate P (mg/L, calculated)	DOC (mg/L)
N/A	4/6/2017	0.19	0.13	0.05	2.66	2.35	0.31	0.07	N/D
N/A	4/25/2017	0.22	0.14	0.00	2.78	2.42	0.36	0.08	N/D
N/A	5/5/2017	0.26	0.18	0.06	2.35	1.86	0.49	0.08	N/D
1	5/12/2017	0.16	0.13	0.07	1.92	1.77	0.15	0.03	N/D
5	7/28/2017	0.30	0.23	0.07	2.28	1.98	0.31	0.07	N/D
N/A	2/10/2018	0.20	0.15	0.02	2.62	2.44	0.18	0.05	7.40
13	4/16/2018	0.09	0.06	0.02	1.68	1.50	0.18	0.04	11.94
14	4/27/2018	0.16	0.12	0.06	1.94	1.76	0.18	0.04	26.19
16	5/15/2018	0.24	0.16	0.09	2.34	1.99	0.35	0.08	29.08
20	6/2/2018	0.15	0.13	0.08	2.72	2.58	0.14	0.02	20.94
22	6/10/2018	0.12	0.08	0.03	3.49	3.23	0.25	0.04	12.82
23	7/21/2018	0.14	0.10	0.05	1.24	1.15	0.10	0.04	13.77
24	7/22/2018	0.20	0.13	0.08	1.27	1.13	0.14	0.07	18.34
39	10/26/2018	0.08	0.05	0.02	2.66	2.47	0.19	0.03	12.99
N/A	4/15/2019	0.14	0.11	0.07	3.15	2.82	0.33	0.03	32.62
41	5/5/2019	0.16	0.12	0.08	3.25	3.04	0.21	0.04	37.18
49	7/8/2019	0.28	0.20	0.12	7.42	2.78	4.84	0.08	32.78
51	7/17/2019	0.24	0.18	0.14	4.64	4.39	0.24	0.06	39.06
54	10/16/2019	0.38	0.21	0.07	4.49	4.17	0.47	0.17	22.12
55	10/20/2019	0.18	0.15	0.09	3.47	3.32	0.10	0.03	28.32
57	10/27/2019	0.19	0.15	0.06	3.14	3.01	0.14	0.04	23.83

58	10/30/2019	0.17	0.14	0.08	2.51	2.46	0.04	0.03	27.41
59	10/31/2019	0.16	0.13	0.05	2.40	2.23	0.17	0.03	21.05
74	8/3/2020	0.19	0.10	0.06	8.15	6.92	1.23	0.08	33.58
75	8/4/2020	0.14	0.10	0.04	4.21	3.95	0.26	0.04	16.81
76	8/12/2020	0.14	0.08	0.05	3.86	3.51	0.37	0.06	26.06
78	8/14/2020	0.08	0.08	0.05	2.43	2.33	0.10	0.00	15.70
86	10/29/2020	0.09	0.06	0.04	3.34	3.31	0.06	0.02	16.08
N/A	11/11/2020	0.08	0.05	0.03	2.63	2.48	0.15	0.03	12.21
N/A	12/24/2020	0.02	0.02	0.01	0.68	0.67	0.01	0.01	2.47
N/A	2/15/2021	0.03	0.02	0.01	1.92	1.88	0.05	0.01	2.76
N/A	3/18/2021	0.09	0.05	0.04	4.28	4.13	0.15	0.04	3.26
88	3/24/2021	0.09	0.06	0.03	3.62	3.48	0.14	0.03	12.31
90	3/31/2021	0.11	0.09	0.05	2.75	2.69	0.06	0.02	24.90
94	5/28/2021	0.26	0.16	0.10	4.28	2.71	1.57	0.10	37.02
98	7/1/2021	0.43	0.32	0.24	5.82	5.44	0.38	0.11	68.05
103	8/17/2021	0.30	0.24	0.17	4.69	4.51	0.18	0.06	52.14
105	9/1/2021	0.34	0.23	0.15	4.77	4.44	0.33	0.11	36.58
111	10/29/2021	0.20	0.15	0.05	1.53	1.26	0.27	0.05	12.29
133	4/28/2023	0.18	0.13	0.05	1.98	1.78	0.21	0.05	16.18
134	4/30/2023	0.18	0.13	0.07	1.94	1.71	0.23	0.05	19.62
138	8/6/2023	0.19	0.13	0.05	3.89	3.65	0.23	0.06	22.23
139	9/10/2023	0.19	0.14	0.05	2.17	1.97	0.21	0.06	18.10
141	9/23/2023	0.12	0.09	0.04	1.48	1.33	0.15	0.03	17.24
142	10/14/2023	0.13	0.10	0.06	2.27	2.13	0.14	0.03	23.83
144	3/23/2024	0.11	0.08	0.03	1.44	1.31	0.12	0.03	10.81

146	4/1/2024	0.13	0.10	0.04	1.59	1.47	0.12	0.04	15.47
147	4/2/2024	0.12	0.10	0.03	0.99	0.89	0.09	0.02	12.63
148	4/3/2024	0.10	0.09	0.03	0.74	0.68	0.06	0.02	10.10
153	6/5/2024	0.21	0.14	0.07	3.46	3.19	0.26	0.07	20.82
154	8/7/2024	0.14	0.12	0.06	2.86	2.80	0.07	0.02	31.27
155	8/8/2024	0.14	0.12	0.04	2.61	2.52	0.09	0.03	18.34
156	8/18/2024	0.16	0.12	0.06	4.91	4.76	0.15	0.04	23.05
157	9/26/2024	0.19	0.12	0.05	2.17	1.91	0.27	0.07	15.54

Table SI-7(C). Underdrain event mean concentrations (EMCs) for all events characterized at EC-BS1 (2017-24). Note that blue-shaded winter events were not included in statistical analyses. Data shaded in yellow were collected as part of the CBT-funded project (2022-2025).

Event No.	Dates	Cr (μg/L)	Cu (μg/L)	Zn (μg/L)	Cd (μg/L)	Pb (μg/L)	Na (mg/L)	K (mg/L)	Mg (mg/L)	Ca (mg/L)
N/A	4/6/2017	0.94	44.51	96.03	0.08	1.44	116.19	2.37	1.67	16.70
N/A	4/25/2017	1.15	56.62	125.49	0.09	2.23	98.73	2.76	1.58	15.16
N/A	5/5/2017	1.06	34.15	105.89	0.07	2.11	47.35	1.98	1.02	9.16
1	5/12/2017	0.97	39.74	112.62	0.07	2.65	67.11	1.77	1.23	11.67
5	7/28/2017	0.76	49.97	126.20	0.09	1.60	43.33	4.31	1.88	16.21
N/A	2/10/2018	0.14	9.12	62.88	0.06	0.29	204.30	5.64	4.66	35.44
13	4/16/2018	0.54	29.42	87.93	0.07	0.58	182.99	4.91	2.27	21.43
14	4/27/2018	1.82	58.12	112.89	0.17	2.21	141.22	4.11	1.55	13.90
16	5/15/2018	1.39	66.13	157.78	0.16	4.02	83.61	3.13	1.56	15.65
20	6/2/2018	0.91	52.45	131.37	0.12	2.25	71.36	3.86	1.74	19.50
22	6/10/2018	0.58	28.91	179.37	0.12	1.37	45.38	4.04	2.15	24.70
23	7/21/2018	0.94	37.83	128.06	0.13	1.90	26.54	1.70	0.95	8.74
24	7/22/2018	1.43	45.19	139.07	0.11	3.97	29.41	2.17	1.26	12.88
39	10/26/2018	0.45	27.36	143.88	0.13	0.41	27.08	2.60	2.24	20.69
N/A	4/15/2019	1.88	78.07	124.60	0.20	3.07	200.02	4.06	1.94	16.29
41	5/5/2019	2.30	92.02	166.18	0.23	3.47	171.19	3.14	1.52	15.14
49	7/8/2019	4.42	103.44	156.23	0.29	9.22	70.56	1.89	0.72	6.65
51	7/17/2019	3.58	104.42	209.58	0.53	8.87	121.97	3.36	1.43	14.53
54	10/16/2019	1.48	57.01	101.84	0.14	2.55	70.46	2.55	1.01	10.04
55	10/20/2019	1.56	72.86	100.01	0.16	3.53	78.57	2.64	1.14	10.92

57	10/27/2019	1.30	66.93	103.21	0.14	3.45	56.88	2.20	0.90	8.50
58	10/30/2019	1.08	61.24	87.39	0.13	3.01	55.32	2.30	1.00	9.45
59	10/31/2019	1.28	60.79	89.16	0.13	3.58	50.84	2.23	0.85	7.82
74	8/3/2020	1.05	67.92	103.07	0.23	0.41	44.83	2.44	2.25	19.76
75	8/4/2020	0.52	42.12	94.54	0.11	0.30	27.60	1.93	1.44	12.84
76	8/12/2020	0.81	55.43	132.81	0.17	1.56	37.36	2.48	1.91	18.84
78	8/14/2020	0.49	44.97	88.85	0.10	1.01	18.75	1.73	1.34	13.48
86	10/29/2020	0.44	33.80	86.81	0.10	0.23	35.02	1.42	2.08	18.76
N/A	11/11/2020	0.39	29.45	69.14	0.08	0.23	25.33	1.69	1.96	19.07
N/A	12/24/2020	0.06	5.99	149.57	0.32	0.04	174.30	8.42	12.07	85.16
N/A	2/15/2021	0.23	8.29	274.88	1.42	0.04	868.30	6.00	23.36	147.80
N/A	3/18/2021	0.85	32.31	104.68	0.42	0.23	646.04	8.74	6.00	55.75
88	3/24/2021	0.71	37.02	135.96	0.19	0.34	333.48	7.26	3.20	29.21
90	3/31/2021	1.07	72.62	92.93	0.23	0.83	321.97	5.49	1.45	14.70
94	5/28/2021	1.55	104.84	107.55	0.21	1.61	166.98	3.35	0.71	7.58
98	7/1/2021	3.01	189.21	152.28	0.43	3.17	168.20	3.17	0.83	9.83
103	8/17/2021	1.88	125.87	103.72	0.29	1.70	162.51	2.94	0.87	10.10
105	9/1/2021	1.50	109.56	79.56	0.19	2.04	82.12	2.52	0.74	8.08
111	10/29/2021	0.60	35.55	32.41	0.08	0.50	37.51	1.61	0.43	3.78
133	4/28/2023	0.58	36.66	42.75	0.08	0.61	28.13	2.35	0.60	6.45
134	4/30/2023	0.58	38.70	42.41	0.09	0.67	26.37	3.01	0.96	9.51
138	8/6/2023	0.63	60.64	75.97	0.09	0.29	31.23	3.30	1.45	14.49
139	9/10/2023	0.62	48.04	60.73	0.09	0.30	22.49	2.63	0.82	7.93
141	9/23/2023	0.66	38.16	65.09	0.09	0.40	27.11	2.99	1.18	11.41
142	10/14/2023	0.73	50.15	53.95	0.11	0.34	35.70	3.36	1.70	16.69

144	3/23/2024	0.58	47.41	55.26	0.10	1.01	101.63	3.53	1.25	10.32
146	4/1/2024	0.65	45.71	54.93	0.10	0.52	80.13	3.58	1.20	10.46
147	4/2/2024	0.46	38.36	31.92	0.07	0.29	58.52	2.85	0.76	6.61
148	4/3/2024	0.41	29.52	26.10	0.06	0.31	53.00	2.65	0.72	6.29
153	6/5/2024	1.05	63.20	75.63	0.13	0.50	49.93	3.35	1.01	9.18
154	8/7/2024	0.91	73.11	69.01	0.16	0.60	53.25	3.18	1.15	11.09
155	8/8/2024	0.58	52.47	68.71	0.11	0.37	40.04	3.58	1.12	9.73
156	8/18/2024	0.80	51.65	62.66	0.13	0.33	49.77	3.53	1.47	13.30
157	9/26/2024	0.68	47.35	59.95	0.09	0.67	27.36	2.45	0.78	7.23

Table SI-8(A). Event mean concentrations (EMCs) for all events characterized at EC-GS (2017-24). Note that blue-shaded winter events were not included in statistical analyses. Data shaded in yellow were collected as part of the CBT-funded project (2022-2025).

Event No.	Dates	Spec. Cond. (µS/cm)	TSS (mg/L)	ANC (µeq/L)	Chloride (mg/L)	Sulfate (mg/L)	Ortho-P (mg/L)	Ammonia-N (mg/L)	Nitrite-N (mg/L)	Nitrate-N + Nitrite-N (mg/L)	Nitrate-N (mg/L)	DON (mg/L, calc.)
1	5/12/2017	403.41	6.62		45.72	3.43	0.11	0.05	0.01	0.02	0.01	1.59
5	7/28/2017	254.64	15.79		21.54	5.03	0.62	0.44	0.07	0.31	0.25	2.04
N/A	2/11/2018	1689.35	15.30	1282.11	445.23	7.34	0.16	0.03	0.01	0.15	0.14	0.54
13	4/16/2018	580.73	45.33	732.24	145.15	3.22	0.26	0.12	0.01	0.19	0.18	0.89
14	4/27/2018	961.46	6.97	2843.10	184.65	4.66	0.11	0.06	0.02	0.04	0.03	1.98
16	5/15/2018	131.76	20.71	750.30	15.96	1.23	0.11	0.09	0.02	0.16	0.14	0.91
20	6/2/2018	520.94	7.49	2828.24	79.86	1.61	0.12	0.11	0.02	0.18	0.15	2.42
22	6/10/2018	142.36	15.24	969.03	13.16	1.01	0.09	0.04	0.01	0.09	0.08	0.73
23	7/21/2018	168.24	2.96	988.17	17.05	3.03	0.42	0.07	0.05	0.43	0.37	0.89
24	7/22/2018	195.41	3.52	1161.21	20.94	2.63	0.30	0.08	0.04	0.33	0.29	1.54
39	10/26/2018	257.59	3.97	1367.12	28.50	7.69	0.64	0.03	0.02	0.50	0.48	1.13
41	5/5/2019	718.75	8.59	2491.00	153.19	5.12	0.11	0.05	0.02	0.03	0.02	1.68
46	6/13/2019	728.79	9.03	2519.04	157.56	5.29	0.11	0.06	0.01	0.04	0.02	1.60
47	7/4/2019	177.72	11.22	577.55	27.81	3.48	0.90	0.10	0.08	0.31	0.23	1.32
48	7/6/2019	235.35	6.70	1222.44	32.11	3.13	0.52	0.47	0.05	0.20	0.15	2.34
49	7/8/2019	127.93	3.72	969.40	12.19	1.23	0.17	0.03	0.01	0.05	0.04	0.80
51	7/17/2019	356.92	8.66	1340.50	62.06	7.57	2.44	1.13	0.01	0.01	0.00	2.61
52	8/22/2019	194.43	14.23	711.05	28.07	5.03	1.79	0.99	0.10	1.00	0.90	1.86
53	8/23/2019	845.29	26.49	3207.38	154.64	21.21	2.28	0.57	0.03	0.02	0.00	6.96
55	10/20/2019	361.04	2.81	1571.08	56.47	10.38	0.87	0.07	0.02	0.77	0.75	1.81

56	10/27/2019	181.35	5.66	1160.53	21.24	3.26	0.39	0.11	0.01	0.15	0.14	0.93
58	10/30/2019	529.60	6.55	2773.08	80.68	8.87	0.44	0.08	0.01	0.10	0.08	2.14
59	10/31/2019	61.03	2.67	452.28	5.05	0.74	0.14	0.07	0.01	0.05	0.04	0.34
74	8/3/2020	351.14	27.83	1589.88	44.35	12.14	3.39	0.22	0.01	0.01	0.00	4.03
75	8/4/2020	135.00	2.62	1187.85	5.36	2.23	0.34	0.04	0.01	0.10	0.08	0.79
76	8/12/2020	162.12	8.78	1194.07	9.10	3.29	0.46	0.34	0.07	0.56	0.50	2.74
77	8/13/2020	414.94	4.47	3504.49	27.81	6.71	0.20	0.05	0.02	0.06	0.05	3.63
78	8/14/2020	99.71	4.38	842.36	4.42	1.24	0.23	0.16	0.02	0.28	0.26	1.16
84	9/29/2020	171.41	9.56	1089.32	15.26	5.07	0.34	0.13	0.02	0.61	0.59	1.79
85	10/12/2020	406.08	7.26	2381.23	44.11	14.01	0.65	0.39	0.06	1.20	1.13	2.33
86	10/29/2020	126.55	8.85	886.33	7.40	2.88	0.39	0.08	0.02	0.58	0.57	1.05
N/A	11/11/2020	197.79	5.77	1529.15	12.16	4.08	0.26	0.07	0.01	0.20	0.18	1.15
N/A	12/24/2020	1005.13	11.45	930.70	281.55	3.52	0.12	0.04	0.01	0.09	0.08	0.49
N/A	2/4/2021	14269.45	10.86	1529.48	4548.38	27.77	0.07	0.02	0.01	0.08	0.07	0.83
N/A	2/15/2021	4056.02	36.82	1121.16	1388.21	10.36	0.13	0.08	0.02	0.18	0.16	0.58
N/A	3/18/2021	3494.37	13.02	2176.22	863.67	12.90	0.33	0.22	0.02	0.21	0.19	1.87
88	3/24/2021	759.58	20.23	1109.68	198.49	3.05	0.28	0.06	0.02	0.22	0.20	1.19
89	3/31/2021	1168.19	13.00	2911.45	296.72	3.86	0.15	0.06	0.02	0.07	0.05	1.88
94	5/28/2021	757.60	17.85	1681.81	181.00	5.21	0.43	0.05	0.03	0.32	0.29	2.52
95	6/14/2021	437.95	17.86	1422.49	87.11	2.93	0.49	0.12	0.03	0.51	0.48	2.61
98	7/1/2021	756.27	15.44	2215.94	163.79	4.95	0.27	0.07	0.03	0.27	0.24	3.64
103	8/17/2021	429.10	7.10	2246.89	62.69	3.15	0.44	0.13	0.02	0.22	0.19	2.43
104	8/20/2021	719.29	7.10	3728.12	97.98	3.19	0.30	0.12	0.03	0.12	0.09	3.46
105	9/1/2021	199.01	6.85	813.54	29.27	2.89	0.49	0.10	0.02	1.48	1.46	1.31
110	10/25/2021	256.19	8.08	941.44	42.87	5.22	0.96	0.13	0.05	1.30	1.26	1.47

111	10/29/2021	112.57	4.30	815.72	14.68	1.80	0.30	0.03	0.01	0.13	0.12	0.65
133	4/28/2023	225.35	8.43	1966.27	8.32	2.16	0.23	0.02	0.01	0.00	0.00	1.00
134	4/30/2023	187.74	7.74	1670.28	6.34	1.24	0.09	0.02	0.01	0.03	0.02	0.91
136	7/21/2023	159.44	10.67	955.08	9.06	3.90	0.90	0.29	0.17	1.59	1.42	2.16
138	8/7/2023	167.66	9.28	924.90	13.38	4.90	0.90	0.37	0.05	1.41	1.36	1.63
140	9/12/2023	133.67	7.02	770.44	7.87	3.67	1.05	0.22	0.07	1.96	1.89	1.21
141	9/23/2023	193.74	5.41	1509.40	8.16	4.50	0.70	0.11	0.02	0.84	0.83	1.18
142	10/14/2023	281.93	20.34	1492.06	27.47	9.10	1.44	0.39	0.03	1.28	1.24	2.60
144	3/23/2024	422.73	9.29	1192.94	89.78	1.84	0.25	0.06	0.01	0.06	0.05	0.83
146	4/1/2024	307.64	27.55	1323.43	51.92	1.72	0.14	0.05	0.01	0.15	0.14	0.73
147	4/2/2024	303.18	33.11	1598.91	43.75	1.19	0.08	0.04	0.01	0.06	0.06	0.52
148	4/3/2024	215.03	22.53	1314.28	25.06	0.88	0.05	0.02	0.00	0.02	0.02	0.27
152	5/27/2024	86.61	16.21	369.38	11.42	0.96	0.31	0.07	0.01	0.13	0.12	0.64
153	6/5/2024	140.10	12.90	656.67	17.49	1.61	0.42	0.10	0.02	0.18	0.15	1.11
154	8/7/2024	449.71	6.28	2725.83	45.62	11.06	1.15	0.07	0.02	0.28	0.26	2.72
155	8/8/2024	169.58	5.47	1056.80	16.20	2.11	0.60	0.06	0.01	0.17	0.16	0.79
156	8/18/2024	90.11	5.23	613.82	5.78	1.55	0.39	0.05	0.01	0.13	0.12	0.63
157	9/26/2024	191.30	9.34	859.70	21.35	5.41	0.83	0.23	0.03	0.29	0.26	1.27

Table SI-8(B). Event mean concentrations (EMCs) for all events characterized at EC-GS (2017-21). Note that blue-shaded winter events were not included in statistical analyses. Data shaded in yellow were collected as part of the CBT-funded project (2022-2025).

Event No.	Dates	Total P (mg/L)	Total Dissolved P (mg/L)	DOP (mg/L, calculated)	Total Nitrogen (mg/L)	Total Dissolved N (mg/L)	Particulate N (mg/L, calculated)	Particulate P (mg/L, calculated)	DOC (mg/L)
1	5/12/2017	0.21	0.16	0.05	1.91	1.66	0.25	0.05	N/D
5	7/28/2017	0.82	0.68	0.07	3.59	2.79	0.79	0.14	N/D
N/A	2/11/2018	0.24	0.19	0.03	0.97	0.71	0.25	0.05	6.84
13	4/16/2018	0.39	0.29	0.02	1.65	1.20	0.46	0.10	10.37
14	4/27/2018	0.22	0.18	0.06	2.28	2.08	0.20	0.04	30.13
16	5/15/2018	0.25	0.14	0.03	1.65	1.15	0.51	0.11	12.34
20	6/2/2018	0.30	0.21	0.11	3.22	2.70	0.52	0.08	29.21
22	6/10/2018	0.18	0.11	0.02	1.21	0.86	0.35	0.06	9.76
23	7/21/2018	0.51	0.47	0.05	1.62	1.38	0.24	0.05	12.95
24	7/22/2018	0.42	0.34	0.05	2.24	1.95	0.29	0.08	22.31
39	10/26/2018	0.73	0.66	0.01	2.05	1.66	0.39	0.08	14.25
41	5/5/2019	0.23	0.16	0.05	2.04	1.77	0.27	0.08	22.64
46	6/13/2019	0.23	0.16	0.04	1.97	1.69	0.27	0.08	21.58
47	7/4/2019	1.21	0.70	0.04	3.07	1.72	1.34	0.51	19.01
48	7/6/2019	0.66	0.60	0.09	3.30	3.00	0.33	0.06	27.18
49	7/8/2019	0.26	0.21	0.04	1.16	0.88	0.27	0.05	10.65
51	7/17/2019	2.68	2.47	0.07	4.36	3.75	0.61	0.22	34.85
52	8/22/2019	1.93	1.79	0.03	4.56	3.85	0.71	0.14	21.11
53	8/23/2019	3.13	2.82	0.54	9.56	7.55	2.01	0.31	71.79
55	10/20/2019	0.99	0.97	0.10	3.03	2.65	0.38	0.04	21.20
56	10/27/2019	0.47	0.42	0.03	1.46	1.19	0.27	0.05	11.78

58	10/30/2019	0.57	0.49	0.05	2.67	2.32	0.35	0.08	28.20
59	10/31/2019	0.20	0.16	0.02	0.69	0.46	0.22	0.04	5.11
74	8/3/2020	4.47	3.83	0.45	5.07	4.26	0.82	0.64	63.38
75	8/4/2020	0.40	0.36	0.02	1.14	0.93	0.20	0.04	11.10
76	8/12/2020	0.75	0.70	0.24	4.19	3.64	0.54	0.06	28.67
77	8/13/2020	0.46	0.46	0.26	4.26	3.75	0.51	0.01	43.21
78	8/14/2020	0.34	0.30	0.08	1.86	1.59	0.27	0.04	14.20
84	9/29/2020	0.50	0.40	0.06	3.40	2.53	0.87	0.10	21.98
85	10/12/2020	0.82	0.73	0.07	4.54	3.92	0.62	0.10	27.23
86	10/29/2020	0.49	0.43	0.04	2.14	1.72	0.42	0.07	9.96
N/A	11/11/2020	0.35	0.30	0.05	1.69	1.41	0.28	0.04	12.33
N/A	12/24/2020	0.17	0.14	0.02	0.79	0.62	0.17	0.03	4.61
N/A	2/4/2021	0.13	0.08	0.01	1.08	0.94	0.14	0.05	3.32
N/A	2/15/2021	0.23	0.15	0.02	1.28	0.85	0.43	0.07	5.26
N/A	3/18/2021	0.48	0.40	0.07	2.65	2.30	0.35	0.09	4.25
88	3/24/2021	0.40	0.32	0.04	1.89	1.47	0.42	0.08	12.46
89	3/31/2021	0.26	0.21	0.06	2.25	2.00	0.25	0.05	20.11
94	5/28/2021	0.69	0.50	0.07	4.11	2.89	1.22	0.19	28.56
95	6/14/2021	0.75	0.58	0.09	4.18	3.24	0.94	0.16	29.85
98	7/1/2021	0.49	0.39	0.12	4.55	3.98	0.57	0.10	41.04
103	8/17/2021	0.56	0.52	0.08	3.00	2.77	0.23	0.05	26.33
104	8/20/2021	0.46	0.40	0.10	4.08	3.70	0.38	0.06	34.88
105	9/1/2021	0.60	0.54	0.05	3.53	3.14	0.39	0.06	16.39
110	10/25/2021	1.16	1.02	0.06	3.64	2.90	0.73	0.14	13.62
111	10/29/2021	0.36	0.32	0.02	1.07	0.81	0.26	0.05	6.66

133	4/28/2023	0.34	0.26	0.03	1.41	1.02	0.39	0.08	14.35
134	4/30/2023	0.20	0.12	0.03	1.36	0.96	0.40	0.08	12.29
136	7/21/2023	1.10	0.98	0.08	4.68	4.05	0.64	0.12	26.05
138	8/7/2023	1.07	0.95	0.04	4.08	3.42	0.66	0.12	18.24
140	9/12/2023	1.15	1.08	0.02	3.81	3.38	0.43	0.08	14.38
141	9/23/2023	0.79	0.73	0.03	2.45	2.13	0.32	0.06	14.77
142	10/14/2023	1.68	1.52	0.07	5.15	4.27	0.88	0.17	26.56
144	3/23/2024	0.35	0.28	0.03	1.30	0.96	0.34	0.07	8.31
146	4/1/2024	0.26	0.16	0.03	1.33	0.93	0.39	0.10	9.22
147	4/2/2024	0.19	0.10	0.02	0.97	0.62	0.35	0.09	7.35
148	4/3/2024	0.12	0.06	0.01	0.54	0.31	0.23	0.06	4.57
152	5/27/2024	0.45	0.34	0.03	1.40	0.85	0.56	0.11	8.54
153	6/5/2024	0.57	0.46	0.03	1.99	1.39	0.60	0.11	13.85
154	8/7/2024	1.31	1.25	0.10	3.47	3.08	0.39	0.07	32.49
155	8/8/2024	0.67	0.63	0.03	1.28	1.02	0.26	0.04	12.85
156	8/18/2024	0.46	0.41	0.02	1.12	0.81	0.31	0.05	7.80
157	9/26/2024	0.98	0.88	0.05	2.41	1.80	0.62	0.10	12.55

Table SI-8(C). Event mean concentrations (EMCs) for all events characterized at EC-GS (2017-24). Note that blue-shaded winter events were not included in statistical analyses. Data shaded in yellow were collected as part of the CBT-funded project (2022-2025).

Event No.	Dates	Cr (μg/L)	Cu (μg/L)	Zn (μg/L)	Cd (μg/L)	Pb (μg/L)	Na (mg/L)	K (mg/L)	Mg (mg/L)	Ca (mg/L)
1	5/12/2017	0.77	11.16	30.93	0.07	1.77	74.40	2.81	1.00	10.77
5	7/28/2017	0.69	10.39	52.55	0.07	1.10	31.98	9.97	1.94	11.77
N/A	2/11/2018	0.69	4.34	19.61	0.03	0.63	283.30	4.33	2.94	31.60
13	4/16/2018	0.64	7.06	30.78	0.03	0.57	99.06	1.57	0.54	6.14
14	4/27/2018	1.07	14.81	18.36	0.08	1.81	197.21	0.97	1.11	14.86
16	5/15/2018	1.86	6.87	47.86	0.03	0.86	24.46	3.22	0.29	2.21
20	6/2/2018	0.77	9.43	48.59	0.07	1.27	86.33	4.12	1.47	18.36
22	6/10/2018	0.42	3.77	44.20	0.03	0.61	21.24	3.70	0.69	7.40
23	7/21/2018	0.90	8.24	29.71	0.04	0.67	26.38	3.61	0.90	6.48
24	7/22/2018	0.92	9.91	37.67	0.06	0.84	31.29	3.32	0.90	8.20
39	10/26/2018	0.45	6.54	25.18	0.03	0.15	31.70	6.43	1.54	13.50
41	5/5/2019	1.70	13.45	23.60	0.10	1.67	132.30	2.37	1.36	14.47
46	6/13/2019	1.66	12.42	23.07	0.09	1.59	136.33	2.44	1.44	14.97
47	7/4/2019	1.69	12.39	23.13	0.09	1.59	138.85	2.52	1.51	15.43
48	7/6/2019	1.88	13.67	23.66	0.10	1.14	44.20	7.46	1.10	6.79
49	7/8/2019	2.00	6.41	16.48	0.09	1.06	24.14	3.40	0.64	4.29
51	7/17/2019	1.70	13.82	29.43	0.17	0.69	51.84	23.34	1.55	8.99
52	8/22/2019	1.43	10.24	26.51	0.07	0.62	28.60	13.28	1.46	4.72
53	8/23/2019	2.05	30.60	51.47	0.30	4.21	149.38	2.51	6.31	35.58
55	10/20/2019	1.53	12.51	15.18	0.08	0.72	61.09	7.22	1.95	9.97

56	10/27/2019	0.93	8.01	13.39	0.05	0.68	32.02	3.10	1.03	5.76
58	10/30/2019	0.81	10.99	15.06	0.07	0.88	90.64	6.78	2.71	19.06
59	10/31/2019	0.66	2.96	15.59	0.04	1.03	10.93	1.65	0.53	2.70
74	8/3/2020	0.79	18.05	30.97	0.06	0.85	30.02	34.78	4.20	16.50
75	8/4/2020	0.37	5.16	4.57	0.03	0.38	12.27	7.18	1.67	9.98
76	8/12/2020	0.72	9.46	9.67	0.07	0.74	21.05	7.52	1.51	10.24
77	8/13/2020	0.76	10.50	11.09	0.11	3.58	61.17	7.44	3.42	27.70
78	8/14/2020	0.47	4.59	5.68	0.04	0.45	4.59	5.68	0.04	0.45
84	9/29/2020	0.68	8.42	7.32	0.05	0.39	25.12	6.05	1.19	8.88
85	10/12/2020	0.45	11.54	9.18	0.06	0.50	54.40	17.40	3.13	21.88
86	10/29/2020	0.48	5.53	5.49	0.03	0.29	13.12	6.16	1.25	8.65
N/A	11/11/2020	0.42	6.37	5.47	0.05	0.37	29.05	3.88	1.64	14.70
N/A	12/24/2020	0.33	4.03	4.63	0.03	0.18	156.98	3.34	3.62	36.67
N/A	2/4/2021	0.24	4.70	18.74	0.56	0.27	2225.35	6.69	41.40	528.54
N/A	2/15/2021	0.49	4.80	10.11	0.10	0.26	807.90	6.42	14.80	73.91
N/A	3/18/2021	1.09	11.04	8.78	0.11	0.67	634.76	7.80	7.92	76.80
88	3/24/2021	1.30	12.42	12.12	0.06	0.98	151.45	1.93	0.68	8.67
89	3/31/2021	1.20	15.28	11.01	0.08	1.75	206.13	1.09	1.29	18.50
94	5/28/2021	1.04	18.09	16.56	0.10	1.61	143.92	17.35	1.28	10.40
95	6/14/2021	1.13	18.49	21.81	0.10	1.08	102.52	7.72	0.69	6.15
98	7/1/2021	1.40	22.50	16.92	0.14	2.53	182.42	5.25	1.02	11.91
103	8/17/2021	1.06	12.72	11.94	0.10	1.97	138.39	5.08	0.86	8.23
104	8/20/2021	1.34	17.53	12.39	0.13	2.54	206.24	5.79	1.43	16.25
105	9/1/2021	0.54	8.35	8.44	0.05	0.87	33.84	4.06	0.48	3.50
110	10/25/2021	0.75	9.12	7.76	0.08	0.75	64.81	7.12	0.99	5.22

111	10/29/2021	0.87	4.70	4.76	0.04	0.52	27.40	3.17	0.69	3.98
133	4/28/2023	0.65	7.37	7.00	0.05	0.90	35.57	3.87	1.22	10.39
134	4/30/2023	0.46	5.54	6.65	0.05	0.73	29.61	2.70	1.03	9.02
136	7/21/2023	0.65	12.11	11.56	0.06	0.58	23.17	8.34	1.23	6.16
138	8/7/2023	0.53	7.79	11.20	0.05	0.46	18.11	12.30	1.73	7.46
140	9/12/2023	0.40	7.36	7.75	0.05	0.33	15.55	8.94	1.45	5.76
141	9/23/2023	0.51	7.34	5.07	0.03	0.52	28.03	5.41	1.77	10.45
142	10/14/2023	0.58	12.19	11.28	0.09	0.65	42.30	14.95	2.20	10.60
144	3/23/2024	0.75	7.38	6.68	0.06	0.59	80.31	0.88	0.78	8.35
146	4/1/2024	0.48	6.49	7.75	0.04	0.53	60.81	0.72	0.61	6.88
147	4/2/2024	0.39	4.42	4.84	0.05	0.36	59.21	0.63	0.80	8.74
148	4/3/2024	0.32	2.91	3.59	0.02	0.27	41.08	0.66	0.61	6.38
152	5/27/2024	0.34	4.17	8.52	0.02	0.29	13.85	0.26	5.78	1.54
153	6/5/2024	1.13	8.70	19.19	0.05	0.57	24.38	4.66	0.35	2.43
154	8/7/2024	0.77	14.85	11.85	0.08	1.35	72.23	15.16	2.40	16.20
155	8/8/2024	0.35	6.20	8.28	0.05	0.52	26.65	6.15	0.89	4.52
156	8/18/2024	0.37	3.58	4.35	0.20	0.25	12.05	3.29	0.56	3.26
157	9/26/2024	0.44	7.47	7.49	0.04	0.41	22.42	13.23	1.42	6.73

Table SI-9(A). Flume event mean concentrations (EMCs) for all events characterized at EC-BS2 (2020-24). Note that blue-shaded winter events were not included in statistical analyses. Data shaded in yellow were collected as part of the CBT-funded project (2022-2025).

Event No.	Dates	Spec. Cond. (µS/cm)	TSS (mg/L)	ANC (µeq/L)	Chloride (mg/L)	Sulfate (mg/L)	Ortho-P (mg/L)	Ammonia-N (mg/L)	Nitrite-N (mg/L)	Nitrate-N + Nitrite-N (mg/L)	Nitrate-N (mg/L)	DON (mg/L, calc.)
75	8/4/2020	118.31	4.61	934.69	6.00	2.09	0.61	0.07	0.01	0.15	0.13	0.82
78	8/14/2020	44.56	6.63	316.63	1.92	0.88	0.34	0.16	0.02	0.31	0.29	0.54
N/A	12/24/2020	1072.51	29.64	520.61	290.13	2.71	0.13	0.09	0.01	0.13	0.13	0.43
111	10/29/2021	106.35	45.82	803.50	7.27	1.70	0.60	0.02	0.01	0.07	0.06	0.63
140	9/12/2023	68.95	11.87	482.51	3.20	1.70	0.53	0.01	0.01	0.12	0.11	0.71
147	4/2/2024	110.25	94.15	724.89	10.90	1.11	0.13	0.03	0.01	0.10	0.09	0.30
152	5/27/2024	115.12	20.99	439.66	14.68	1.57	0.83	0.17	0.02	0.22	0.20	1.01
155	8/8/2024	114.46	7.96	898.48	4.84	1.39	0.60	0.02	0.00	0.03	0.02	0.61
157	9/26/2024	74.40	16.20	480.40	4.36	0.99	0.61	0.02	0.01	0.06	0.04	0.65

Table SI-9(B). Flume event mean concentrations (EMCs) for all events characterized at EC-BS2 (2020-24). Note that blue-shaded winter events were not included in statistical analyses. Data shaded in yellow were collected as part of the CBT-funded project (2022-2025).

Event No.	Dates	Total P (mg/L)	Total Dissolved P (mg/L)	DOP (mg/L, calculated)	Total Nitrogen (mg/L)	Total Dissolved N (mg/L)	Particulate N (mg/L, calculated)	Particulate P (mg/L, calculated)	DOC (mg/L)
75	8/4/2020	0.69	0.62	0.02	1.29	1.04	0.25	0.07	11.47
78	8/14/2020	0.43	0.36	0.02	1.34	1.02	0.32	0.07	8.41
N/A	12/24/2020	0.21	0.14	0.01	0.95	0.66	0.29	0.06	6.13
111	10/29/2021	0.77	0.62	0.03	1.22	0.72	0.51	0.15	10.13
140	9/12/2023	0.63	0.55	0.02	1.29	0.84	0.45	0.08	11.63
147	4/2/2024	0.35	0.14	0.02	0.99	0.42	0.57	0.20	5.18
152	5/27/2024	1.07	0.88	0.05	2.43	1.41	1.03	0.19	13.45
155	8/8/2024	0.69	0.63	0.02	1.02	0.66	0.37	0.07	9.52
157	9/26/2024	0.73	0.64	0.03	1.09	0.72	0.36	0.08	9.34

Table SI-9(C). Flume event mean concentrations (EMCs) for all events characterized at EC-BS2 (2020-24). Note that blue-shaded winter events were not included in statistical analyses. Data shaded in yellow were collected as part of the CBT-funded project (2022-2025).

Event No.	Dates	Cr (µg/L)	Cu (µg/L)	Zn (µg/L)	Cd (µg/L)	Pb (µg/L)	Na (mg/L)	K (mg/L)	Mg (mg/L)	Ca (mg/L)
75	8/4/2020	0.21	4.39	6.31	0.01	0.10	17.79	9.10	1.53	3.71
78	8/14/2020	0.14	2.14	4.63	0.02	0.26	4.66	3.83	0.62	2.09
N/A	12/24/2020	0.15	1.96	4.53	0.02	0.12	140.06	8.15	6.21	47.42
111	10/29/2021	0.44	3.37	2.80	0.01	0.37	84.55	4.89	0.47	1.53
140	9/12/2023	0.25	3.02	3.36	0.01	0.09	7.84	6.71	0.93	1.93
147	4/2/2024	0.22	1.79	0.91	0.01	0.11	23.73	0.78	0.20	1.25
152	5/27/2024	0.51	3.34	3.84	0.02	0.13	12.86	15.36	0.35	1.22
155	8/8/2024	1.61	2.37	2.88	0.02	0.11	17.64	8.17	0.94	1.77
157	9/26/2024	7.38	3.20	3.66	0.03	0.14	10.12	6.86	0.55	1.23

Table SI-10(A). Underdrain event mean concentrations (EMCs) for all events characterized at EC-BS2 (2020-24). Note that blue-shaded winter events were not included in statistical analyses. Data shaded in yellow were collected as part of the CBT-funded project (2022-2025).

Event No.	Dates	Spec. Cond. (µS/cm)	TSS (mg/L)	ANC (µeq/L)	Chloride (mg/L)	Sulfate (mg/L)	Ortho-P (mg/L)	Ammonia-N (mg/L)	Nitrite-N (mg/L)	Nitrate-N + Nitrite-N (mg/L)	Nitrate-N (mg/L)	DON (mg/L, calc.)
75	8/4/2020	199.43	8.41	1045.99	11.94	7.37	0.16	0.03	0.01	5.10	5.09	0.78
76	8/12/2020	313.21	12.42	1884.11	8.70	15.78	0.05	0.03	0.01	8.53	8.52	1.89
78	8/14/2020	155.54	6.61	1156.70	3.00	4.90	0.10	0.03	0.01	2.26	2.25	2.03
86	10/29/2020	255.92	14.67	1082.49	13.90	22.96	0.08	0.04	0.01	6.13	6.12	1.29
N/A	11/11/2020	192.44	30.97	1127.39	10.89	9.11	0.09	0.02	0.01	3.01	3.00	1.09
N/A	12/24/2020	952.30	1.74	494.77	275.23	2.84	0.02	0.01	0.00	0.44	0.44	0.24
N/A	2/4/2021	3259.73	5.28	500.08	1029.95	14.75	0.00	0.00	0.01	2.31	2.30	0.34
N/A	2/15/2021	3586.56	3.68	498.67	1129.77	9.06	0.02	0.06	0.01	1.43	1.42	0.29
N/A	3/24/2021	1812.79	12.09	914.22	518.87	7.45	0.15	0.09	0.01	1.57	1.56	1.03
N/A	3/31/2021	1185.09	9.42	2209.92	302.82	6.49	0.07	0.07	0.01	0.96	0.95	1.82
94	5/28/2021	973.84	44.38	2182.56	196.76	21.87	0.20	0.37	0.04	2.04	2.00	4.64
95	6/14/2021	772.11	48.09	2850.95	138.69	20.06	0.15	0.07	0.05	4.08	4.02	3.79
105	9/1/2021	542.36	48.95	1939.69	78.22	33.52	0.27	0.06	0.04	3.44	3.40	3.52
110	10/25/2021	354.34	54.66	1895.06	23.26	20.10	0.30	0.05	0.02	8.26	8.23	3.20
111	10/29/2021	218.12	47.54	1647.71	13.20	4.98	0.36	0.05	0.02	1.13	1.12	1.69
133	4/28/2023	182.02	44.60	1369.88	3.36	7.11	0.20	0.22	0.01	0.88	0.87	1.73
134	4/30/2023	173.83	39.49	1451.47	2.38	4.72	0.15	0.11	0.02	0.74	0.72	1.81
138	8/7/2023	250.08	26.11	1054.80	10.23	24.44	0.55	0.20	0.03	6.36	6.33	1.35
139	9/10/2023	136.20	19.95	958.06	5.39	6.69	0.35	0.03	0.02	0.31	0.29	1.76
141	9/23/2023	177.98	9.22	1548.45	4.12	4.93	0.13	0.03	0.01	0.22	0.22	1.24

144	3/23/2024	367.55	9.20	1107.08	72.49	3.29	0.14	0.04	0.01	0.43	0.42	1.05
146	4/1/2024	257.37	27.81	1307.61	33.63	2.94	0.15	0.04	0.01	0.45	0.44	1.00
147	4/2/2024	168.03	32.45	1049.55	17.46	1.60	0.11	0.02	0.01	0.11	0.10	0.56
148	4/3/2024	217.58	19.45	1469.43	21.13	1.62	0.12	0.04	0.01	0.06	0.05	0.89
152	5/27/2024	167.98	21.42	684.53	19.54	4.29	0.51	0.09	0.02	1.25	1.23	1.31
153	6/5/2024	209.59	26.26	1157.22	16.44	5.24	0.50	0.07	0.02	2.13	2.11	1.62
155	8/8/2024	218.34	9.77	1374.53	13.41	7.19	0.37	0.03	0.01	2.05	2.04	1.48
157	9/26/2024	129.13	28.72	790.03	5.55	6.54	0.34	0.04	0.01	0.72	0.71	1.34

Table SI-10(B). Underdrain event mean concentrations (EMCs) for all events characterized at EC-BS2 (2020-24). Note that blue-shaded winter events were not included in statistical analyses. Data shaded in yellow were collected as part of the CBT-funded project (2022-2025).

Event No.	Dates	Total P (mg/L)	Total Dissolved P (mg/L)	DOP (mg/L, calculated)	Total Nitrogen (mg/L)	Total Dissolved N (mg/L)	Particulate N (mg/L, calculated)	Particulate P (mg/L, calculated)	DOC (mg/L)
75	8/4/2020	0.24	0.18	0.02	6.99	5.91	1.08	0.05	18.58
76	8/12/2020	0.15	0.11	0.05	11.15	10.45	0.70	0.04	24.32
78	8/14/2020	0.21	0.18	0.08	4.56	4.33	0.23	0.03	17.56
86	10/29/2020	0.17	0.13	0.05	8.25	7.46	0.79	0.04	19.10
N/A	11/11/2020	0.18	0.13	0.04	4.29	4.12	0.17	0.05	14.14
N/A	12/24/2020	0.04	0.03	0.01	0.76	0.70	0.07	0.01	3.10
N/A	2/4/2021	0.04	0.00	0.00	2.80	2.65	0.15	0.04	4.46
N/A	2/15/2021	0.04	0.03	0.01	1.86	1.78	0.08	0.02	2.76
N/A	3/24/2021	0.24	0.19	0.04	3.00	2.70	0.30	0.05	11.06
N/A	3/31/2021	0.17	0.13	0.06	2.99	2.85	0.13	0.04	23.78
94	5/28/2021	0.52	0.38	0.18	8.38	6.90	1.48	0.14	45.07
95	6/14/2021	0.56	0.35	0.20	9.00	7.93	1.06	0.20	56.71
105	9/1/2021	0.62	0.47	0.20	7.65	7.02	0.63	0.16	48.32
110	10/25/2021	0.69	0.50	0.20	12.31	11.51	0.80	0.19	34.39
111	10/29/2021	0.62	0.49	0.13	3.37	2.87	0.50	0.13	22.99
133	4/28/2023	0.46	0.29	0.10	3.55	2.83	0.71	0.16	19.98
134	4/30/2023	0.41	0.28	0.13	3.16	2.67	0.49	0.13	24.93
138	8/7/2023	0.77	0.61	0.06	8.59	7.91	0.68	0.15	24.68
139	9/10/2023	0.51	0.43	0.08	2.43	2.10	0.34	0.08	25.41
141	9/23/2023	0.21	0.18	0.05	1.65	1.49	0.16	0.04	18.52
144	3/23/2024	0.24	0.19	0.05	1.73	1.52	0.22	0.05	12.47

146	4/1/2024	0.29	0.19	0.04	1.81	1.48	0.32	0.10	16.46
147	4/2/2024	0.22	0.14	0.03	0.93	0.69	0.23	0.08	8.05
148	4/3/2024	0.24	0.15	0.03	1.47	0.99	0.48	0.09	9.84
152	5/27/2024	0.74	0.58	0.07	3.42	2.65	0.77	0.16	17.63
153	6/5/2024	0.72	0.58	0.09	4.37	3.82	0.55	0.13	22.60
155	8/8/2024	0.47	0.42	0.05	3.81	3.55	0.26	0.05	20.96
157	9/26/2024	0.51	0.40	0.06	2.51	2.10	0.41	0.11	16.85

Table SI-10(B). Underdrain event mean concentrations (EMCs) for all events characterized at EC-BS2 (2020-24). Note that blue-shaded winter events were not included in statistical analyses. Data shaded in yellow were collected as part of the CBT-funded project (2022-2025).

Event No.	Dates	Cr (µg/L)	Cu (µg/L)	Zn (µg/L)	Cd (µg/L)	Pb (µg/L)	Na (mg/L)	K (mg/L)	Mg (mg/L)	Ca (mg/L)
75	8/4/2020	0.58	45.74	94.49	0.06	0.22	30.78	4.39	1.72	11.64
76	8/12/2020	0.90	56.20	77.30	0.07	0.34	40.96	6.43	2.86	21.09
78	8/14/2020	0.58	38.45	116.63	0.06	0.70	20.14	4.26	1.59	12.09
86	10/29/2020	0.60	41.40	176.01	0.07	0.22	26.17	4.88	2.97	21.78
N/A	11/11/2020	0.60	36.66	135.95	0.05	0.17	19.15	4.08	2.28	16.72
N/A	12/24/2020	0.11	8.07	154.13	0.13	0.04	106.72	10.89	7.93	55.11
N/A	2/4/2021	0.16	10.40	308.33	0.59	0.02	377.44	8.24	31.56	212.29
N/A	2/15/2021	0.21	7.63	303.12	0.53	0.03	545.23	11.43	31.79	142.96
N/A	3/24/2021	0.71	24.81	187.16	0.14	0.37	300.00	11.67	4.70	37.87
N/A	3/31/2021	1.09	67.38	116.57	0.10	0.49	240.15	8.72	2.15	17.34
94	5/28/2021	1.76	129.24	184.90	0.21	1.04	200.30	9.58	2.04	16.17
95	6/14/2021	2.96	157.12	82.13	0.14	0.58	178.21	7.52	1.62	14.15
105	9/1/2021	2.16	127.99	187.74	0.16	1.34	105.97	7.07	1.27	11.43
110	10/25/2021	1.92	89.06	106.82	0.10	1.38	122.86	5.13	0.90	7.42
111	10/29/2021	1.24	56.03	57.28	0.06	0.59	89.56	4.15	0.59	3.99
133	4/28/2023	0.95	42.52	61.80	0.08	0.71	27.91	2.44	2.15	5.61
134	4/30/2023	0.91	40.97	59.82	0.07	0.60	27.65	3.89	0.75	6.16
138	8/7/2023	0.75	50.03	100.59	0.08	0.29	35.06	7.74	1.61	10.88
139	9/10/2023	0.88	56.51	80.80	0.05	0.36	22.25	5.67	0.84	5.34
141	9/23/2023	0.72	43.96	82.71	0.05	0.28	28.35	5.31	1.34	8.99

144	3/23/2024	0.88	37.71	53.54	0.05	0.45	66.83	4.40	1.11	8.18
146	4/1/2024	0.76	32.18	45.76	0.06	0.37	48.90	3.71	0.81	5.98
147	4/2/2024	0.41	21.75	22.23	0.02	0.16	35.02	2.42	0.45	3.42
148	4/3/2024	0.42	20.52	22.24	0.06	0.24	43.78	2.89	0.57	4.39
152	5/27/2024	0.56	27.54	39.47	0.04	0.33	26.84	10.05	0.63	3.81
153	6/5/2024	1.08	44.92	63.95	0.05	0.37	34.80	7.72	0.87	5.99
155	8/8/2024	0.65	36.47	66.11	0.05	0.35	36.37	7.32	1.14	6.45
157	9/26/2024	0.80	40.87	53.04	0.05	0.34	21.93	5.01	0.64	4.26

Table SI-11(A). Flume event mean concentrations (EMCs) for all events characterized at LT-BS (2019-24). Data shaded in yellow were collected as part of the CBT-funded project (2022-2025).

Event No.	Dates	Spec. Cond. (µS/cm)	TSS (mg/L)	ANC (µeq/L)	Chloride (mg/L)	Sulfate (mg/L)	Ortho-P (mg/L)	Ammonia-N (mg/L)	Nitrite-N (mg/L)	Nitrate-N + Nitrite-N (mg/L)	Nitrate-N (mg/L)	DON (mg/L, calc.)
2	4/14/2019	316.69	151.89	702.92	85.44	1.69	0.07	0.04	0.01	0.14	0.13	0.61
5	5/3/2019	209.10	48.50	430.08	59.84	1.69	0.11	0.14	0.01	0.25	0.24	0.42
7	5/5/2019	254.40	26.48	1118.34	58.96	1.70	0.07	0.03	0.01	0.02	0.01	0.47
14	6/13/2019	122.37	150.80	586.02	20.62	1.09	0.24	0.04	0.01	0.08	0.07	0.54
16	7/8/2019	96.53	14.56	580.03	11.36	1.07	0.37	0.04	0.01	0.14	0.13	0.66
20	10/31/2019	72.11	55.60	574.75	5.24	0.82	0.25	0.02	0.01	0.03	0.03	0.39
36	5/3/2021	156.17	89.82	513.41	30.93	0.78	0.18	0.02	0.01	0.10	0.09	0.51
43	8/18/2021	128.09	14.69	726.45	16.09	0.98	0.36	0.03	0.01	0.10	0.09	0.72
46	8/25/2021	51.05	21.29	298.25	3.70	0.75	0.28	0.01	0.02	0.29	0.27	0.44
49	9/1/2021	59.17	17.33	511.80	3.03	0.40	0.08	0.01	0.00	0.02	0.02	0.19
79	4/3/2024	161.50	10.00	952.90	18.93	1.24	0.05	0.03	0.01	0.14	0.13	0.29
81	5/25/2024	93.92	18.61	377.21	13.10	0.98	0.27	0.06	0.02	0.22	0.20	0.79
87	8/8/2024	123.49	5.18	1075.32	4.69	0.72	0.13	0.01	0.00	0.00	0.00	0.44

Table SI-11(B). Flume event mean concentrations (EMCs) for all events characterized at LT-BS (2019-24). Data shaded in yellow were collected as part of the CBT-funded project (2022-2025).

Event No.	Dates	Total P (mg/L)	Total Dissolved P (mg/L)	DOP (mg/L, calculated)	Total Nitrogen (mg/L)	Total Dissolved N (mg/L)	Particulate N (mg/L, calculated)	Particulate P (mg/L, calculated)	DOC (mg/L)
2	4/14/2019	0.37	0.09	0.03	2.08	0.79	1.29	0.27	9.03
5	5/3/2019	0.30	0.12	0.01	1.29	0.82	0.47	0.18	7.25
7	5/5/2019	0.16	0.08	0.01	0.65	0.51	0.14	0.08	6.86
14	6/13/2019	0.55	0.26	0.02	1.58	0.66	0.93	0.28	8.94
16	7/8/2019	0.45	0.40	0.04	1.06	0.84	0.23	0.05	8.08
20	10/31/2019	0.36	0.26	0.01	0.82	0.44	0.38	0.10	6.77
36	5/3/2021	0.32	0.20	0.02	1.16	0.64	0.52	0.12	6.08
43	8/18/2021	0.44	0.39	0.02	1.01	0.85	0.16	0.05	10.20
46	8/25/2021	0.38	0.31	0.02	1.07	0.74	0.34	0.07	6.06
49	9/1/2021	0.12	0.09	0.01	0.33	0.22	0.12	0.04	2.97
79	4/3/2024	0.26	0.06	0.01	0.96	0.45	0.51	0.20	5.38
81	5/25/2024	0.45	0.30	0.03	1.72	1.06	0.65	0.15	10.60
87	8/8/2024	0.17	0.14	0.01	0.59	0.45	0.14	0.03	7.01

Table SI-11(C). Flume event mean concentrations (EMCs) for all events characterized at LT-BS (2019-24). Data shaded in yellow were collected as part of the CBT-funded project (2022-2025).

Event No.	Dates	Cr (μg/L)	Cu (μg/L)	Zn (μg/L)	Cd (μg/L)	Pb (μg/L)	Na (mg/L)	K (mg/L)	Mg (mg/L)	Ca (mg/L)
2	4/14/2019	3.39	7.56	35.93	0.08	7.47	64.07	1.24	0.22	1.81
5	5/3/2019	2.19	5.40	26.39	0.13	4.10	44.71	0.54	0.23	2.41
7	5/5/2019	1.63	4.14	14.32	0.09	2.02	58.34	0.22	0.29	2.58
14	6/13/2019	4.11	8.51	41.77	0.14	11.13	22.70	1.90	0.38	2.76
16	7/8/2019	1.53	4.50	15.04	0.11	1.18	21.91	1.67	0.52	1.88
20	10/31/2019	0.97	4.26	15.61	0.06	3.37	15.46	1.42	0.53	1.88
36	5/3/2021	0.44	2.96	1.37	0.03	0.23	32.07	0.47	0.19	1.76
43	8/18/2021	0.31	2.73	2.02	0.01	0.14	41.34	2.05	0.66	2.35
46	8/25/2021	0.49	1.71	1.79	0.01	0.13	14.31	1.17	0.23	1.03
49	9/1/2021	0.20	0.80	1.02	0.01	0.08	13.18	0.58	0.29	2.00
79	4/3/2024	0.23	1.47	0.87	0.01	0.09	33.27	0.71	0.40	2.36
81	5/25/2024	0.36	3.24	3.40	0.02	0.10	16.18	3.58	0.39	2.14
87	8/8/2024	0.45	1.71	1.48	0.01	0.06	21.88	1.29	0.86	3.13

Table SI-12(A). Underdrain event mean concentrations (EMCs) for all events characterized at LT-BS (2019-24). Data shaded in yellow were collected as part of the CBT-funded project (2022-2025).

Event No.	Dates	Spec. Cond. (µS/cm)	TSS (mg/L)	ANC (µeq/L)	Chloride (mg/L)	Sulfate (mg/L)	Ortho-P (mg/L)	Ammonia-N (mg/L)	Nitrite-N (mg/L)	Nitrate-N + Nitrite-N (mg/L)	Nitrate-N (mg/L)	DON (mg/L, calc.)
2	4/14/2019	857.95	12.32	2097.01	192.96	4.67	0.12	0.03	0.01	0.89	0.88	0.99
5	5/3/2019	556.58	23.54	2099.41	110.24	7.15	0.10	0.06	0.02	2.53	2.52	1.03
7	5/5/2019	681.69	5.94	2382.52	136.36	4.22	0.10	0.03	0.01	0.28	0.27	0.85
14	6/13/2019	371.51	26.32	1835.51	60.29	4.49	0.12	0.04	0.01	0.84	0.83	0.99
15	6/17/2019	587.17	8.90	2297.72	111.99	6.72	0.10	0.07	0.01	0.72	0.72	0.92
16	7/8/2019	364.10	19.18	1505.96	60.63	6.60	0.15	0.02	0.01	0.97	0.96	1.15
17	7/22/2019	361.40	16.21	1774.43	58.90	8.32	0.15	0.02	0.01	0.88	0.87	1.05
18	10/27/2019	319.77	19.28	1301.17	50.49	11.52	0.22	0.03	0.01	2.82	2.82	0.71
19	10/30/2019	408.10	12.23	2005.91	61.43	10.28	0.26	0.02	0.01	0.82	0.81	1.14
20	10/31/2019	199.23	11.14	1419.24	17.37	4.99	0.16	0.02	0.01	0.90	0.89	0.86
25	8/4/2020	300.14	10.93	1909.57	27.52	8.48	0.17	0.01	0.02	2.24	2.22	0.90
27	8/12/2020	204.15	10.30	1338.97	14.59	8.65	0.12	0.04	0.02	1.62	1.60	1.07
32	10/29/2020	264.93	10.94	1348.45	27.69	11.37	0.20	0.28	0.01	1.75	1.74	1.38
33	11/11/2020	288.83	12.95	1412.08	26.70	12.97	0.14	0.01	0.01	3.03	3.02	2.14
34	11/12/2020	280.80	7.33	1847.60	23.73	8.22	0.12	0.01	0.01	1.01	1.00	1.03
36	5/3/2021	311.81	64.61	903.53	63.29	2.97	0.21	0.04	0.01	0.85	0.84	0.91
38	5/29/2021	843.83	6.54	2083.27	199.33	8.64	0.18	0.04	0.01	1.17	1.16	1.00
39	7/1/2021	454.38	18.06	1649.77	83.49	6.71	0.27	0.02	0.02	1.08	1.06	1.57
41	7/17/2021	332.99	36.43	1452.56	55.90	8.28	0.26	0.02	0.02	1.24	1.22	1.45
42	8/16/2021	275.56	26.90	1159.02	39.15	10.25	0.35	0.02	0.02	2.19	2.16	1.24
43	8/18/2021	286.07	25.49	1564.02	35.80	3.93	0.24	0.04	0.02	1.67	1.65	1.53

46	8/25/2021	239.30	41.70	1237.60	28.40	4.70	0.33	0.04	0.02	1.83	1.81	0.98
49	9/1/2021	271.61	10.87	1758.90	27.13	1.39	0.12	0.01	0.01	0.67	0.66	0.79
55	10/29/2021	263.21	20.18	1595.91	49.61	10.64	0.21	0.02	0.01	3.87	3.86	1.18
72	4/28/2023	256.89	59.87	1507.91	28.70	3.44	0.14	0.09	0.02	0.28	0.26	0.97
73	4/30/2023	223.69	27.38	1633.46	17.42	2.39	0.08	0.04	0.01	0.11	0.10	1.05
N/A	9/23/2023	443.27	9.31	2624.37	45.69	11.22	0.17	0.03	0.01	3.16	3.15	1.05
76	3/23/2024	585.07	98.51	1356.98	132.77	2.79	0.13	0.05	0.01	0.25	0.24	0.89
77	4/1/2024	544.98	75.80	1524.41	115.30	2.93	0.10	0.04	0.01	0.24	0.23	0.87
78	4/2/2024	453.60	75.87	1820.83	83.45	1.97	0.06	0.02	0.01	0.07	0.06	0.70
79	4/3/2024	377.42	15.16	2095.39	52.14	1.55	0.05	0.03	0.01	0.06	0.06	0.63
81	5/25/2024	509.03	17.73	2323.72	80.27	4.44	0.12	0.03	0.01	0.45	0.43	1.73
82	5/26/2024	518.33	12.28	2805.21	71.41	3.84	0.10	0.02	0.01	0.24	0.23	1.55
84	6/5/2024	782.30	9.50	2853.10	143.70	7.63	0.07	0.02	0.01	0.68	0.68	1.29
85	6/29/2024	368.60	13.00	1471.80	45.44	8.30	0.22	0.03	0.31	5.96	5.65	2.05
86	8/7/2024	434.14	9.93	2676.95	47.98	6.90	0.12	0.02	0.00	0.71	0.71	1.01
87	8/8/2024	274.33	4.99	2166.41	17.86	2.04	0.12	0.01	0.00	0.09	0.09	0.86

Table SI-12(B). Underdrain event mean concentrations (EMCs) for all events characterized at LT-BS (2019-24). Data shaded in yellow were collected as part of the CBT-funded project (2022-2025).

Event No.	Dates	Total P (mg/L)	Total Dissolved P (mg/L)	DOP (mg/L, calculated)	Total Nitrogen (mg/L)	Total Dissolved N (mg/L)	Particulate N (mg/L, calculated)	Particulate P (mg/L, calculated)	DOC (mg/L)
2	4/14/2019	0.20	0.15	0.04	2.22	1.92	0.31	0.05	16.94
5	5/3/2019	0.22	0.15	0.05	3.78	3.62	0.16	0.07	24.04
7	5/5/2019	0.15	0.12	0.03	1.18	1.15	0.03	0.03	14.29
14	6/13/2019	0.22	0.16	0.04	2.11	1.87	0.25	0.06	16.97
15	6/17/2019	0.17	0.15	0.04	1.83	1.72	0.11	0.03	14.90
16	7/8/2019	0.26	0.20	0.06	2.33	2.13	0.19	0.06	13.97
17	7/22/2019	0.25	0.20	0.04	2.17	1.95	0.22	0.05	16.67
18	10/27/2019	0.29	0.25	0.03	3.75	3.56	0.19	0.03	12.71
19	10/30/2019	0.40	0.29	0.03	2.18	1.97	0.20	0.11	20.17
20	10/31/2019	0.26	0.19	0.03	2.01	1.77	0.23	0.06	15.65
25	8/4/2020	0.22	0.19	0.02	3.30	3.15	0.15	0.03	13.39
27	8/12/2020	0.20	0.16	0.04	2.98	2.72	0.26	0.04	14.57
32	10/29/2020	0.26	0.23	0.04	3.74	3.40	0.34	0.02	13.13
33	11/11/2020	0.22	0.17	0.04	5.50	5.19	0.31	0.04	19.05
34	11/12/2020	0.20	0.17	0.04	2.18	2.05	0.13	0.03	16.25
36	5/3/2021	0.35	0.25	0.04	2.27	1.80	0.47	0.10	13.55
38	5/29/2021	0.29	0.21	0.02	2.87	2.20	0.67	0.08	12.99
39	7/1/2021	0.39	0.33	0.06	2.94	2.67	0.27	0.06	22.27
41	7/17/2021	0.42	0.32	0.06	3.06	2.71	0.35	0.10	21.93
42	8/16/2021	0.47	0.39	0.04	3.70	3.45	0.25	0.08	16.66
43	8/18/2021	0.36	0.29	0.05	3.41	3.23	0.18	0.07	23.84

46	8/25/2021	0.50	0.37	0.04	3.41	2.85	0.57	0.13	14.60
49	9/1/2021	0.17	0.14	0.02	1.57	1.46	0.11	0.03	11.86
55	10/29/2021	0.31	0.24	0.03	5.54	5.06	0.48	0.08	14.17
72	4/28/2023	0.26	0.17	0.03	1.68	1.34	0.34	0.10	12.62
73	4/30/2023	0.17	0.12	0.04	1.43	1.20	0.23	0.06	14.80
N/A	9/23/2023	0.23	0.20	0.03	4.33	4.24	0.09	0.03	16.59
76	3/23/2024	0.29	0.17	0.04	1.59	1.19	0.40	0.12	9.32
77	4/1/2024	0.29	0.13	0.04	1.61	1.15	0.46	0.16	12.70
78	4/2/2024	0.24	0.09	0.03	1.22	0.79	0.42	0.15	9.10
79	4/3/2024	0.13	0.09	0.03	0.85	0.72	0.13	0.04	8.56
81	5/25/2024	0.24	0.18	0.06	2.45	2.21	0.24	0.06	21.50
82	5/26/2024	0.19	0.16	0.06	1.94	1.81	0.13	0.03	23.35
84	6/5/2024	0.16	0.13	0.06	2.14	1.99	0.15	0.03	21.52
85	6/29/2024	0.37	0.28	0.06	8.34	8.04	0.30	0.09	29.30
86	8/7/2024	0.21	0.17	0.05	1.90	1.73	0.17	0.04	16.04
87	8/8/2024	0.18	0.16	0.04	1.06	0.97	0.09	0.02	11.61

Table SI-12(C). Underdrain event mean concentrations (EMCs) for all events characterized at LT-BS (2019-24). Data shaded in yellow were collected as part of the CBT-funded project (2022-2025).

Event No.	Dates	Cr (μg/L)	Cu (μg/L)	Zn (μg/L)	Cd (μg/L)	Pb (μg/L)	Na (mg/L)	K (mg/L)	Mg (mg/L)	Ca (mg/L)
2	4/14/2019	1.57	8.07	37.31	0.04	1.39	163.10	2.10	1.06	12.16
5	5/3/2019	2.31	8.22	54.38	0.09	1.66	100.93	0.83	1.14	16.64
7	5/5/2019	1.68	5.90	31.55	0.04	1.04	116.43	0.81	1.12	16.46
14	6/13/2019	2.48	7.46	36.75	0.08	1.52	67.47	0.66	0.96	15.13
15	6/17/2019	1.61	6.26	50.53	0.17	0.96	108.25	0.67	1.67	21.76
16	7/8/2019	1.77	7.32	34.15	0.18	1.34	67.96	0.53	1.08	14.07
17	7/22/2019	1.67	8.07	38.80	0.08	1.18	74.30	0.65	1.04	15.13
18	10/27/2019	4.52	4.98	23.57	0.07	1.08	58.58	1.01	1.05	10.30
19	10/30/2019	0.66	6.46	21.61	0.04	0.99	75.26	1.45	1.28	13.16
20	10/31/2019	1.11	6.28	27.42	0.05	2.11	38.12	1.02	0.84	9.78
25	8/4/2020	0.45	6.01	14.69	0.02	0.16	54.08	0.51	1.17	11.92
27	8/12/2020	0.48	5.19	26.21	0.03	0.42	27.80	0.55	1.20	13.80
32	10/29/2020	0.43	4.51	14.00	0.02	0.11	40.08	1.33	1.41	15.80
33	11/11/2020	0.46	5.33	18.46	0.02	0.17	41.65	1.76	1.94	21.30
34	11/12/2020	0.30	5.20	13.27	0.02	0.15	41.90	2.28	1.79	21.28
36	5/3/2021	0.50	4.71	9.46	0.02	0.20	57.98	0.87	0.69	8.20
38	5/29/2021	0.51	5.54	19.39	0.03	0.30	167.61	1.31	1.80	17.10
39	7/1/2021	1.09	8.79	22.23	0.05	0.39	125.26	0.74	0.89	10.63
41	7/17/2021	0.93	8.07	29.98	0.08	0.25	96.93	0.94	0.94	12.60
42	8/16/2021	0.72	6.40	13.43	0.03	0.15	57.59	0.83	0.78	9.51
43	8/18/2021	0.65	6.97	12.76	0.03	0.25	103.95	1.82	0.77	9.96

46	8/25/2021	0.60	4.90	20.40	0.03	0.20	0.13	0.57	2.79	0.04
49	9/1/2021	0.32	3.90	9.17	0.02	0.20	47.58	0.87	0.92	13.20
55	10/29/2021	0.47	4.80	11.95	0.02	0.28	61.08	1.52	1.51	16.59
72	4/28/2023	0.53	4.66	10.17	0.03	0.27	41.99	0.57	0.84	9.94
73	4/30/2023	0.39	4.56	14.31	0.04	0.26	34.84	0.51	0.91	11.89
N/A	9/23/2023	0.20	7.66	8.57	0.04	0.12	74.83	1.64	2.07	20.64
76	3/23/2024	0.56	11.58	11.75	0.03	0.24	113.72	0.72	1.17	10.55
77	4/1/2024	0.53	4.67	8.03	0.02	0.13	108.01	0.74	1.23	12.03
78	4/2/2024	0.33	3.83	5.00	0.02	0.14	85.27	0.89	0.77	10.47
79	4/3/2024	0.28	3.90	5.19	0.05	0.15	71.18	0.81	1.06	12.64
81	5/25/2024	0.77	9.83	12.53	0.03	0.18	102.23	0.81	1.36	16.03
82	5/26/2024	0.63	9.50	11.15	0.03	0.20	96.58	0.77	1.41	16.47
84	6/5/2024	0.52	7.50	16.95	0.03	0.17	133.29	0.98	2.34	26.61
85	6/29/2024	0.69	10.69	25.34	0.07	0.21	62.93	2.30	1.27	15.70
86	8/7/2024	0.44	6.11	8.92	0.05	0.09	81.10	0.85	1.29	14.09
87	8/8/2024	0.30	4.57	7.32	0.04	0.16	47.14	0.81	0.88	11.75

Table SI-13(A). Event mean concentrations (EMCs) for all events characterized at LT-GS (2019-24). Data shaded in yellow were collected as part of the CBT-funded project (2022-2025).

Event No.	Dates	Spec. Cond. (µS/cm)	TSS (mg/L)	ANC (µeq/L)	Chloride (mg/L)	Sulfate (mg/L)	Ortho-P (mg/L)	Ammonia-N (mg/L)	Nitrite-N (mg/L)	Nitrate-N + Nitrite-N (mg/L)	Nitrate-N (mg/L)	DON (mg/L, calc.)
2	4/14/2019	545.68	34.18	1121.20	129.21	2.76	0.05	0.06	0.01	0.07	0.06	0.90
5	5/3/2019	340.37	61.03	531.63	91.67	3.37	0.12	0.13	0.02	0.24	0.23	0.67
7	5/5/2019	471.77	9.38	1766.63	97.04	3.04	0.04	0.02	0.01	0.01	0.00	0.78
14	6/13/2019	164.59	74.96	629.63	27.93	2.34	0.25	0.05	0.01	0.05	0.04	0.74
15	6/17/2019	513.32	13.97	1200.12	110.63	9.76	0.26	0.24	0.01	0.02	0.01	1.61
16	7/8/2019	126.46	7.45	537.69	19.64	3.59	0.28	0.03	0.02	0.11	0.09	0.65
17	7/22/2019	307.31	9.81	1086.95	59.85	8.99	0.44	0.02	0.02	0.11	0.09	1.37
18	10/27/2019	155.14	7.43	765.73	19.05	5.44	0.45	0.05	0.01	0.19	0.18	0.73
19	10/30/2019	354.41	5.47	1656.10	49.30	13.23	1.11	0.02	0.02	0.14	0.12	1.46
20	10/31/2019	105.94	22.00	729.99	10.46	2.11	0.33	0.02	0.01	0.02	0.02	0.56
27	8/12/2020	100.82	10.45	580.03	10.67	3.13	0.90	0.24	0.04	0.48	0.44	1.48
31	10/12/2020	286.58	8.00	1198.25	39.89	9.91	0.87	0.02	0.01	0.07	0.06	1.30
32	10/29/2020	226.74	11.85	899.52	30.00	10.44	0.99	0.06	0.02	0.54	0.52	1.37
33	11/11/2020	242.70	18.42	1080.78	30.17	10.01	1.63	0.03	0.01	0.28	0.27	1.35
36	5/3/2021	211.98	58.51	534.42	46.34	1.40	0.20	0.04	0.01	0.12	0.11	0.61
38	5/29/2021	1072.02	13.22	1750.07	179.07	15.40	0.23	0.05	0.04	1.06	1.03	1.65
39	7/1/2021	514.14	16.53	1191.07	115.27	6.56	0.53	0.03	0.03	0.41	0.37	1.83
40	7/12/2021	734.39	25.08	1008.93	185.96	12.31	1.29	0.03	0.08	0.29	0.21	2.30
41	7/17/2021	280.10	25.84	415.11	67.58	4.68	0.96	0.02	0.02	0.29	0.27	1.32
42	8/16/2021	125.72	19.06	573.43	19.83	2.16	0.51	0.03	0.02	0.20	0.19	0.80

43	8/18/2021	207.37	11.76	943.52	32.42	2.51	0.47	0.03	0.01	0.04	0.03	1.28
45	8/20/2021	206.33	10.53	1247.44	24.58	1.55	0.56	0.05	0.01	0.03	0.01	1.49
46	8/25/2021	73.30	10.75	372.99	6.80	1.21	0.51	0.02	0.02	0.34	0.32	0.71
49	9/1/2021	141.66	7.82	986.30	14.60	0.79	0.17	0.02	0.01	0.01	0.01	0.61
55	10/29/2021	262.17	19.93	1054.94	52.57	6.40	1.20	0.02	0.01	0.08	0.07	0.94
72	4/28/2023	393.72	17.48	1253.99	72.77	8.61	0.16	0.05	0.02	0.41	0.39	1.35
73	4/30/2023	258.24	28.13	1340.85	34.50	3.90	0.09	0.06	0.01	0.07	0.05	1.20
76	3/23/2024	652.38	41.56	1183.33	158.66	4.39	0.19	0.05	0.01	0.20	0.19	1.06
77	4/1/2024	616.77	64.30	1354.28	138.84	4.31	0.08	0.05	0.01	0.13	0.12	1.17
78	4/2/2024	590.42	39.29	1967.33	116.74	3.60	0.05	0.02	0.01	0.02	0.01	0.89
79	4/3/2024	258.15	96.68	1307.30	37.13	1.77	0.05	0.03	0.01	0.09	0.08	0.41
81	5/25/2024	92.07	32.23	264.18	16.07	1.30	0.21	0.01	0.01	0.17	0.16	0.72
82	5/26/2024	159.14	59.56	633.41	25.64	1.68	0.20	0.09	0.01	0.12	0.10	1.37
83	5/27/2024	503.40	37.50	2254.70	84.01	2.66	0.10	0.03	0.01	0.01	0.00	2.33
84	6/5/2024	365.56	20.40	767.27	80.97	2.16	0.37	0.04	0.02	0.16	0.14	1.46
85	6/29/2024	471.55	18.74	1047.90	95.96	8.48	1.08	0.04	0.44	1.66	1.22	2.73
86	8/7/2024	159.98	6.71	1134.27	11.96	2.06	0.27	0.02	0.01	0.00	0.00	1.11
87	8/8/2024	159.55	4.61	1322.88	7.74	1.31	0.18	0.01	0.00	0.00	0.00	0.92
88	9/26/2024	196.58	11.86	1182.33	18.31	3.54	0.47	0.02	0.01	0.00	0.00	1.09

Table SI-13(B). Event mean concentrations (EMCs) for all events characterized at LT-GS (2019-24). Data shaded in yellow were collected as part of the CBT-funded project (2022-2025).

Event No.	Dates	Total P (mg/L)	Total Dissolved P (mg/L)	DOP (mg/L, calculated)	Total Nitrogen (mg/L)	Total Dissolved N (mg/L)	Particulate N (mg/L, calculated)	Particulate P (mg/L, calculated)	DOC (mg/L)
2	4/14/2019	0.21	0.08	0.03	1.73	1.03	0.70	0.13	12.82
5	5/3/2019	0.36	0.14	0.02	1.35	1.04	0.31	0.22	10.65
7	5/5/2019	0.11	0.07	0.02	0.92	0.81	0.11	0.05	11.67
14	6/13/2019	0.42	0.27	0.02	1.64	0.84	0.80	0.15	11.78
15	6/17/2019	0.38	0.31	0.05	2.34	1.87	0.47	0.08	24.27
16	7/8/2019	0.36	0.31	0.03	1.02	0.79	0.23	0.04	8.61
17	7/22/2019	0.56	0.50	0.06	1.90	1.50	0.40	0.07	19.72
18	10/27/2019	0.51	0.47	0.02	1.18	0.97	0.21	0.04	11.12
19	10/30/2019	1.24	1.19	0.07	2.02	1.63	0.39	0.05	27.80
20	10/31/2019	0.41	0.34	0.02	0.97	0.60	0.33	0.08	10.31
27	8/12/2020	1.11	1.01	0.10	2.81	2.20	0.61	0.10	19.03
31	10/12/2020	0.98	0.91	0.04	1.75	1.39	0.36	0.07	21.52
32	10/29/2020	1.07	1.03	0.05	2.40	1.97	0.44	0.04	18.57
33	11/11/2020	1.68	1.58	0.00	2.25	1.67	0.58	0.10	22.40
36	5/3/2021	0.35	0.23	0.03	1.38	0.77	0.62	0.12	7.16
38	5/29/2021	0.34	0.27	0.04	3.22	2.76	0.45	0.07	17.60
39	7/1/2021	0.67	0.58	0.06	2.78	2.26	0.52	0.09	25.17
40	7/12/2021	1.62	1.36	0.07	4.03	2.62	1.41	0.25	32.48
41	7/17/2021	1.15	1.01	0.05	2.47	1.63	0.85	0.15	19.37
42	8/16/2021	0.64	0.53	0.02	1.53	1.04	0.48	0.10	10.87
43	8/18/2021	0.57	0.52	0.05	1.62	1.35	0.27	0.06	17.09

45	8/20/2021	0.66	0.60	0.04	1.94	1.56	0.38	0.06	19.52
46	8/25/2021	0.63	0.55	0.03	1.54	1.07	0.48	0.08	9.60
49	9/1/2021	0.22	0.19	0.02	0.80	0.65	0.15	0.03	8.33
55	10/29/2021	1.38	1.23	0.03	1.55	1.03	0.52	0.15	15.64
72	4/28/2023	0.28	0.20	0.04	2.25	1.82	0.43	0.08	17.63
73	4/30/2023	0.23	0.14	0.05	1.73	1.32	0.40	0.09	16.75
76	3/23/2024	0.35	0.22	0.04	1.81	1.32	0.49	0.13	11.00
77	4/1/2024	0.29	0.12	0.04	2.01	1.35	0.67	0.17	16.24
78	4/2/2024	0.20	0.08	0.03	1.33	0.93	0.41	0.12	11.38
79	4/3/2024	0.30	0.06	0.01	1.24	0.53	0.71	0.24	6.37
81	5/25/2024	0.39	0.24	0.03	1.59	0.90	0.69	0.15	10.80
82	5/26/2024	0.47	0.25	0.05	2.57	1.57	1.00	0.22	18.55
83	5/27/2024	0.31	0.17	0.07	3.04	2.37	0.67	0.14	31.67
84	6/5/2024	0.57	0.42	0.05	2.50	1.66	0.85	0.15	20.98
85	6/29/2024	1.39	1.19	0.11	5.39	4.43	0.96	0.21	40.05
86	8/7/2024	0.36	0.31	0.04	1.39	1.13	0.27	0.05	16.07
87	8/8/2024	0.25	0.22	0.03	1.09	0.93	0.16	0.03	12.16
88	9/26/2024	0.58	0.50	0.04	1.52	1.11	0.40	0.08	17.83

Table SI-13(C). Event mean concentrations (EMCs) for all events characterized at LT-GS (2019-24). Data shaded in yellow were collected as part of the CBT-funded project (2022-2025).

Event No.	Dates	Cr (μg/L)	Cu (μg/L)	Zn (μg/L)	Cd (μg/L)	Pb (μg/L)	Na (mg/L)	K (mg/L)	Mg (mg/L)	Ca (mg/L)
2	4/14/2019	1.90	5.16	17.26	0.05	2.33	102.01	1.32	1.11	9.84
5	5/3/2019	2.15	4.81	21.54	0.05	5.01	59.21	0.82	0.91	6.84
7	5/5/2019	1.61	4.44	12.72	0.04	1.20	91.60	0.42	1.09	9.15
14	6/13/2019	2.36	4.52	17.88	0.06	2.63	31.79	1.70	0.53	20.08
15	6/17/2019	2.61	9.43	17.70	0.11	1.23	94.24	1.95	1.98	14.32
16	7/8/2019	1.89	5.42	11.98	0.05	0.75	24.95	0.88	0.60	3.80
17	7/22/2019	1.66	7.38	13.00	0.04	0.80	68.60	2.20	1.52	9.15
18	10/27/2019	0.96	4.28	11.89	0.03	0.54	31.14	2.25	0.84	3.08
19	10/30/2019	0.67	5.65	10.96	0.03	0.67	61.75	5.17	2.13	9.85
20	10/31/2019	0.87	3.05	13.64	0.03	1.35	21.20	2.04	0.70	2.63
27	8/12/2020	0.37	4.61	6.55	0.03	0.29	15.44	3.01	0.74	2.71
31	10/12/2020	0.40	5.57	3.48	0.03	0.13	46.08	6.32	1.97	9.49
32	10/29/2020	0.44	4.37	4.02	0.02	0.12	38.03	4.38	1.29	6.69
33	11/11/2020	0.43	4.88	4.79	0.02	0.16	38.87	8.28	1.94	8.58
36	5/3/2021	0.36	2.58	2.42	0.02	0.21	69.85	0.61	0.40	3.03
38	5/29/2021	1.84	8.63	3.76	0.05	0.81	205.47	1.38	3.88	27.72
39	7/1/2021	1.72	8.66	7.11	0.05	0.48	149.71	1.79	1.69	11.56
40	7/12/2021	0.60	7.47	7.70	0.05	0.32	141.53	9.01	3.30	19.13
41	7/17/2021	0.57	4.38	4.17	0.03	0.15	51.91	5.15	1.06	5.85
42	8/16/2021	0.58	2.96	2.84	0.02	0.19	25.72	2.64	0.59	2.32

43	8/18/2021	0.48	3.51	3.47	0.02	0.26	89.98	1.83	0.77	3.92
45	8/20/2021	0.57	4.28	3.22	0.03	0.29	106.75	1.64	0.60	3.64
46	8/25/2021	0.71	2.11	3.40	0.02	0.18	13.55	1.61	0.20	0.97
49	9/1/2021	0.25	1.53	1.38	0.01	0.18	37.87	0.93	0.51	3.43
55	10/29/2021	0.46	3.39	3.56	0.01	0.15	53.06	6.29	1.24	6.07
72	4/28/2023	0.65	5.16	2.64	0.03	0.34	64.55	0.48	1.51	10.89
73	4/30/2023	0.44	4.13	2.83	0.03	0.33	43.39	0.34	0.94	7.03
76	3/23/2024	0.60	3.84	2.02	0.02	0.16	119.57	0.68	2.05	13.53
77	4/1/2024	0.50	3.89	1.96	0.03	0.13	112.73	0.58	2.19	14.88
78	4/2/2024	0.34	3.01	1.38	0.02	0.16	107.75	0.40	2.13	15.03
79	4/3/2024	0.19	1.76	0.74	0.01	0.10	52.53	0.25	0.67	4.70
81	5/25/2024	0.28	2.36	3.21	0.01	0.11	16.20	1.94	0.25	1.69
82	5/26/2024	0.44	4.03	4.71	0.02	0.26	29.64	1.27	0.56	3.95
83	5/27/2024	0.69	5.70	4.52	0.04	0.38	91.53	1.20	2.20	15.64
84	6/5/2024	0.32	5.14	3.56	0.02	0.08	67.14	2.83	0.89	5.98
85	6/29/2024	0.68	9.64	6.89	0.03	0.13	74.64	9.67	2.53	13.31
86	8/7/2024	0.39	4.17	2.54	0.02	0.16	30.66	1.66	0.83	4.01
87	8/8/2024	0.35	3.27	1.73	0.03	0.19	31.01	1.10	0.70	4.01
88	9/26/2024	0.30	3.31	2.61	0.02	0.22	32.86	4.66	1.66	6.35